UNIVERSITY OF CALIFORNIA, SAN DIEGO

Transcriptomic Profiling of the Giant Kelp, *Macrocystis pyrifera,* Across Environmental Gradients

A dissertation submitted in partial satisfaction of the
Requirements for the degree Doctor of Philosophy

in

Oceanography

by

Talina Helen Konotchick

Committee in charge:

Paul K. Dayton, Co-Chair
James J. Leichter, Co-Chair
Andrew E. Allen
Jules S. Jaffe
Lisa A. Levin
P. Ed Parnell
Shankar Subramaniam

2012

The Dissertation of Talina Helen Konotchick is approved, and it is acceptable in quality and form for publication on microfilm and electronically:

_____

_____

_____

_____

_____

_____
Co-Chair

_____
Co-Chair

University of California, San Diego

2012

TABLE OF CONTENTS

LIST OF ABBREVIATIONS

bp	base pair
BLAST	Basic Local Alignment Search Tool
cDNA	complementary DNA
CD-HIT	Cluster Database at High Identity with Tolerance
DNA	deoxyribonucleic acid
EST	expressed sequence tag
Gbp	giga (=10^9) basepairs
HMM	hidden Markov models
JCVI	J. Craig Venter Institute
KEGG	Kyoto Encyclopedia of Genes and Genomes
KO	Kegg orthology
mab	meters above bottom
Mbp	mega (=10^6) basepairs
pfam	protein family annotated using HMM approach
µM	micromolar
ORF	open reading frame
PSII	Photosystem II
PCR	Polymerase Chain Reaction
qPCR	quantitative Polymerase Chain Reaction
RNA	ribonucleic acid
RT	room temperature

rRNA	ribosomal RNA
SCUBA	self contained underwater breathing apparatus
TU	transcriptional unit

LIST OF FIGURES

Chapter 2

Chapter 3

Chapter 4

Chapter 5

Appendix 1

Appendix 2

LIST OF TABLES

Chapter 3

Chapter 4

Chapter 5

Appendix 1

Appendix 2

ACKNOWLEDGEMENTS

The time and effort of many people have contributed to the successful completion of my dissertation. I would like to start by acknowledging the guidance and support of my PhD advisors: Jim Leichter, Paul Dayton and Andrew Allen.

To Jim Leichter, thank you for your time and valuable advice during my progression through graduate school, for allowing me the independence to develop my own research interests and providing guidance when needed. To Paul Dayton, who has provided unwavering support throughout the years, thank you for sharing your passion for the natural world and for leading many unforgettable camping and fieldtrips. To Andy Allen for the opportunity to work in his lab at the J. Craig Venter Institute (JCVI) and allowing me to find my way into the fields of molecular biology and genomics that became a large portion of my dissertation.

To the other members of my dissertation committee, I feel privileged to have worked with all of you. To Lisa Levin, for being an inspiring role model and for insightful feedback. To Ed Parnell for valuable discussions about the kelp forest, help with data processing and genuine support. To Jules Jaffe, for his enthusiasm, encouragement and thought-provoking discussions. To Shankar Subramaniam, I am truly impressed by your efficient and insightful manner. Thank you to my entire committee for your ideas, support and mentorship.

Thank you to all the past and present members of the Dayton and Leichter Labs who provided an engaging academic and social atmosphere on the third floor of Ritter Hall. Special thanks to Kristen Riser and Ryan Darrow for their friendship and help in

the field. Thank you to my office mates Cynthia Catton, Marcel Croon, Christian Anderson, Doug Krause, and Jillian Maloney for discussions and advice in all matters relating to grad school.

I have learned a tremendous amount from collaborations with researchers and co-authors at JCVI. Thank you for your time and energy in support of my dissertation. Special thanks to Chris Dupont, who has been a motivating force and reliable source of quality advice and guidance throughout this project. Thank you to Jonathan Badger and Ruban Valas, for your help with bioinformatic analyses and for your patience in answering my questions. Thanks to Jing Bai who initially got me up and running in the lab, and to Hong Zheng, the glue of the Allen lab. Thank you to the many others at JCVI who have helped me along the way including: Mauricio Arriagada, Karen Beeri, Stephan Lefebvre, Flip McCarthy, Jeff McQuaid, Graham Peers, Greg Wanger, and Lisa Zeigler.

The fieldwork in this project could not have been completed without the help of the SIO diving and boating program and all of my many diving buddies. Thank you to DSO Christian McDonald and to Eddie Kisfaludy. A special thanks to Rich Walsh for diving and boating assistance and for bringing heat packs on the boat to keep my hands warm enough to process my samples.

The intellectual and personal experiences during my time as Scripps would not have been the same without the engaging friendships that I have made. First, to my Biological Oceanography cohort and their families: Geoff Cook, Marco Hatch, Elizabeth Henderson, Megan McKenna, and Andrew Thurber, I am grateful for your friendship and for many shared experiences, from departmental studying to scientific

and not-so-scientific discussions over beer. Thanks to Marco and Renee for hosting many enjoyable dinners. Thanks to the faculty, staff and graduate students of SIO who have enriched my experience, including: Peter Franks, Miriam Goldstein, Kristian Gustavson, Davey Kline, Greg Mitchell, Danny Richter and the entire Center for Marine Biodiversity and Conservation community. To my north-of-the-pier surfing buddies: Marco Hatch, Nate Huffnagle, Spencer Kawamoto, Ben Maurer, Gino Passalacqua, Andrew Thurber, and Rich Walsh, thank you for making my time at SIO that much more enjoyable. Thanks as well to the UCSD triathlon team and especially to Tim Ray. Your passion for getting the most out of life and possessing the initiative to actually make it happen is a true inspiration. To my other friends who have been there for me during this journey: Clairine Cadena, Christy Decker Goodson, Paola Lopez, Ryan Drobek, and Charles McKeown. Thanks to Annie Rorick, Imad Ajjawi, Eric Moellering, and the rest of the rotating RB & Sunday Dinner crowd.

I would not be getting a PhD in Oceanography without the encouragement of many teachers along the way. A special thanks goes to Bill Hamner for motivating me to pursue a career in Oceanography. Thanks as well to Dan Reineman for convincing me to get my scientific diving certification and for sharing his enthusiasm for ocean sciences.

Finally, I would like to give a special thanks to my family for their encouragement throughout the years. I am lucky to have been born into such a loving, supportive and caring family. To my Mom and Dad, my sisters Kristi, Karin, Kim and Anna, and their families, I would not be where I am today without you!

The research presented in this dissertation was made possible by funding provided by a National Defense Science and Engineering Graduate Fellowship, a National Science Foundation (NSF) Graduate Research Fellowship, the Center for Marine Biodiversity and Conservation's Integrative Graduate Education and Research and Training (IGERT) program, a P.E.O. Mary Louise Remy Endowed Scholar Award, a Mia J. Tegner Fellowship for Coastal Ecology Fieldwork, and a Sigma Xi Grant in aid of Research, the Jaffe Lab, and the J. Craig Venter Institute.

Chapter 2, in full, is currently in preparation for submission. Konotchick, T., C. Dupont, R.E. Valas, and A.E. Allen. Brown Algal Genomics. The dissertation author was the primary investigator and author of this manuscript.

Chapter 3, in full, has been submitted for publication in Estuarine, Coastal and Shelf Science. Konotchick, T., P.E. Parnell, P.K. Dayton, and J.J. Leichter. Vertical Distribution of *Macrocystis pyrifera* Nutrient Exposure in Southern California. The dissertation author was the primary investigator and author of this manuscript.

Chapter 4, in full, is currently in preparation for submission. Konotchick, T., C. Dupont, J. Badger, R.E. Valas, and A.E. Allen. Transcriptomic Analysis of Metabolic Function in the Giant Kelp, *Macrocystis pyrifera*, Across Depth and Season. The dissertation author was the primary investigator and author of this manuscript.

Chapter 5, in full, is currently in preparation for submission. Konotchick, T., C. Dupont, R.E. Valas, and A.E. Allen. Transcriptional Profiling of the Giant Kelp, *Macrocystis pyrifera*, Spanning Water Column Gradients in Light, Temperature, and Nutrients. The dissertation author was the primary investigator and author of this manuscript.

VITA

Education

2012 Ph.D. in Oceanography
University of California, San Diego
Dissertation title: "Transcriptomic Profiling of the Giant Kelp, *Macrocystis pyrifera,* Across Environmental Gradients"

2008 M.S. in Oceanography
University of California, San Diego

2004 B.S. in Marine Biology, *summa cum laude*
University of California, Los Angeles

Publications

Konotchick, T., P.E. Parnell, P.K. Dayton, and J.J. Leichter. (in review). Vertical distribution of *Macrocystis pyrifera* nutrient exposure in southern California. Estuarine, Coastal and Shelf Science.

Levin, L.A., G.F. Mendoza, **T. Konotchick**, and R. Lee. 2009. Macrobenthos community structure and trophic relationships within active and inactive Pacific hydrothermal sediments. *Deep Sea Research II* 56(19-20): 1632-1648.

Erisman, B., **T. Konotchick**, and S. Blum. 2009. Observations of spawning in the Leather Bass, *Dermatolepis dermatolepis* (Teleostei: Epinephelidae) at Cocos Island, Costa Rica. *Environmental Biology of Fishes* 85: 15-20.

Sandin, S.A., J.E. Smith, E.E. DeMartini, E.A. Dinsdale, S.D. Donner, A.M. Friedlander, **T. Konotchick**, M. Malay, J.E. Maragos, D. Obura, O. Pantos, G. Paulay, M. Richie, F. Rohwer, R.E. Schroeder, S. Walsh, J.B.C. Jackson, N. Knowlton, and E. Sala. 2008. Baselines and degradation of coral reefs in the Northern Line Islands. *PLoS ONE* 3(2): e1548.

Benham, C., A.M. Cawood, G.S. Cook, A. Darnell, P.C. Davison, M.C. Goldstein, A.E. Johnson, **T. Konotchick**, E.M. Maldonado, A.L. Pasulka, J.C. Prairie, S.M. Moseman, V. Tai, C.A. Tanner, T. Vardi, T.S. Whitty, and L.A. Levin 2008. Review of J.P. Kritzer and P.F. Sale, *Marine Metapopulations* (2006) in *Marine Ecology* 29(2): 319. (book review)

Fields of Study

Studies in Biodiversity and Conservation
Professors F. Joyce; J. Jackson, N. Knowlton
UC Los Angeles, Education Abroad Program; UC San Diego

Studies in Oceanography
Professors L. Aluwihare, K. Barbeau, S. Cande, C. Charles, M. Hendershott, D. Hilton, R. Keeling, L. Talley
UC San Diego

Studies in Marine Biology
Professors W. Hamner, P. Fong, D. Jacobs, R. Vance; A. Kohn, G. Paulay, R. Strathmann; L. Levin
UC Los Angeles; University of Washington; UC San Diego

Studies in Marine Molecular Ecology
Professor R. Burton
UC San Diego

Studies in Natural History
Professor P. Dayton
UC San Diego

Studies in Physical-Biological Interactions
Professors James Leichter, Peter Franks; D. Grunbaum
UC San Diego; University of Washington

Studies in Plant Physiology and Marine Botany
Professors E. Zieger and Peggy Fong
UC Los Angeles

Studies in Antarctic Biology
Professors D. Manahan, M. Denny, D. Karentz, A. Murray, G. Somero
McMurdo Station, Antarctica

ABSTRACT OF THE DISSERTATION

Transcriptomic Profiling of the Giant Kelp,
Macrocystis pyrifera,
Across Environmental Gradients

by

Talina Helen Konotchick

Doctor of Philosophy in Oceanography

University of California, San Diego, 2012

Professor Paul K. Dayton, Co-Chair
Professor James J. Leichter, Co-Chair

The giant kelp, *Macrocystis pyrifera,* spans gradients in light, temperature and nutrient availability both within its geographic distribution and the range of depths that individual sporophytes span. *M. pyrifera* is a member of the brown algae (Phaeophyceae), a complex multicellular group divergent from other eukaryotes; the application of sequence-based tools to study the ecology and evolution of this group is reviewed. To understand the biological response of this ecologically important alga to its environment, it is important to quantify the temporal scales of environmental variation. A several-year thermistor chain time series examined depth-specific variations in temperature and nutrients within a kelp bed. In addition to long-term seasonal changes, rapid vertical variations in the depth of the nutricline were observed, as much as 10m vertical displacement over the span of a few hours. Tools capable of examining the *M. pyrifera* physiological response on this temporal scale had not yet

been developed. Due to the lack of available genomic data for the giant kelp, I utilized next-generation transcriptomic sequencing to increase the number of annotated transcriptional units for this species. *M. pyrifera* samples collected at different depths enabled transcriptomic exploration of metabolic function across environmental gradients. Depth-dependent transcription patterns were apparent and transcript annotation facilitated the identification of physiological responses to environmental factors. At the surface, where irradiance levels are highest and the potential for oxidative damage is most intense, physiological processes were focused on the capture of light energy for photosynthesis as well as protection from the damaging effects of the sun. *M. pyrifera* has multiple light harvesting complexes, including some in the LI818 group. Genes involved in nutrient acquisition, genetic information processing and degradation were more highly expressed at depth where colder temperatures and more nutrients occur. This dissertation provides the first transcriptomic characterization of *M. pyrifera,* develops sequenced-based tools and demonstrates their use to study transcriptional patterns in the context of this alga's natural and variable environment.

CHAPTER 1

Introduction

Macrocystis pyrifera is the largest alga in the world and a dominant competitor on rocky substrates for light in the temperate nearshore of many coastlines worldwide including the west coast of North America. What physiological features and evolutionary traits have contributed to the success of *M. pyrifera*? In this dissertation, I discuss how genomic information in the brown algae (Phaeophyceae) can be used to address evolutionary and ecological areas of research; explore the depth-specific temperature variability in a *M. pyrifera* kelp forest; establish a transcript catalogue using next generation transcriptomics to develop sequenced-based tools to explore *M. pyrifera*'s gene expression patterns in relation to physical environmental factors; and develop a sequence-based resource for this ecologically important organism.

The Ecosystem Roles of *Macrocystis pyrifera*

Macrocystis pyrifera is a dominant species on temperate shallow rocky shores. The complex structure of *M. pyrifera* supports a diversity of species (containing many more phyla than terrestrial forests) that use the kelp as a habitat, a nursery, or for food (detritivores and decomposers and fish and invertebrate herbivores). *M. pyrifera* competes for space and light with other algae. Other kelp genera that comprise the biodiversity of kelps in southern California include *Pterygophora*, *Laminaria*, *Eisenia*, *Pelagophycus*, and *Egregia*. Herbivorous predators include the purple and red sea urchins (*Strongylocentrotus purpuratus* and *S. franciscanus,* respectively), several

species of abalone (*Haliotis spp.*), and several fish species feeding on the blades or on encrusting epiphytes. Kelp forests also provide many benefits for humans. They provide a habitat for commercially and recreationally harvested fish and invertebrate species, produce chemical products such as alginate that are used in a variety of products, and have intrinsic value as a bio-diverse ecosystem to explore.

Macrocystis **Biology**

Taxonomy and Evolution

M. pyrifera is currently placed in the taxonomic InfraKingdom Heterokonta. Heterokonts (or Stramenopiles) are a major lineage of eukaryotes, with cellular morphologies that span seven orders of magnitude in size. The Heterokonts are believed to have diverged from other major eukaryotic groups, including plants and animals ~1 billion years ago (Douzery et al., 2004). This group contains the brown algae, diatoms, Oomycetes and some protists. Heterokonts are characterized by the presence of cells with two unequal flagella, plastids with four membranes and lamellae with three stacked thylakoids. Heterokonts are thought to be a product of secondary endosymbiosis (Moustafa et al., 2009). When examining the genetic make-up of the brown algae, we must consider the nuclear and organelle (i.e. chloroplast and mitochondria) genomes of the heterotrophic eukaryote, and the primary and secondary photosynthetic endosymbionts. Red algae likely originated from an endosymbiosis of a eukaryotic protist and a cyanobacterium, then brown algae arose from secondary endosymbiosis of a protist of the red alga (Moustafa et al., 2009). *M. pyrifera* is a member of the Class Phaeophyceae (the brown algae), which is characterized by the

ability to form complex multicellular thalli. The general thallus morphology of an *M. pyrifera* sporophyte includes a holdfast that attaches to the substrate, and long stipes to which blades are attached. At the base of each blade is a pneumatocyst, a small gas bladder that helps keep the kelp afloat in the water column. The golden color of *M. pyrifera* comes from the carotenoid pigments fucoxanthin and violaxanthin found in their plastids in addition to the chlorophyll *a, c1 c2* pigments. *M. pyrifera* is in the Order Laminariales (e.g. the kelps), and Family Laminariaceae.

Algae lack a significant fossil record and often display highly plastic phenotypes, which makes genetic data an appropriate metric to measure evolutionary relationships. Morphological differences in blade and holdfast morphology have historically been used to designate the different species in the genus *Macrocystis* (Setchell, 1932). However, environmental factors have been shown to alter blade morphology (Druehl, 1978; Hurd et al., 1996; Hurd, 2000). Variability in holdfast morphology can also be induced environmentally (Demes et al., 2009); all thalli begin with a characteristic *M. pyrifera* conical holdfast morphology and morphological differences are a result of an interaction between vertical growth of the haptera along the basal stipes and the lifetime height of the basal stipe. However, the physiological mechanisms behind such sensitive phenotypic plasticity are unresolved though they may be related to light availability. In the brown kelp, *Nereocystis luetkeana*, the incidence of far red light affected stipe elongation (Duncan and Foreman, 1980).

Reproductive isolation is one designation for defining a species (Mayr, 1969); the species in the genus *Macrocystis* are not completely reproductively isolated according to this definition. Additionally, *Macrocystis angustifolia* has been shown to

hybridize with other genera in the Family Laminariaceae: *Pelagophycus* and *Nereocystis* (Sanbonsuga and Neushul, 1978). Hybridization is seen in other Phaeophyte orders as well (Coyer et al., 2002). The currently described species in the genus *Macrocystis* may actually only be one species even though it has a large geographic range. Demes et al. proposes collapsing the four currently recognized species of the genus *Macrocystis* (i.e. *M. pyrifera, M. integrifolia, M. angustifolia,* and *M. laevis*) into *M. pyrifera* on the basis of extreme morphological plasticity and demonstrated interfertility and the argument that morphological differences should be considered as ecotypes (Demes et al., 2009).

Knowledge of phylogenetic relationships within brown algae has improved with recent advances in molecular techniques and sequencing technology (Table 14.1 in Reviers et al. 2007). A monospecific *Macrocystis* genus is supported by this molecular work as well. *M. pyrifera* and *M. integrifolia,* two morphologically disparate congeners display less chloroplast DNA diversity than did two morphologically similar populations of *M. integrifolia* from the northern and southern hemispheres (Druehl and Saunders, 1992). More recent studies using genomic internal transcribed spaces (ITS) regions found low levels of population divergence (<1%) between *M. integrifolia* and *M. pyrifera* and the possibility of gene flow between Southern and Northern hemisphere (Mackenzie, 1997). Additionally, larger genetic differences were found between geographically separated members of the same species as compared to different species in closer geographic range on the basis of ITS1 and ITS2 sequences (Coyer et al., 2001). A restructuring of family level classifications in kelp combined the genera *Macrocystis, Pelagophycus, Postelsia* and

Nereocystis into the *Macrocystis* clade on the basis of ribulose-1,5-bisphosphate carboxylase oxygenase (rubisco), an enzyme involved in carbon fixation, and ITS sequence data; this classification is consistent with the interfertility observations of Sanbonsuga and Neushul (1978). Despite these single gene population studies, there is relatively little genomic data available for *M. pyrifera.*

Reproduction

M. pyrifera has a diplohaplontic life cycle (e.g. alternation of generations) with a macroscopic diploid (2N) sporophyte stage and a microscopic haploid (1N) gametophyte stage. The sporophyte stage can grow to many tens of meters in size. Located near the base of the sporophyte are reproductive blades called sporophylls that release spores. Production of spores occurs throughout the year. These spores become the haploid female and male gametophytes (1N). The female gametophyte produces an egg and the male releases motile sperm that acts on chemical cues to find the egg. After fertilization, the sporophyte grows on top of the female gametophyte and eventually grows into the large sporophyte stage. The sporophyte is often perennial. *M. pyrifera* samples collected in this dissertation were from mature blades of the sporophyte stage.

The Kelp Forest: a Variable Physical Environment

Macrocystis pyrifera exists across large gradients in light, temperature and nutrients that are present both within the geographic range of this species as well as through the range of depths spanned by individual sporophytes within the water

column. In North America, *Macrocystis* ranges from Alaska to central Baja California (Foster and Schiel, 1985). In the Southern hemisphere, *Macrocystis* is found along the West and Southern East coasts of South America, South Africa and New Zealand. At higher latitudes *Macrocystis* is limited by light, and at lower latitudes the genus is limited by nutrients, warmer temperatures and other algae (Dayton, 1985; Steneck et al., 2002). The congener *M. laevis* has been found at 68 meters depth in the Southern Ocean (Perissinotto and McQuaid, 1992). Several kelp species have been found in tropical waters near the Galapagos (Taylor, 1945). *M. pyrifera* is a subtidal species that spans the water column, reaching heights up to 40-50 meters and thus individuals experience gradients in temperature, light, and nutrients in the vertical dimension as well as the horizontal, or geographic dimension. Other variable factors in the environment include currents and wave exposure, pollution, pH, O_2 and CO_2. La Nina events have been shown to amplify low-oxygen and low-pH events off California (Nam et al., 2011). Nutrients and light are critical for growth and reproduction. Understanding how *M. pyrifera* responds at a molecular level to gradients in physical conditions may help researchers to predict how the species will react to rising ocean temperatures and changes in upwelling that are predicted to accompany climate change in southern California (Bakun, 1990; Diffenbaugh et al., 2004; King et al., 2011; Doney et al., 2012).

Temperature & Nutrients

There is a strong linear relationship between nitrate and temperature in the southern California nearshore at temperatures below 14.5°C, with colder waters

possessing more nitrate (Kamykowski and Zentara, 1986; Zimmerman and Kremer, 1986; Dayton et al., 1999; Lucas et al., 2011). At temperatures above 14.5°C, nitrate levels are not typically appreciable. While anomalous temperature-nitrate events have been documented in the southern part of *M. pyrifera*'s North American geographic range (Ladah, 2003), in general the relationship between temperature and nitrate concentrations is strong enough to allow estimation of seawater nitrate concentrations from concurrent temperature records. Surface nitrate concentrations are low for most of the year, but increase during the winter when the water column is well mixed (Jackson, 1977). In the summer months, when the surface temperatures rise and nutrient concentrations decrease, kelps begin to die (North and Zimmerman, 1984; Jackson, 1997). Interestingly, parts of kelp below the thermocline (not seen in aerial surveys) usually remain healthy (North and Zimmerman, 1984).

Nitrogen is a primary building block in amino acids, which are used to make proteins that are essential in kelp cellular functioning. Biological processes in *M. pyrifera* affected by nutrients include: recruitment, growth, survivorship, reproductive output, and stress tolerance (Mann, 1973; Jackson, 1977; Zimmerman and Kremer, 1986). Unlike plants, *M. pyrifera* (and other algae) absorb their nutrients from the waters that surround them, not from the soil. Thus, the amount of nutrient exposure can have a large effect on the existence and the condition of a kelp bed.

Potential sources of nutrients for kelps include wind-driven upwelling, upwelling from shoaling internal waves, and terrestrial sources. On the coast of California, where the major winds come from the north, surface water is pushed offshore and deeper and colder nutrient-rich water upwells to replace the water that

moves offshore. In Southern California, this cold-water nutrient input is most pronounced in the spring (McPhee-Shaw et al., 2007; Nam et al., 2011). Internal waves form in late summer when stratification is pronounced (Cudaback and McPhee-Shaw, 2009). In the nearshore (within a few kilometers of the coast), the area of internal wave generation is often the continental shelf break, creating internal waves that propagate across the narrow continental shelf toward shore. These waves mix coastal waters and drive cross-shelf transfer of organic matter and larvae (Pineda, 1991; 1999). Internal waves can bring the phytoplankton-rich chlorophyll maximum layers to the benthos (Witman et al., 1993) as well as deliver cold, nutrient-rich waters to higher light levels (Leichter et al., 2003). Nutrient input from land makes its way to the nearshore via rivers, salt marshes/wetlands, and through anthropogenic run-off. In southern California, the effect of this type of nutrient input is likely greatest during the winter when sporadic storms deliver pulses of rain. Longer time-scale fluctuations like the El Niño Southern Oscillation (ENSO) also change isotherm depth and hence, the supply of nutrients these algae experience, affecting their ability to grow and compete with other kelp species (Zimmerman and Robertson, 1985; Dayton et al., 1999).

The warm water and accompanying low surface nutrient conditions found during the late summer are more pronounced during El Niño years and may be expected to increase with climate change. Hydrographic time series of the upper 500m of the coast of southern California and daily temperature records at Scripps Institution of Oceanography's pier have documented the rise in sea surface temperature over the last several decades (Roemmich, 1992). Climate and wind patterns are likely to change

due to changes in land-sea interactions leading to changes in upwelling (Bakun, 1990; Diffenbaugh et al., 2004; King et al., 2011). As spring (70%) and winter (10%) upwelling provide 80% of total nutrient input in the Southern California Bight (McPhee-Shaw et al., 2007), this could have significant impacts on *Macrocystis* nutrition and health (Doney et al., 2012).

Sunlight and Photosynthesis

Macrocystis pyrifera is a photoautotroph, which means it is capable of using energy from sunlight for the synthesis of organic compounds. The photosynthetically available light for *M. pyrifera* is greatest at the surface and decreases exponentially with depth with ~1% of surface light levels reaching 20m in the kelp forest (Gerard, 1984). Available light shows a seasonal peak in the summer (Dean, 1985). Wavelength-specific attenuation of light (i.e. preferential absorption of red and UV light) in the ocean changes the spectrum of light that reaches the depths and the chlorophyll *c* and accessory pigment complex of brown algae allows for highly efficient conversion of the deepest penetrating blue-green wavelengths. Physiological adaptations of deep *M. pyrifera* blades include higher relative amounts of chlorophyll and fucoxanthin in blades found at 20m as compared to surface blades (Smith and Melis, 1987). Fucoxanthin is a pigment that gives *Macrocystis* its characteristic golden brown color, absorbs light energy for photosynthesis and can protect against photodamage.

Light can be a limiting factor in the depth that kelps can survive (North, 1971). *Macrocystis* requires ~ 0.7 E m^{-2} day^{-1} for growth (Neushul and Haxo, 1963). Light

affects the depth of maximum photosynthetic rate and thus the depth distribution of algae (Gail, 1922). Lower light levels can lead to decreased carbon fixation and growth by *M. pyrifera* blades below the canopy (Towle and Pearse, 1973; Schroeter et al., 1995). Photosynthesis occurs in all parts of *Macrocystis*. Canopy shading by the kelp itself and particulate matter (both organic and inorganic) negatively affects light penetration, leading to decreased carbon fixation and growth by *M. pyrifera* blades (Towle and Pearse, 1973; Dean, 1985). *Macrocystis* forms large canopies and can self-shade with the greatest decrease in irradiance occurring in the top 1m of the water column with irradiances low enough (<200 μE m^2/s) to limit photosynthesis (Gerard, 1984); a 70% decrease in quantum irradiance can occur just under a *M. pyrifera* canopy (Dean, 1985). The highest spatial and temporal variability in the irradiance occurs just beneath the canopy and decreases with increasing depth (Gerard, 1984). Factors that cause the canopies to shift (e.g. the ebb and flow of tides, changing the height of the water column, or strong sub-surface currents) also affect light penetration (Wing et al., 1993). In addition to the thickness of canopy kelp, light reaching algae can be affected by many factors: weather (e.g. clouds), season, time of day, turbidity which varies according to the levels of suspended organic and inorganic matter, and algal blooms (Dean, 1985). While low light limits photosynthesis, excess light can lead to photosystem damage and oxidative stress. In response, algae have adaptations to optimize light absorption under a variable light availability through differential expression of light harvesting complexes, some of which are involved in both light capture and photoprotection (Peers et al., 2009).

Primary production in kelp is largely controlled by light and nutrients. McFarland & Prescott (1959) estimate that kelp forest production is the same magnitude as production from other aquatic ecosystems like coral reefs and marine grass flats. *M. pyrifera* has fast rates of growth, with average elongation rates of 7.1 cm/day (Sargent and Lantrip, 1952) to up to .5 m/day (Clenndenning). Wheeler (1980) estimates a maximum net photosynthetic rate of 1040 nmol $0_2/cm^2hr$, and general productivity estimates range from 350-1500 gC/m^2y (Dayton, 1985). The kelp forest ecosystem has higher turnover rates than other productive terrestrial systems (Smith, 1981). The majority of photosynthesis occurs in the surface canopy with half of the standing crop lying between the surface and 1.5 m as fronds reach and spread along the surface (McFarland and Prescott, 1959; Towle and Pearse, 1973; Gerard, 1986). The daily increase in dry weight of growing tip (i.e. apical region) is greater than the products of its photosynthesis; additionally, blades further down the stipe have rates of photosynthesis that exceed their rate of growth, implying a need for transport of materials (Sargent and Lantrip, 1952).

M. pyrifera is the largest known seaweed, yet does not possess a vascular system as in plants to support such a large structure. Instead, *M. pyrifera* translocates material through sieve elements, specialized conducting cells with large pores and large numbers of mitochondria (Oliver, 1887; Sykes, 1908; Sargent and Lantrip, 1952; Parker and Huber, 1965). The composition of sieve tube sap is ~65% mannitol, a major storage carbohydrate, and 15% amino acids, which may represent the transported form of nitrogen (Parker, 1966; Manley, 1983). Other storage carbohydrates in kelp include alginic acid, laminarin and fucoidin (Bidwell and

Ghosh, 1962). This is another major difference compared to plants, which use cellulose, starch, D-glucose, D-fructose, sucrose. Radiolabeled ^{14}C experiments have shown the movement of carbon assimilates along the stipe axis (Schmitz and Srivastava, 1979). There is a source-sink relationship where movement of carbon assimilate flows from older fronds toward younger developing fronds (Sargent and Lantrip, 1952). This transport has a velocity of 0.5 m/hr along the length of the stipe and has been shown to move both upward and downward depending on the starting location of the ^{14}C input and location of nearest carbon sink. Additionally, carbon dioxide is not the main source of inorganic carbon for algae as it is for terrestrial plants, instead algae rely primarily on the bicarbonate form (HCO_3^-) since they inhabit an aquatic environment. Therefore, we might expect that the delivery of CO_2 to rubisco will resemble that of unicellular algae instead of plants.

Transcriptomics: a Tool for Physiological Study

The water-column spanning *M. pyrifera* lives in a highly variable physical environment and spans gradients in light, temperature and nutrients. It is important to consider the time and space scales of hydrographic variation (Chapter 3) in order to understand and appropriately measure the time and space scales of kelp response. For example, during summer months and El Niño years, temperatures rise, nutrients decrease, and ultimately kelp densities decrease (Jackson, 1977). These die-offs are the final result of the sum of integrated physiological responses over time. However, it is unknown how kelps are responding on a cellular level at much shorter time scales of minutes to hours. Changes in gene expression are a preliminary step in changing

the physiological state of an organism and can vary with external environmental conditions, such as variations in nutrients or changes in temperature. One way to take a "snapshot" of the physiological status of an organism is by looking at its transcriptome.

The transcriptome is the set of all messenger RNA molecules, or transcripts, and thus represents the genes that are being expressed at any given time. In comparison, the genome is the collection of all possible genes, whether expressed or not. Sequencing only the expressed genes or expressed sequence tags (ESTs) is a lower cost alternative to whole genome sequencing and is useful in gene discovery, genome annotation, gene structure identification, single nucleotide polymorphism (SNP) characterization and phylogenomic analysis (Adams et al., 1991; Nagaraj et al., 2006; Dunn et al., 2008). RNA-Seq is the direct sequencing of complementary DNA (cDNA) using high-throughput technologies yielding a large quantity of data (i.e. millions of sequences), which allows for quantitative surveys of the transcriptome using density of reads. An organism's transcriptome coverage can vary greatly from the genome because not all genes are expressed at a given time or developmental stage. This approach is not limited to analyses of *a priori* defined regions of a genome; gene discovery and expression profiling are achieved via the same experiment. One example of global transcriptome profiling in algae comes from a recent study that examined the transcriptome response of the red seaweed *Chondrus crispus* to light, temperature, and salt stress in order to identify key stress genes and distinguish the most important natural stressors (Collén et al., 2007). In Chapter 2, I

discuss how transcriptional units derived from sequence-based data can be applied to evolutionary and ecological study.

Due to the lack of available genomic data for the giant kelp, and the desire to understand and develop the tools necessary to understand how *M. pyrifera* is able to contend with a variable environment, I set out to increase the number of transcriptional units for this species. Through transcriptional profiling of *M. pyrifera,* we created a sequence-based tool kit for future physiological study of this species to examine changes in metabolic function in individuals spanning environmental gradients with depth. I use two different sequencing technologies for generating transcriptomic data for *M. pyrifera:* the Roche 454 platform (Chapter 4) and the Illumina Genome Analyzer IIx platform (Chapter 5). These two platforms differ in their amplification approach and sequencing chemistries, read lengths and amount of data generated, as well as cost (Shendure and Ji, 2008; Wilhelm and Landry, 2009; Metzker, 2010).

In brief, the 454 pyrosequencing begins with water-in-oil emulsion based PCR where a droplet containing bead-bound primers bind a DNA template that is then clonally amplified. The beads with DNA are then placed into microtiter wells filled with packing beads. For the sequencing reaction, the different nucleotides are washed over the sample and as individual nucleotides are incorporated into DNA, a luciferase enzyme generates flashes of light. A higher intensity indicates incorporation of multiple nucleotides, also known as homopolymer runs. The most common error for this platform is insertion or deletion errors resulting from inaccuracies in resolving long homopolymer runs. In the case of *M. pyrifera*, the 454 platform was initially

attractive because of the long reads generated which aids in assembly when there is no reference genome.

For the Illumina platform, in a process called bridge amplification, single-stranded DNA fragments with ligated adapters are washed over and bind randomly to primers attached to the surface of a flow cell. Nucleotides are added and repeated denaturation and extension conditions result in localized clusters of amplified DNA fragments. Sequencing proceeds by adding four labeled reversible terminators and fluorescence is recorded upon incorporation. The process is repeated and the identity of each base is recorded based on the fluorescent signal. DNA is extended one nucleotide at a time. The most common error type for the Illumina platform is substitution. Illumina has a much lower cost per Mb than the 454 and generates orders of magnitude more sequence data making a it logical choice to continue our transcriptomic analysis of *M. pyrifera*.

Structure of the Dissertation

In addition to this introduction, this dissertation contains one review chapter, three empirical data chapters, concluding remarks and two appendices. Each chapter is intended to stand alone as a publishable unit. As such, the reader may encounter some redundancy in the introduction and methods.

Chapter 2: Brown Algal Genomics

The brown algae (Phaeophyceae) are a complex multicellular group divergent from other eukaryotes with interesting evolutionary and ecological features and

biotechnological applications. This chapter reviews the current state of genomic knowledge for the Phaeophyceae and discusses how this type of information can be applied to address ecological questions. The current trend of rapidly increasing genomic information provides an opportunity to expand our knowledge in these areas.

Aims and Objectives are to:

2.1 Review the evolutionary and ecological features and biotechnological applications of members of the Phaeophyceae

2.2 Assess the current state of genomic knowledge for this group

2.3 Review examples of sequence-based data being applied to evolutionary and ecological questions to demonstrate the potential for knowledge discovery in the brown algae

Chapter 3: Vertical distribution of *Macrocystis pyrifera* nutrient exposure in southern California

Depth-specific variations in temperature and therefore nutrients occur on a variety of time scales and the vertical distribution of these factors can vary spatially within a kelp bed, with biologically important consequences for *M. pyrifera*. This chapter examines variability in nutrient and temperature climate through time (emphasizing depth differences) in a single kelp bed using an ~4 year thermistor string time series (depths: 0, 2, 6, 10, 14, and 18 meters above the bottom) at two locations in the La Jolla kelp forest. We found that while coherence patterns were similar within a kelp bed, the vertical distributions of temperature and nutrients can vary dramatically across the vertical span of individual kelps. We estimate potential productivity from nutrient availability and find values consistent with published accounts of biological

productivity for kelps. We also show that the amount of nutrient exposure along the length of a *M. pyrifera* individual as calculated by temperature fluctuations can vary by several meters over time scales as short as minutes to hours. The discussion examines various temporal (interdecadal, interannual, seasonal, daily) and spatial scales (geographic range edges, kelp bed, within water column/individual) of nutrient variability focusing on the response of *M. pyrifera*. In order to develop tools to look at kelp physiological state in relation to short-time scale events such as internal waves and before longer term outward signs of stress (sloughing tissue, die-offs, etc.) become apparent, we needed to have sequencing information (see Chapters 4 & 5). This chapter provides the environmental context for why a large-scale transcriptomic effort is appropriate for this *M. pyrifera*.

Aims and Objectives are to:

3.1 Compare the water-column (i.e. depth-specific) variation in temperature and therefore nutrients at two locations in a single kelp forest through time

3.2 Identify the dominant time scales of temperature and nutrient variations

3.3 Calculate water-column integrated nitrate through time and use that to estimate the upper bound of productivity

Chapter 4: Transcriptomic analysis of metabolic function in the giant kelp, *Macrocystis pyrifera*

Through transcriptional profiling of the giant kelp, *M. pyrifera,* we created a sequence-based tool kit for future physiological study of this species and demonstrate changes in metabolic function in individuals spanning environmental gradients with

depth. To obtain a diversity of transcripts, I sequenced four cDNA libraries: a wintertime surface, wintertime 18m depth, summertime surface, and summertime 18m depth sample. The raw sequences were filtered, assembled, annotated, and examined for expression. From the sequencing, we developed tools to look at specific genes using quantitative PCR demonstrating the utility for future physiological studies. We observed patterns of high expression of 'stress' genes and light harvesting complexes in the surface samples. We also found evidence of the phylogenetic clade LI818 known in green algae to be highly responsive to high light (Peers et al., 2009). Genes involved in nutrient acquisition showed up-regulation at depth. The differentiation of function with depth matches patterns seen in physical parameters.

Aims and Objectives are to:

4.1 Increase the number of identified transcriptional units for *M. pyrifera*

4.2 Create a sequence-based tool kit for future physiological study of this species

4.3 Compare gene expression in *M. pyrifera* blades collected at the surface and at depth in two seasons

Chapter 5: Expression patterns with depth in the giant kelp, *Macrocystis pyrifera*

Through the creation of a genomic resource for *Macrocystis pyrifera*, an ecologically important but non-model species, we explore variability in gene expression with depth across a natural environmental gradient. This chapter explores finer scale (compared to top/bottom differences seen in Chapter 4) depth-related patterns in the global transcriptome of *M. pyrifera* across biologically relevant

gradients in light, temperature and nutrients. From a single water-column spanning individual (during summer-time stratified conditions), RNA was extracted from blades collected every 3m from the surface to 18m depth. Three technical replicates for each of the seven depth samples were prepared for cDNA library construction and sequenced on the Illumina Genome Analyzer IIx platform. This yielded 508 million reads of 45 Gbp total sequence which assembled into ~370,000 contigs, of which 8-14% were annotatable via alignment based approaches (e.g. BLAST), greatly expanding the number of identified transcriptional units for this species and enabling the creation of tools for future studies of the molecular physiology of *M. pyrifera*. We see high reproducibility between the technical replicates and distinct grouping by depth from expression profile clustering. Photosynthesis and related pathways showed highest expression levels in the shallow depths, compared to degradation processes at depth.

Aims and Objectives are to:

5.1 Compare gene expression in *M. pyrifera* blades from depths spanning water column gradients in light, temperature and nutrients

5.2 Increase the number of identified transcriptional units for *M. pyrifera* through expanded transcriptomic coverage

Appendices

Appendix 1: Carbon and nitrogen stable isotope patterns with depth in *Macrocystis pyrifera*

Consistent patterns of negative correlations of both $\delta^{13}C$ and $\delta^{15}N$ values with depth in *Macrocystis pyrifera* blades along a stipe were seen in three locations along

the California coastline during the summer; depth-dependent variation was not observed during the winter in La Jolla. $\delta^{13}C$ and $\delta^{15}N$ were positively correlated. Higher $\delta^{13}C$ values near the surface may be due to increased rates of photosynthesis due to higher light availability, thus altering the balance of CO_2 vs. HCO_3^- incorporation (Simenstad et al., 1993). The lower $\delta^{15}N$ values at depth likely reflect oceanic nitrate values and higher values in the surface may be due to recycling of nitrogen or an alternate nitrogen source. The observed patterns warrant further investigation.

Aims and Objectives are to:

A1.1 Explore patterns in $\delta^{13}C$, $\delta^{15}N$, percent carbon, and percent nitrogen of *M. pyrifera* with depth through different seasons at several locations

Appendix 2: Preliminary investigations into the bacteria associated with the blades of *M. pyrifera*

Microorganisms are abundant in the marine environment, occupying both the water column and surfaces of microorganisms. There is rising interest in algal-microbe interactions in recent years (Goecke et al., 2010). These symbioses can affect the kelp physiology, either negatively or positively. The composition and roles of the *Macrocystis*-associated microbial community remains largely unstudied. The first step in being able to explore ecological questions related to *Macrocystis*-microbe interactions is to identify the microbes present. Scanning electron microscopy and culture-based approaches identified bacterial morphotypes and taxa associated with *M.*

pyrifera blades. Several culture-independent bacterial DNA extraction protocols were evaluated.

Aims and Objectives are to:

A2.1 Confirm the presence of bacteria living on blades of *M. pyrifera*

A2.2 Identify taxonomically bacteria capable of growing on a mannitol-based carbon source that were isolated from *M. pyrifera* blades

A2.3 Evaluate several methods for *M. pyrifera*-associated bacteria DNA extraction for future culture-independent studies

References

Adams, M., Kelley, J., Gocayne, J., Dubnick, M., Polymeropoulos, M., Xiao, H., Merril, C., Wu, A., Olde, B., Moreno, R., et al. (1991). Complementary DNA sequencing: expressed sequence tags and human genome project. Science *252*, 1651–1656.

Bakun, A. (1990). Global climate change and intensification of coastal ocean upwelling. Science *247*, 198–201.

Bidwell, R.G.S., and Ghosh, N.R. (1962). Photosynthesis and metabolism in marine algae: IV. The fate of C^{14}-mannitol in *Fucus Vesiculosus*. Canadian Journal of Botany *40*, 803–807.

Clenndenning, K. Photosynthesis and general development. In The Biology of Giant Kelp Beds (*Macrocystis*) In California, W. North, ed. (Beihefte Zur Nova Hedwigia), pp. 169–190.

Collén, J., Marsollier, I.G., Léger, J., and Boyen, C. (2007). Response of the transcriptome of the intertidal red seaweed *Chondrus crispus* to controlled and natural stresses. New Phytologist *176*, 45–55.

Coyer, J., Smith, G., and Anderson, R. (2001). Evolution of *Macrocystis* spp. (Phaeophyceae) as determined by ITS1 and ITS2 sequences. Journal of Phycology *37*, 574–585.

Coyer, J.A., Peters, A.F., Hoarau, G., Stam, W.T., and Olsen, J.L. (2002). Hybridization of the marine seaweeds, *Fucus serratus* and *Fucus evanescens* (Heterokontophyta: Phaeophyceae) in a 100-year-old zone of secondary contact. Proceedings of the Royal Society B: Biological Sciences *269*, 1829–1834.

Cudaback, C., and McPhee-Shaw, E. (2009). Diurnal-period internal waves near Point Conception, California. Estuarine, Coastal and Shelf Science *83*, 349–359.

Dayton, P., Tegner, M., Edwards, P., and Riser, K. (1999). Temporal and spatial scales of kelp demography: The role of oceanographic climate. Ecological Monographs *69*, 219–250.

Dayton, P.K. (1985). Ecology of kelp communities. Annual Review of Ecology and Systematics *16*, 215–245.

Dean, T. (1985). The temporal and spatial distribution of underwater quantum irradiation in a southern California kelp forest. Estuarine, Coastal and Shelf Science *21*, 835–844.

Demes, K.W., Graham, M.H., and Suskiewicz, T.S. (2009). Phenotypic plasticity reconciles incongruous molecular and morphological taxonomies: the Giant Kelp, Macrocystis (Laminariales, Phaeophyceae), is a monospecific genus. Journal of Phycology *45*, 1266–1269.

Diffenbaugh, N., Snyder, M., and Sloan, L. (2004). Could CO_2-induced land-cover feedbacks alter near-shore upwelling regimes? Proceedings of the National Academy of Sciences *101*, 27–32.

Doney, S., Ruckelshaus, M., Duffy, J., Barry, J., Chan, F., English, C., Galindo, H., Grebmeier, J., Hollowed, AB, Knowlton, N., et al. (2012). Climate change impacts on marine ecosystems. Annual Review of Marine Science *4*, 11–37.

Douzery, E., Snell, E., Bapteste, E., Delsuc, F., and Philippe, H. (2004). The timing of eukaryotic evolution: does a relaxed molecular clock reconcile proteins and fossils? Proceedings of the National Academy of Sciences *101*, 15386–15391.

Druehl, L., and Saunders, G. (1992). Molecular explorations in kelp evolution. Progress in Phycological Research *8*, 47–83.

Druehl, L.D. (1978). The distribution of *Macrocystis integrifolia* in British Columbia as related to environmental parameters. Canadian Journal of Botany *56*, 69–79.

Duncan, M., and Foreman, R. (1980). Phytochrome-mediated stipe elongation in the kelp *Nereocystis* (Phaeophyceae). Journal of Phycology *16*, 138–142.

Dunn, C., Hejnol, A., Matus, D., Pang, K., Browne, W., Smith, S., Seaver, E., Rouse, G., Obst, M., Edgecombe, G., et al. (2008). Broad phylogenomic sampling improves resolution of the animal tree of life. Nature *452*, 745–749.

Foster, M.S., and Schiel, D.R. (1985). Ecology of giant kelp forests in California: a community profile (U.S. Fish & Wildlife Services Biological Report).

Gail, F. (1922). Photosynthesis in some of the red and brown algae as related to depth and light. Publications - Puget Sound Biological Station *3*, 177–193.

Gerard, V. (1984). The light environment in a giant kelp forest: influence of *Macrocystis pyrifera* on spatial and temporal variability. Marine Biology *84*, 189–195.

Gerard, V. (1986). Photosynthetic characteristics of the giant kelp (*Macrocystis pyrifera*) determined *in situ*. Marine Biology *90*, 473–482.

Goecke, F., Labes, A., Wiese, J., and Imhoff, J. (2010). Chemical interactions between marine macroalgae and bacteria. Marine Ecology Progress Series *409*, 267–300.

Hurd, C. (2000). Water motion, marine macroalgal physiology and production. Journal of Phycology *36*, 453–472.

Hurd, C., Harrison, P., and Druehl, L. (1996). Effect of seawater velocity on inorganic nitrogen uptake by morphologically distinct forms of *Macrocystis integrifolia* from wave-sheltered and exposed sites. Marine Biology *126*, 205–214.

Jackson, G. (1977). Nutrients and production of giant kelp, *Macrocystis pyrifera*, off southern California. Limnology and Oceanography *22*, 979–995.

Jackson, G. (1997). Currents in the high drag environment of a coastal kelp stand off California. Continental Shelf Research *17*, 1913–1928.

Kamykowski, D., and Zentara, S.-J. (1986). Predicting plant nutrient concentrations from temperature and sigma-*t* in the upper kilometer of the world ocean. Deep Sea Research *33*, 89–105.

King, J., Agostini, V., Harvey, C., McFarlane, G., Foreman, M., Overland, J., DiLorenzo, E., Bond, N., and Aydin, K. (2011). Climate forcing and the California Current ecosystem. ICES Journal of Marine Science *68*, 1199–1216.

Ladah, L.B. (2003). The shoaling of nutrient-enriched subsurface waters as a mechanism to sustain primary productivity off Central Baja California during El Niño winters. Journal of Marine Systems *42*, 145–152.

Leichter, J., Stewart, H., and Miller, S. (2003). Episodic nutrient transport to Florida coral reefs. Limnology and Oceanography *48*, 1394–1407.

Lucas, A., Dupont, C., Tai, V., Largier, J., Palenik, B., and Franks, P. (2011). The green ribbon: Multiscale physical control of phytoplankton productivity and community structure over a narrow continental shelf. Limnology and Oceanography *56*, 611–626.

Mackenzie, I. (1997). Genetic and morphological variation in *Macrocystis* C. Agardh (Laminariales, Phaeophyceae) of the North American coast. Simon Fraser University.

Manley, S. (1983). Composition of sieve tube sap from *Macrocystis pyrifera* (Phaeophyta) with emphasis on the inorganic constituents. Journal of Phycology *19*, 118–121.

Mann, K. (1973). Seaweeds: their productivity and strategy for growth. Science *182*, 975–981.

Mayr, E. (1969). The biological meaning of species. Biological Journal of the Linnean Society *1*, 311–320.

McFarland, W., and Prescott, J. (1959). Standing crop, chlorophyll content and *in situ* metabolism of a Giant Kelp community in Southern California. Publications of the Institute of Marine Science *6*, 109–132.

McPhee-Shaw, E., Siegel, D., Washburn, L., Brzezinski, M., Jones, J., Leydecker, A., and Melack, J. (2007). Mechanisms for nutrient delivery to the inner shelf: Observations from the Santa Barbara Channel. Limnology and Oceanography *52*, 1748–1766.

Metzker, M.L. (2010). Sequencing technologies — the next generation. Nature Reviews Genetics *11*, 31–46.

Moustafa, A., Beszteri, B., Maier, U., Bowler, C., Valentin, K., and Bhattacharya, D. (2009). Genomic footprints of a cryptic plastid endosymbiosis in diatoms. Science *324*, 1724.

Nagaraj, S.H., Gasser, R.B., and Ranganathan, S. (2006). A hitchhiker's guide to expressed sequence tag (EST) analysis. Briefings in Bioinformatics *8*, 6–21.

Nam, S., Kim, H., and Send, U. (2011). Amplification of hypoxic and acidic events by La Niña conditions on the continental shelf off California. Geophysical Research Letters *38*, L22602.

Neushul, M., and Haxo, F.T. (1963). Studies on the Giant Kelp, *Macrocystis* I. Growth of Young Plants. American Journal of Botany *50*, 349–353.

North, W. (1971). The biology of giant kelp beds (Macrocystis) in California (Beihefte Zur Nova Hedwigia, Heft).

North, W., and Zimmerman, R. (1984). Influences of macronutrients and water temperatures on summertime survival of *Macrocystis* canopies. Hydrobiologia *116/117*, 419–424.

Oliver, F. (1887). On the obliteration of the sieve-tubes in Laminarieae. Annals of Botany *1*, 95–117.

Parker, B. (1966). Translocation in *Macrocystis*. III. Composition of sieve tube exudate and identification of the major C^{14}-labeled products. Journal of Phycology *2*, 38–41.

Parker, B.C., and Huber, J. (1965). Translocation in *Macrocystis*. II. Fine structure of the sieve tubes. Journal of Phycology *1*, 172–179.

Peers, G., Truong, T., Ostendorf, E., Busch, A., Elrad, D., Grossman, A., Hippler, M., and Niyogi, K. (2009). An ancient light-harvesting protein is critical for the regulation of algal photosynthesis. Nature *462*, 518–522.

Perissinotto, R., and McQuaid, C. (1992). Deep occurrence of the giant kelp *Macrocystis laevis* in the Southern Ocean. Marine Ecology Progress Series *81*, 89–95.

Pineda, J. (1991). Predictable upwelling and the shoreward transport of planktonic larvae by internal tidal bores. Science *253*, 548–551.

Pineda, J. (1999). Circulation and larval distribution in internal tidal bore warm fronts. Limnology and Oceanography *44*, 1400–1414.

Roemmich, D. (1992). Ocean warming and sea level rise along the southwest U.S. coast. Science *257*, 373–375.

Sanbonsuga, Y., and Neushul, M. (1978). Hybridization of Macrocystis (Phaeophyta) with other float-bearing kelps. Journal of Phycology *14*, 214–224.

Sargent, M., and Lantrip, L. (1952). Photosynthesis, growth and translocation in Giant Kelp. American Journal of Botany *39*, 99–107.

Schmitz, K., and Srivastava, L. (1979). Long distance transport in *Macrocystis integrifolia*. I. translocation of ^{14}C-labeled assimilates. Plant Physiology *63*, 995–1002.

Schroeter, S., Dean, T., Thies, K., and Dixon, J. (1995). Effects of shading by adults on the growth of blade-stage *Macrocystis pyrifera* (Phaeophyta) during and after the 1982-1984 El Nino. Journal of Phycology *31*, 697–702.

Setchell, W. (1932). *Macrocystis* and its holdfast. University of California Publications in Botany *16*, 445–492.

Shendure, J., and Ji, H. (2008). Next-generation DNA sequencing. Nature Biotechnology *26*, 1135–1145.

Simenstad, C.A., Duggins, D.O., and Quay, P.D. (1993). High turnover of inorganic carbon in kelp habitats as a cause of delta^{13}C variability in marine food webs. Marine Biology *116*, 147–160.

Smith, B., and Melis, A. (1987). Photosystem stoichiometry and excitation distribution in chloroplasts from surface and minus 20 meter blades of *Macrocystis pyrifera*, the giant kelp. Plant Physiology *84*, 1325–1330.

Smith, S. (1981). Marine macrophytes as a global carbon sink. Science *211*, 838–840.

Steneck, R., Graham, M., Bourque, B., Corbett, D., Erlandson, J., Estes, J., and Tegner, M. (2002). Kelp forest ecosystems: biodiversity, stability, resilience and future. Environmental Conservation *29*, 436–459.

Sykes, M. (1908). Anatomy and histology of *Macrocystis pyrifera* and *Laminaria saccharina*. Annals of Botany *22*, 291–325.

Taylor, W. (1945). Pacific marine algae of the Allen Hancock Expeditions to the Galapagos Islands.

Towle, D., and Pearse, J. (1973). Production of the giant kelp, *Macrocystis*, estimated by in situ incorporation of ^{14}C in polyethylene bags. Limnology and Oceanography *18*, 155–159.

Wilhelm, B.T., and Landry, J.-R. (2009). RNA-Seq-quantitative measurement of expression through massively parallel RNA-sequencing. Methods *48*, 249–257.

Wing, S., Leichter, J., and Denny, M. (1993). A dynamic model for wave-induced light fluctuations in a kelp forest. Limnology and Oceanography *38*, 396–407.

Witman, J., Leichter, J., Genovese, S., and Brooks, D. (1993). Pulsed phytoplankton supply to the rocky subtidalzone: Influence of internal waves. Proceedings of the National Academy of Sciences *90*, 1686–1690.

Zimmerman, R., and Kremer, J. (1986). In situ growth and chemical composition of the giant kelp, *Macrocystis pyrifera*: response to temporal changes in ambient nutrient availability. Marine Ecology Progress Series *27*, 277–285.

Zimmerman, R., and Robertson, D. (1985). Effects of El Niño on local hydrography and growth of the giant kelp, *Macrocystis pyrifera,* at Santa Catalina Island, California. Limnology and Oceanography *30*, 1298–1302.

CHAPTER 2

Brown Algal Genomics

Abstract

The Phaeophyceae are a complex multicellular group divergent from other eukaryotes with interesting evolutionary and ecological features and biotechnological applications. Genomic knowledge for the Phaeophyceae is limited with only one member with a sequenced genome (e.g. *Ectocarpus siliculosus*), yet ORF-level clustering of available information reveals novel clusters distinct from their closest relatives. I discuss how this sequence-based information can be used to develop tools that can address evolutionary and ecological questions. The current increasing trend in genomic information provides an opportunity to expand our knowledge of this group.

Characteristics and Importance of Brown Algae (Phaeophyceae, Heterokonts)

The Stramenopiles are thought to be a product of secondary endosymbiosis and thus possess a polyphyletic evolutionary history. In this evolutionary development, a protist likely engulfed a red alga, itself a product of an initial endosymbiosis of a cyanobacterium by a protist (Moustafa et al., 2009). Therefore, examining the genetic make-up of the brown algae, we must consider the nuclear and organelle (i.e. chloroplast and mitochondria) genomes of the heterotrophic eukaryote, and the primary and secondary photosynthetic endosymbionts (Bhattacharya et al., 2003; Archibald, 2005; Keeling et al., 2005; Moustafa et al., 2009). Evidence of secondary endosymbiosis exists in plastids with the presence of three or four membranes and sometimes the remnant nucleus of the algal symbiont called a nucleomorph (Bhattacharya et al., 2003). Another trait of secondary endosymbiosis is the presence of a signal sequence on the N-terminus of a protein to ensure passage across the multiple membranes. Sequence-based information and comparison with known groups can help resolve these evolutionary contributions.

Stramenopiles (or Heterokonts) are a major lineage of eukaryotes, which span seven orders of magnitude in size. The Stramenopiles are thought to have diverged from other major eukaryotic groups ~1 billion years ago and contain the brown algae, diatoms, Oomycetes and some protists (Douzery et al., 2004). Stramenopiles are characterized by the presence of two unequal flagella in their motile life cycle stage, plastids with four membranes (as a result of secondary endosymbiosis), lamellae with three stacked thylakoids, chlorophylls *a* and *c* and ß-1,3-linked carbohydrates. The Class Phaeophyceae (e.g. the brown algae) falls within the Stramenopile lineage and

thus possesses the features described above as well as other unique features, including the ability to form complex multicellular thalli. Class Phaeophyceae includes 1784 recognized species (Guiry, 2012), ranging from microscopic filaments to the largest alga on earth, the giant kelp, *Macrocystis pyrifera* (Figure 2.1). The Phaeophyceae are morphologically diverse, containing both benthic and pelagic forms (e.g. *Sargassum,* Figure 2.1) and have adapted to a variety of environments worldwide, from the polar regions to the tropics. They are mostly marine and found in coastal waters though some freshwater species exist (e.g. *Sphacelaria* and *Herbaudiella*). The intertidal Phaeophytes are dominated by the Fucoids and the subtidal by the Laminariales (i.e. the kelps). The Phaeophyceae is an important group for evolutionary, ecological and economic reasons.

Evolutionary Importance

Only five eukaryotic lineages have independently evolved multicellularity; these are animals, fungi, green plants, red algae, and chromalveolates (which include the Stramenopiles as well as Alveolates (Peters et al., 2004; Keeling et al., 2005). Phaeophytes are evolutionarily distant from other photoautotrophs, thus the applicability of results learned from model species such as the plant *Arabidopsis* remain somewhat limited for this group. The Stramenopiles are very distantly related to other multicellular photoautotrophs (i.e. plants and red algae); therefore, this is a unique group in which to examine differences in physical structure, communication between multiple cells, and photochemistry. For example, metabolite transfer in Stramenopiles between the cytosol and plastids crosses four membranes; this is not the

case for plants. It has been suggested that the element iodine played a key role in the emergence of multicellularity, helping organisms counteract the cellular generation of toxic reactive oxygen species corresponding with the emergence of photosynthesis; kelps accumulate iodine to higher concentrations than any other living organism, at levels up to 30,000 fold higher than the environment (Kupper et al., 1998; 2008; La Barre et al., 2010). The development of extracellular matrix is another feature related to the transition to multicellularity. Brown algal cell wells have components from a variety of evolutionary events: cellulose (in common with plants; inherited from a red algal symbiont); sulfated fucans (common with animals; ancestral origin); and alginates (from horizontal gene transfer from an Actinobacterium) (Michel et al., 2010b). D-mannitol and laminarin (β-1,3-glucan) are the primary storage carbohydrate of brown algae as compared to the α-1,4-glucans (glycogen or starch) of most living organisms (Michel et al., 2010a). These sorts of evolutionary novelties and biotechnologically relevant chemistries in the Phaeophyceae are beginning to be discovered through comparative studies with *Ectocarpus siliculosus*, the first brown algae to have its genome sequenced, and other current databases (Cock et al., 2010).

Ecological Importance

The Phaeophytes are ecologically important members of the coastal environment. Like other algae and plants, they are photosynthetic and contribute significantly to global primary production (Smith, 1981). Kelp forests are thought to be among the most productive ecosystems on the planet with estimated production of

6.8 gC/m^2day. (Towle and Pearse, 1973). Their golden color comes from the carotenoid pigments fucoxanthin and violaxanthin found in their plastids in addition to chlorophyll *a, c1 c2* that allows them to exploit the deepest penetrating blue-green wavelengths of light, expanding their photosynthetic niche. Brown algal primary production fuels intertidal and subtidal ecosystems and provides a food source for fish and invertebrates with the majority of material being utilized by detritivores and decomposers. Some Phaeophyceae, notably the giant kelp, provide habitat for other species from their physical structure. The morphology of the brown algae ranges from the simplest forms (i.e. branching filaments), to encrusting or calcareous forms, to the specialized tissues and structural complexity found in the kelps (Order Laminariales) (Figures 2.1 & 2.2). For example, *Macrocystis pyrifera* possesses specialized conducting cells with large pores and large numbers of mitochondria called sieve tube cells which have the ability to translocate material including mannitol and amino acids (Sykes, 1908; Manley, 1983).

Economic Importance

The brown algae are also economically important as food or as source for alginate extraction and currently, the United States depends on imports from other countries (Roesijadi et al., 2010). The entire seaweed industry (i.e. Phaeophyta, Rhodophyta and Chlorophyta) has an annual total value of production of almost 6 billion US Dollars as of 2001 (McHugh, 2003). China has the largest edible seaweed production, followed by the Republic of Korea and Japan (McHugh, 2003). Brown algae possess a high lipid content and long chain poly unsaturated fatty acids

(Eichenberger et al., 1993). Attractive qualities for human consumption include high protein content, low fat content, and many vitamins and minerals. Edible Phaeophyceae species include: *Laminaria* (kombu/haidai), *Undaria* (wakame/quandai-cai); *Hizikia, Cladosiphon* (Mozuku) and *Alaria* (McHugh, 2003). There is also a market for animal feed as well, especially in Norway, where brown seaweeds are collected, dried and milled, and used for sheep, cattle, and horses (McHugh, 2003). Also, alginates (discussed below) are used to coagulate fish feed and help to keep it from dissolving in water.

As of 2001, the market value of alginate products derived from brown algae was USD $195 million (McHugh, 2003). Brown algae used for alginate production are harvested from natural populations rather than cultivated due to expense. Alginate is found in cell walls of brown algae and contributes to their flexibility in the dynamic intertidal and subtidal zones. Attractive properties of sodium alginate include the ability to increase viscosity of aqueous solutions and form gels that do not melt when heated (McHugh, 2003). The extent of these properties varies depending on the species of brown algae. Alginates improve a whole suite of products including cosmetics, beer, medical wound dressings and textile printing inks (McHugh, 2003). Other commercial uses of algae include use as a crop fertilizer, where it is mixed into the soil and allowed to compost, resulting in increased moisture retention and addition of trace metals. This method does not supply phosphorous to the same extent as chemical fertilizers, but is attractive for organic farming and home gardening (McHugh, 2003). Chemical properties of brown algae are being exploited in other fields including for use in high-capacity batteries (Kovalenko et al., 2011), as a

component in natural and copper-free anti-fouling paint (Pinori et al., 2011), and in toxic metal removal (Davis et al., 2003). During World War I, the extraction of extraction of potash and acetone from *M. pyrifera* was used in the production of gunpowder (Neushul, 1989). Thus, the unique chemistry and metabolisms of this group have great potential biotechnology applications.

Increasing energy costs and decreasing fossil fuel reserves have prompted research into biofuels and microbial fermentation of biomass. In the late 1970s and early 1980s, the feasibility of ocean farms of the fast-growing giant kelp, *M. pyrifera*, for natural gas production was investigated by the United States Congress Office of Technology Assessment (US Congress, 1980). They concluded that macroalgal-based methane production was considered competitive with that of terrestrial biomass, though research efforts were scaled back as fuel costs recovered in the 1980s. Estimates were that a 1 million acre kelp farm could potentially supply 1% of U.S. gas needs at the time. New government initiatives such as the 2007 Energy Independence and Security Act (EISA), which requires the development of domestic supply of diverse biomass feedstocks, have revived interest in macroalgae as a potential contributor to meeting the energy needs of the United States. The marine biomass resource potential is considered "very high," though the infrastructure (i.e. the supply chain for macroalgae-to-biofuels market) and scalability to support such an effort need to be developed further (Roesijadi et al., 2010). Current estimates suggest that to replace 1% of our current domestic gasoline supply needs, the macroalgal production would have to occur at 10.5 times the current worldwide production. However, a very recent breakthrough in genetic engineering has improved the process of

converting brown algal sugars into ethanol and estimates placing macroalgal ethanol productivity at two and five times higher productivity than sugarcane and corn respectively (Wargacki et al., 2012). Previously, the main limitation had been the breakdown of alginates. Wargacki and colleagues engineered a microbial platform for alginate depolymerization and ethanol production by transplanting *Vibrio spendidus* genes for alginate degradation, transport and metabolism into *Escherichia coli*. Attractive properties of brown algae as compared to plants are that they do not contain lignin, a chemical compound found in the cell wall of plants that requires costly thermal or chemical breakdown prior to the fermentation process and because their photosynthetic efficiencies are greater than terrestrial biomass (Roesijadi et al., 2010). Macroalgae are also seen as a promising resource because they do not utilize arable land, fertilizer or freshwater resources and thus do not compete with land-based energy or food crops (Roesijadi et al., 2010).

Sequencing the Brown Algae

Early work on brown algal genetics investigated the count number of chromosomes in brown algae. The results of studies provided evidence for polyploidy, were used to distinguish closely related species, and to elucidate the alternation of generations (Cole, 1967; Lewis, 1996). Sequence based studies started with the analysis of individual gene sequences (e.g. SSU rRNA, cytochrome oxidase subunit 1, internal transcribed spacer regions). These are used to create phylogenies and in population studies, or to assay specific physiological genes of interest.

Microarrays extended the physiological assay power by being able to examine the expression of many *a priori* determined genes at a time.

Expressed sequence tag (EST) analysis uses sequencing to identify actively expressed genes in a more cost effective manner compared to whole genome sequencing (Adams et al., 1991). ESTs focus on protein coding sequence by only sequencing the mRNA. This is often the first step in a genomics project and connects sampling conditions with the expression of genes in an organism, and can be used to identify genes for further gene or protein specific studies. In brown algae, ESTs have been used to identify specific genes and expression patterns involved in various processes (e.g. specific life stages or various experimentally manipulated conditions such as stressful light or temperature) (Crepineau et al., 2000; Roeder et al., 2005); determine phylogenetic analysis/evolutionary relationships (Phillips et al., 2008); investigate metabolic processes such as carbon metabolism (Moulin et al., 1999); and develop sequenced based molecular toolkits (Moulin et al., 1999).

Eukaryotic genome sequencing has lagged behind microbial genome sequencing and initial efforts focused on the smaller integrated plastid and mitochondrial genomes. To date (January 2012), there are 168 complete eukaryotic genome projects vs. 2762 for bacteria (Pagani et al., 2012). Of those, only four are Stramenopiles: two diatoms, *Phaeodactylum tricornutum* and *Thalassiosira pseudonana*, a pelagophyte *Aureococcus anophageefferens* and a small filamentous Phaeophyte *Ectocarpus siliculosus*. Recognizing the need for brown algal model species (Waaland et al., 2004), Peters et al. (2004) proposed *Ectocarpus siliculosus* because of its small genome size, rapid life cycle and facility with which laboratory

and genetic approaches can be applied. For a review of the use of *Ectocarpus siliculosus* as a genomic and genetic model, see Charrier et al 2008. The Laminariales and Fucales, though economically and ecologically important, were dismissed on the basis of their large genome sizes and long life cycles which make genetic studies difficult (Peters et al., 2004). However, many of these ecologically important species may possess important pathways or structures (e.g. the sieve tube system) that are not represented in the laboratory model organisms. There are few genomes sequenced from ecologically important species in the marine environment and even fewer analyses from field studies (Dupont et al., 2007). Applications of next generation sequencing in non-model organisms include transcriptome characterization, expression level analyses, assessment of genetic variation, SNP discovery, microsatellite discovery and construction, candidate gene finding and whole genome assembly (Table 2, Ekblom and Galindo, 2010). Sequences will continue to be generated with increasing rapidity especially with widespread use of next generation platforms and thus large quantities of genetic data can be attained affordably, and comparative studies will likely extend beyond the model organisms.

A major assumption of comparative biology is that the more closely two organisms are related, the more they will share molecular, biochemical, and morphological features (Keeling et al. 2005). Comparative studies can identify parts of genes related to morphological and physiological variations. Comparative genomics continues to improve and offers valuable insights with the addition of more reference genomes and more annotated genes. For example, sequencing *Ectocarpus* genome aided the discovery of new protein-kinase families important in multicellular

signaling and features relevant for survival in a stressful intertidal environment including halide metabolism and a variety of light harvesting complexes (Cock et al., 2010).

Comparative Genomics of Available Phaeophyceae Data with Other Algal Groups

To assess the 'uniqueness' of the currently available Phaeophyceae genomic knowledge we compare three scenarios in a cluster-based Venn diagram analysis (Figure 2.3). Venn diagrams display the distribution of clusters sharing 60% sequence identity between a given subset of brown algae and various related groups described below (Li and Godzik, 2006). These clusters group together closely related protein families that share a recent ancestral sequence. Annotations were assigned using phyloDB, a J. Craig Venter Institute internal database, containing all completed and draft algal genomes and all Phaeophyceae EST libraries available in NCBI GenBank. The brown algae category includes information from the *Ectocarpus siliculosus* genome and ESTs for the "other brown" include: *Fucus serratus*, *Fucus vesiculosus*, *Sargassum binderi*, and *Laminaria digitata*. Diatom genomes include *Fragilariopsis cylindrus*, *Phaeodactylum tricornutum, Chaetoceros* sp. RS-19, *Thalassiosira pseudonana*, *Nitzschia* I-146, and *Pseudo-nitzschia granii*. Pelagophyte genomes include *Aureococcus anophagefferens*, and *Pelagomonas calceolata*. Other Stramenopiles genomes include *Phytophthora infestans, Phytophthora ramorum,* and *Phytophthora sojae.* Green genomes include: *Chlamydomonas reinhardtii*, *Volvox carteri, Micromonas* sp. RCC299, *Micromonas pusilla* CCMP1545, *Ostreococcus* sp.

RCC809, *Ostreococcus tauri,* and *Ostreococcus lucimarinus* CCE9901. Red genomes include: *Porphyra haitanensis, Porphyra yezoensis, Cyanidioschyzon merolae,* and *Porphyridium purpureum*.

Figure 2.3a compares the distribution of brown algal clusters with 60% sequence identity to *Ectocarpus* (in the same class), red algae, green algae, or a combined group containing the diatoms, pelagophytes and other stramenopiles. There were 3954 total clusters in the brown algae (not including *Ectocarpus*), 34% of which shared identity with at least one of the other four groups. Of the clusters in the Venn, The highest similarity of clusters in the Venn was with *Ectocarpus* (753), which is related at the class level, followed by the combined group X (153), which is the next most closely related group. The mean size of clusters outside the Venn was three to six-fold smaller than for each of the groups in the Venn. Also, clusters not in the Venn had a much smaller percentage with annotation (14.5% vs. 83.7% to 98.4%). Of the 10 largest brown algal clusters, four did not have any identity matches with a single group in the Venn. Of the 10 largest other brown clusters, 4 were not found in any of the Venn groups. Annotations included several heat shock proteins, ribosomal proteins and a chlorophyll *a/b* binding protein.

Figure 2.3b compares the distribution of clusters that were found in either brown algal EST clusters or *Ectocarpus* (18047) with that of the red algae, green algae, diatoms/pelagophytes and other stramenopiles. Only 6% shared identities with the groups represented in the Venn, indicating that the addition of the genome of *Ectocarpus* greatly expanded the number of known protein families. The highest number of matches was to the most closely related diatom/pelagophyte group. The

outside-Venn cluster size was smaller than the cluster size found in the Venn. Of the 10 largest clusters found in either other brown or *Ectocarpus*, 6 were not found in any of the other groups in the Venn. Annotations of these top 10 included several heat shock proteins, ribosomal proteins, and a chlorophyll *a/b* binding protein.

Figure 2.3c compares the distribution of clusters that were found in both brown algal EST clusters and *Ectocarpus* (977) with that of the red algae, green algae, diatoms/pelagophytes and other stramenopiles; 23% of which shared identity with at least one of the other groups. There were more identity matches with the closer taxonomic groups, the combined diatom/pelagophyte (57) and the other stramenopile group (18). The mean cluster size was again much smaller than the clusters found within the Venn (3.2 vs. 16.6 to 25.7). Of the 10 largest brown algal clusters (*Ectocarpus* and other brown), 4 did not have any identity matches to the groups in the Venn. Annotations of the top 10 included several ribosomal proteins, a chlorophyll *a/b* binding protein, and ABC transporter and WD domain G-beta repeat.

Many currently available brown algal sequences are novel (i.e. not found in related groups) and are not annotatable via comparative approaches. In general, cluster size is smaller when they are not shared with related groups and consequently have a smaller percentage of annotations. Comparisons of the Phaeophyte sequences generated thus far indicate a high level of novel protein discovery in this group.

Developing Sequence-based Tools

We briefly outline the general process of developing sequence based tools and focus on RNA sequence data that yields information on gene expression (i.e. what

genes are up or down regulated under different conditions). Potential applications of expressed sequence data include discovery of new genes and identification of coding regions at a fraction of the cost of complete genome sequencing (Adams et al., 1991).

The Process

(1) Choose and sample your organism. What features make it worth sequencing (e.g. ecologically important, endangered, invasive, etc.)? What conditions or processes (e.g. stress response, ontogeny shifts, environmental gradients) are you interested in?

(2) Extract the RNA or DNA from the algal tissue. For the Phaeophyceae, this can be difficult because of the large quantity of mucus polysaccharides. However, protocols exist for some species (e.g. a protocol *M. pyrifera* RNA extraction can be found in Chapter 4) that can be modified to fit a species of interest. In general, macroalgae are not be limited by biomass for RNA extraction as can be the case for plankton.

(3) Decide on a platform depending on your application and prepare libraries for sequencing. There are commercial kits available and this process takes from one to several days. Trade-offs between sequencing platforms mainly exist in length of reads vs. coverage. Cost, while an important consideration, is becoming less of a limiting factor than in the past. For assembly, longer reads (such as with the Roche 454 platform) can be helpful when there is no reference genome to scaffold onto. For a comparison of the Roche 454 platform and Illumina Genome Analyzer chemistries and features, see Chapter 1 of this dissertation.

(4) Most laboratories and universities do not have their own sequencing facilities, so the actual sequencing is often done off site. Bioinformatic analysis of these large biological datasets sometimes requires collaboration and challenges lie in computer power and time. The steps include quality control, assembly, annotation, and in some cases, read mapping. Quality control steps are sequencing platform dependent. Short reads can then be assembled into contigs (overlapping reads that represent a consensus region). A critical step in the analysis of next generation sequencing is annotation, the process of assigning function to a given sequence. This is most often done using homology based approaches such as Basic Local Alignment Search Tool (BLAST), where the unknown query sequences are compared against databases containing annotated sequences. The utility of this approach, therefore, will depend heavily on the data in the reference database. Problems may arise if the original sequences were mis-annotated, causing a cascading effect that can be difficult to remedy. For annotation of transcriptomic data, where conditions or treatments may be linked to expression data, other approaches for determining unknown function may be used. For example, another form of clustering from that described above (i.e. grouping by similar expression patterns) can assign reads of unknown function with pathways and proteins of known function. These can be used to develop hypotheses to pursue further in a rigorous experimental design.

(5) Sequencing is the first step in identifying genes and determining function and interactions. Once transcriptional units have been identified, they can be used to create markers for specific genes of interest (e.g. primers for specific genes, microarrays) and to design experiments. What scale of response is necessary to

answer your question of interest? Perhaps analysis of one gene might be enough – in that case, simple qPCR experiments would be sufficient, requiring only the development of specific primers for one or several genes. Microarrays can be developed to assess rapidly the expression of tens to thousands of genes. As costs decrease, next generation sequencing of different experimental conditions becomes more realistic. A benefit of this approach is that no prior sequence-based knowledge is needed and expression patterns of unknown genes could provide new areas of the transcriptome to focus studies on.

Tying Genomics with Biology/Ecology

Ecology is the study of the interactions of living organisms with each other and with their environment. Evolution can be thought of as the net consequence of ecological factors acting over many generations. Here we provide a few examples of sequence-based data being applied to ecological and evolutionary questions. The molecular ecology approaches described in other taxonomic groups could easily be adapted for the brown algae.

Elucidating Evolutionary Relatedness

Genomic data can be used to improve resolution of phylogenetic relationships. An increase in sequence data has been shown to resolve incongruence in phylogenies (Rokas et al., 2003). Single genes may not be enough to resolve phylogenies across large groups (due to differences in rates of evolutionary change) and efforts have shifted to multi gene trees to gain a more complete picture. Algae lack a significant

fossil record[1] and often display highly plastic phenotypes, which makes genetic data an appropriate metric to measure evolutionary relationships. For Phaeophyceae, even our single gene data (18S) is lacking (Figure 2.2). Approximately half the orders in Phaeophyceae do not have this sequence data for this one gene available. Reproductive isolation is one designation for defining a species (Mayr, 1969). *Macrocystis angustifolia* has been shown to hybridize with other genera in the Family Laminariaceae: *Pelagophycus* and *Nereocystis* (Sanbonsuga and Neushul, 1978). Hybridization is seen in other Phaeophyte orders as well (Coyer et al., 2002). Determining phylogenetic relationships within brown algae has improved and will continue to improve with recent advances in molecular techniques and sequencing technology (table 14.1, de Reviers and Rousseau, 2007).

The Interaction of Biology and the Environment

How is X responding to Y? In this question, X could be a particular organism or tissue type, and Y could be factors such as changing environmental conditions or exposure to abiotic stressors). Intertidal algae contend with a variable light, temperature, and salinity environment due to changing tidal conditions. To identify genes that may play a role in stress tolerance, gene expression changes resulting from an induced stress can be used. To study desiccation stress in the intertidal Fucoid *Fucus vesiculosus*, researchers used suppression subtractive hybridization (SSH) to examine differences in gene expression (Pearson et al., 2001). This technique is a PCR-amplification approach that identifies differentially expressed transcripts

[1] However, fossil Phaeophyceae have been found in Miocene deposits (B. Parker & Dawson, 1965).

between an experimental condition and a control condition by removing cDNAs of similar abundance. Of the genes they were able to identify by sequence homology with known gene sequences, several chloroplast-encoded transcripts are differentially regulated in desiccated vs. hydrated conditions. Similarly, to identify key stress genes and distinguish the most important stressors in nature for *Chondrus crispus*, a red alga, researchers assessed the transcriptome response of *C. crispus* to high light, high temperature, and hypo- and hyper-osmotic stress using microarrays (Collén et al., 2007). The majority of genes showed differential expression in response to only one stressor. This identifies key stress genes that could be useful for targeted monitoring of those particular stressors in the future. Some genes showed regulation by several stressors, though osmotic stress was found to be the most significant natural stressor in terms of changes in gene expression for this intertidal alga. Another study aimed to understand the reaction of the ecologically important seagrass, *Zostera,* to heat stress predicted with climate change. Researchers compared the heat-stress and recovery transcriptomic profiles of two *Zostera* populations from along their geographic range (Franssen et al., 2011). They use this approach to identify the physiological and genetic basis of thermal tolerances. They suggest that the differences in the recovery transcriptomic patterns may predict how populations adapted to thermal stress. This approach would be worth repeating with the giant kelp, *M. pyrifera*, another ecosystem structuring species. In the future, rapid-response monitoring programs could use sequence-based tools to assess stress levels before phenotypic changes manifest.

Species Interactions

The interplay of symbiotic (beneficial or not) interactions is a key area in ecology. For example, invasive species threaten biodiversity worldwide. Genomics can identify cryptic species and examine population consequences of mixed populations. Have there been multiple invasions or just a single invasion? What are the traits of successful invaders? Booth et al. (2007) reviews how molecular approaches can be used to study invasive seaweeds. Brown algal invaders include *Turbinaria, Sargassum, Ascophyllum* and *Undaria.*

Commercially farmed algae are susceptible to disease (Craigie and Correa, 1996; Woo et al., 2002). *Porphyra,* also known as Nori, has estimated financial losses of 40-60 million USD/year due to disease (Woo et al., 2002). The first step of identifying the pathogens and understanding their mechanism of interaction with the host can be accomplished through the use of sequence-based tools. For example, to gain information on the host genes that are affected by *white spot syndrome virus* in shrimp, researchers examined cDNA microarray of infected vs. non-infected shrimp (Dhar et al., 2003). They identified many cellular genes with differential expression, providing a framework for further studies on infection mechanisms. This approach could be applied to commercially-important algal species and the viruses that have been identified in brown algae to date (Kapp, 1998). Potential future applications include developing transgenic strains with disease resistance.

Predator/prey relationships are another important area of bio-ecological study. Sequencing can help elucidate predator/prey relationships when visual observations are difficult or impossible, by using gene markers employed in gut content analysis.

To identify the prey of the elusive giant squid (*Architeuthis* sp.), PCR-based detection of gut contents was employed (Deagle et al., 2005). Researchers were able to identify the squid's fish prey to species and also found evidence for cannibalism. Applying this approach to algae, one could screen the gut contents of animals found in brown algal habitats to learn who is eating which species. Knowing the full complement of consumers can help with modeling and investigations of top-down affects on algal communities.

Applied Phycology

Genetic transformations, the introduction of foreign DNA into a living organism (genes, promoters, etc.), have been used in terrestrial plant crops to introduce desirable characteristics. This methodology could be applied to select for algal properties of value, for example, high lipid content for fuel or desirable alginate characteristics for other products. Genetic engineering approaches are being developed to improve microalgae as a source of renewable biofuels (Radakovits et al., 2010). There are few examples of successful genetic engineering in Phaeophyceae. For the Phaeophyceae, progress in genetic engineering in *Laminaria japonica*, an economically important algal food crop in China (Qin et al., 1999) has been made, including identification of successful reporter genes and DNA introduction methods. As sequencing costs decline, it may become feasible to sequence whole genomes of valuable genetic lines to identify the genomic diversity and potential areas of the genome to manipulate, as has been done with plants. This is likely to be an expanding area of focus in algae in coming years.

Future Directions

The cost of existing sequencing technologies is decreasing and newer technologies with improved read length, accuracy, and sequence coverage continue to be developed. The acquisition of sequence data is straightforward. It is in the analysis of these large and complex data sets where the challenge lies; bioinformatic support will be needed. As the technology moves forward at an accelerated pace, so too will the tools for bioinformatic analysis. Computational biology is a rapidly progressing field and its importance will increase as we continue to generate more sequences. Many universities have developed graduate and undergraduate programs in this field in the last decade (Zauhar, 2001). Scientists ranging the spectrum from computer science to ecology need to understand the methods and language from each other's discipline to communicate effectively and to lead to progress in the field. These studies are moving away from an era of single scientist studies because extracting information from these complex datasets requires collaborative efforts for both funding and informational needs.

Integrating results from diverse experiments is key to being able to understand complex systems (Hawkins et al., 2010). It is now becoming possible to integrate other 'omics' as additional layers of data. In addition to genomics and transcriptomics, there are other similar approaches looking at slightly different processes in the DNA → RNA→ protein pathway, that when used in conjunction with other methods can yield a richer view of the entire process. This has mostly been done in other fields such as human biology, but has not yet been applied to algae. Examples

include: GRO-Seq which examines transcriptionally-engaged RNA polymerases (Core et al., 2008), Chip-Seq studies protein-DNA interactions (can be feasible once you have protein models and a genome), MeDIP-Seq, MethylC-Seq (Lister et al., 2009). Data visualization programs such as the University of California Santa Cruz genome browser (Fujita et al., 2011) or gView (Petkau et al., 2010) help with the interpretation of these large datasets.

It is important to tie the genomic information with experimental data in an interactive approach. Next generation sequencing is a tool for studying biology. Data collection for these projects should be consistent with appropriate ecological approaches and knowledge. Just as the microscope or SCUBA allowed for exploration of unknown aspects of biology, sequencing technology also provides an opportunity for the generation of new hypotheses and a suite of tools to extend the study of biology. It lends itself especially well to exploring evolutionary trails left in the genetic record and functional comparisons of related organisms. As with any tool, the results or observations must be interpreted with knowledge of the organisms and ecosystems.

Chapter 2, in full, is currently in preparation for submission. Konotchick, T., C. Dupont, R. Valas, and A.E. Allen. Brown Algal Genomics. The dissertation author was the primary investigator and author of this manuscript.

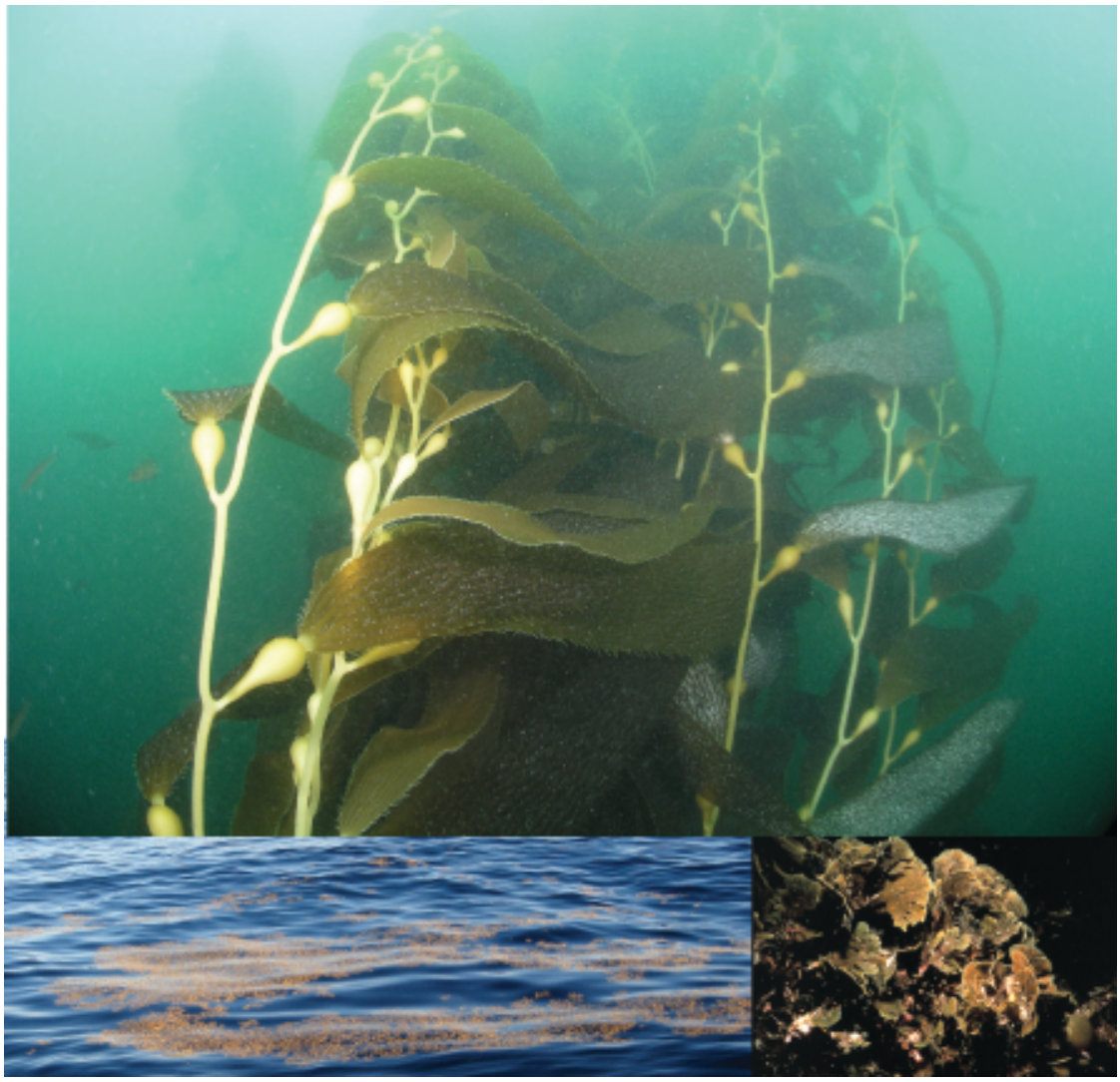

Figure 2.1: Photographs representing some of the diversity of the brown algae (Phaeophyceae). Clockwise from top: *Macrocystis* pyrifera, the largest alga on earth and also one of the more structurally complex with sieve cells that allows the transport of metabolites, photo credit: Steve Gardner; a pelagic form of *Sargassum*, photo credit: Greg Wanger; *Lobophora,* photo credit: A. Shepard, OAR/National Undersea Research Program (NURP), University of North Carolina at Wilmington; NOAA/Department of Commerce.

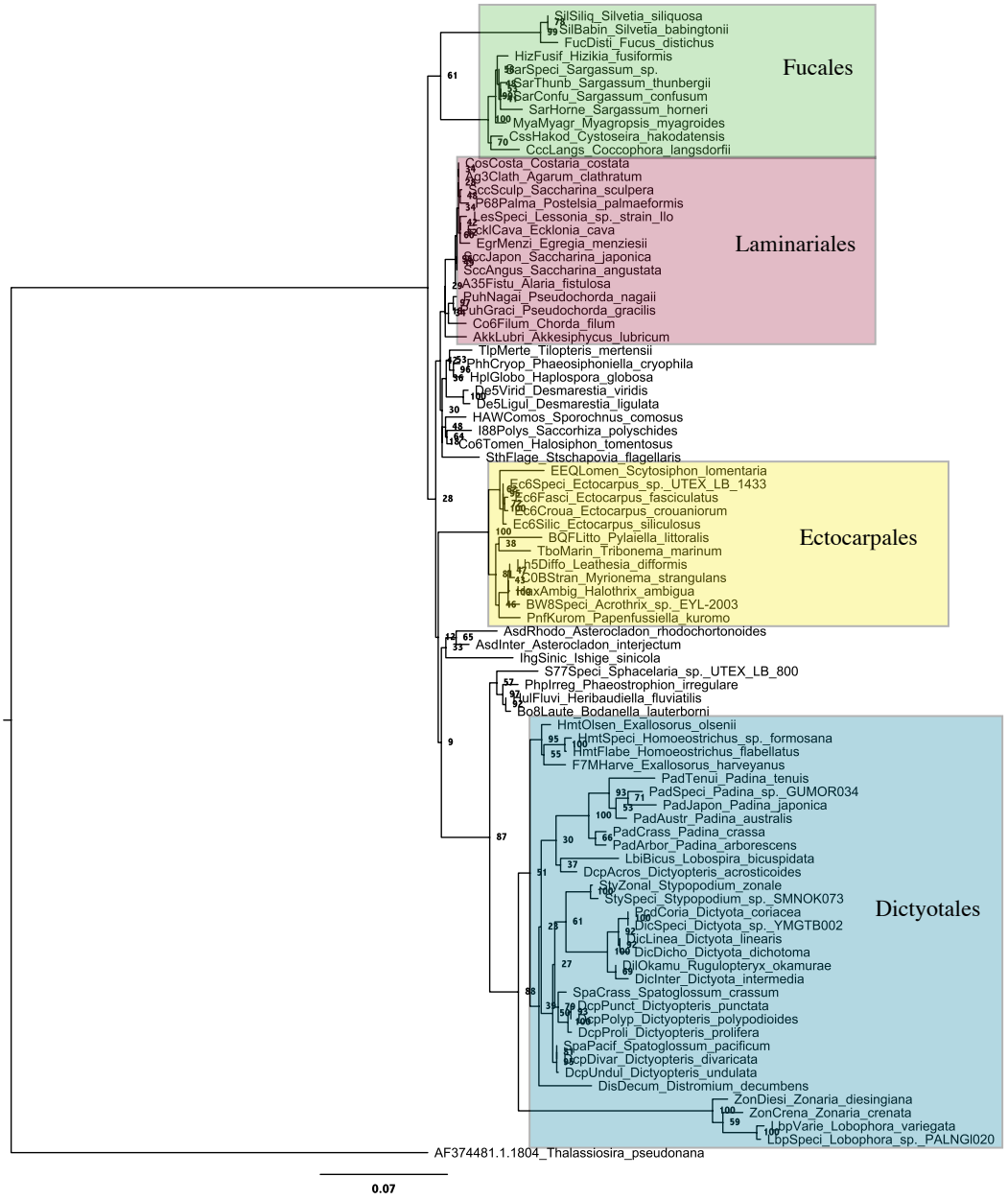

Figure 2.2: Phaeophyceae phylogenetic tree based on 18S rRNA sequences. Orders of brown algae differ in their thallus growth and construction and their reproductive strategies and increased coverage of these groups has the potential to yield insights into these developmental processes. Phaeophyceae 18S sequences were extracted from the online SILVA database, sequences with quality value scores less than 75 were removed, and only one representative from each species was included. *Chlamydomonas* was added as an outgroup. Sequences were aligned using muscle, and PHyML used to create the tree (100 bootstraps, BioNJ starting tree, HKY85 model).

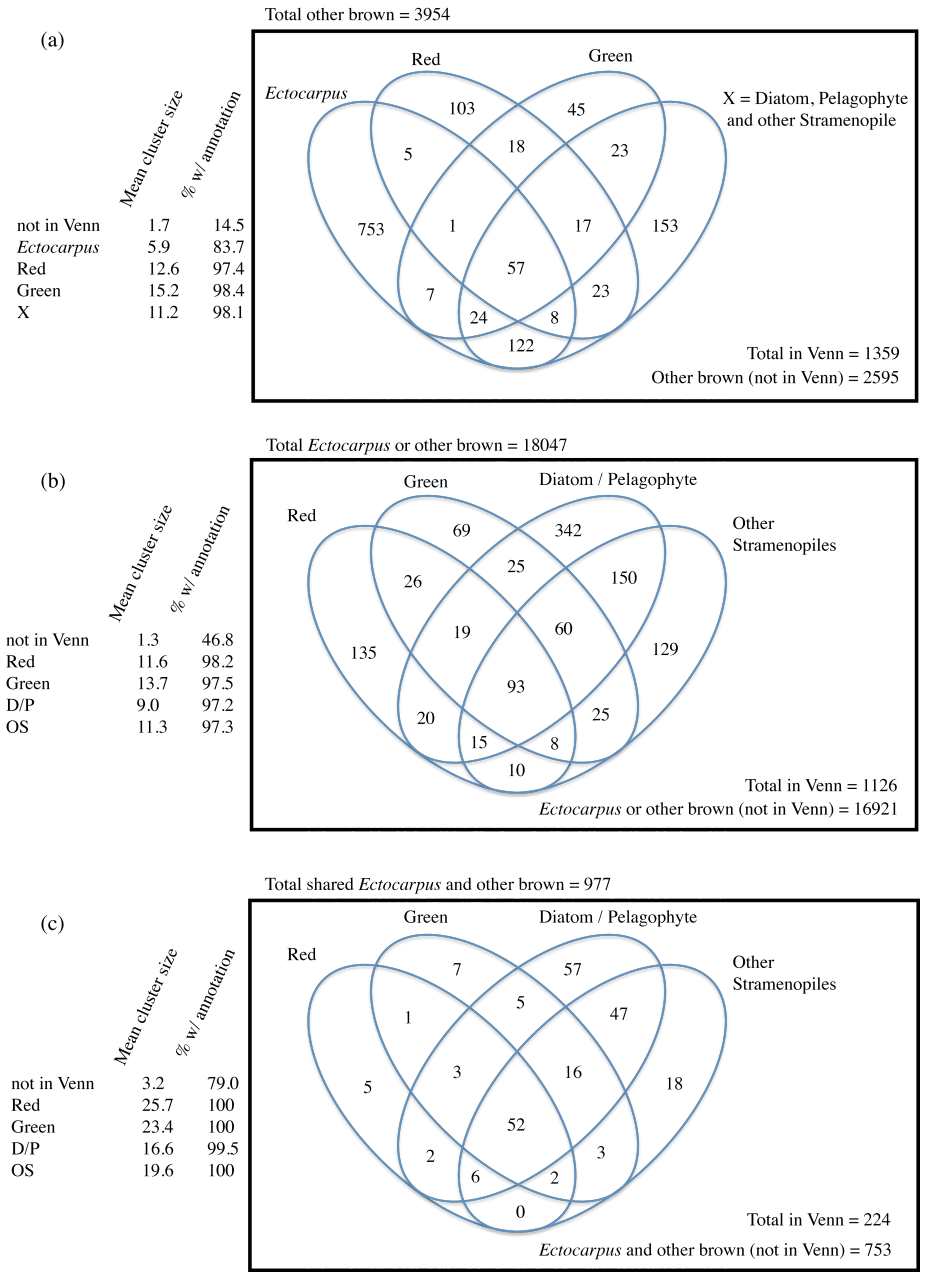

Figure 2.3: Comparative genomics of available Phaeophyceae sequence data with other algal groups. Panel (a) compares the distribution of brown algal clusters with 60% sequence identity to *Ectocarpus* (in the same class), red algae, green algae, or a combined group containing the diatoms, pelagophytes and other stramenopiles. (b) compares the distribution of clusters that were found in either brown algal EST clusters or *Ectocarpus* (18047) with that of the red algae, green algae, diatoms/pelagophytes and other stramenopiles. (c) compares the distribution of clusters that were found in both brown algal EST clusters and *Ectocarpus* (977) with that of the red algae, green algae, diatoms/pelagophytes and other stramenopiles. Areas of overlap represent shared clusters.

References

Adams, M., Kelley, J., Gocayne, J., Dubnick, M., Polymeropoulos, M., Xiao, H., Merril, C., Wu, A., Olde, B., Moreno, R., et al. (1991). Complementary DNA sequencing: expressed sequence tags and human genome project. Science *252*, 1651–1656.

Archibald, J. (2005). Jumping genes and shrinking genomes - probing the evolution of eukaryotic photosynthesis with genomics. IUBMB Life *57*, 539–547.

Bhattacharya, D., Yoon, H., and Hackett, J. (2003). Photosynthetic eukaryotes unite: endosymbiosis connects the dots. BioEssays *26*, 50–60.

Booth, D., Provan, J., and Maggs, C.A. (2007). Molecular approaches to the study of invasive seaweeds. Botanica Marina *50*, 385–396.

Cock, J., Sterck, L., Rouzé, P., Scornet, D., Allen, A., Amoutzias, G., Anthouard, V., Artiguenave, F., Aury, J.-M., Badger, J., et al. (2010). The *Ectocarpus* genome and the independent evolution of multicellularity in brown algae. Nature *465*, 617–621.

Cole, K. (1967). Chromosome numbers in the Phaeophyceae. Canadian Journal of Genetics and Cytology *9*, 519–530.

Collén, J., Marsollier, I.G., Léger, J., and Boyen, C. (2007). Response of the transcriptome of the intertidal red seaweed *Chondrus crispus* to controlled and natural stresses. New Phytologist *176*, 45–55.

Core, L., Waterfall, J., and Lis, J. (2008). Nascent RNA sequencing reveals widespread pausing and divergent initiation at human promoters. Science *322*, 1845–1848.

Coyer, J.A., Peters, A.F., Hoarau, G., Stam, W.T., and Olsen, J.L. (2002). Hybridization of the marine seaweeds, *Fucus serratus* and *Fucus evanescens* (Heterokontophyta: Phaeophyceae) in a 100-year-old zone of secondary contact. Proceedings of the Royal Society B: Biological Sciences *269*, 1829–1834.

Craigie, J., and Correa, J. (1996). Etiology of infectious diseases in cultivated *Chondrus crispus* (Gigartinales, Rhodophyta). Hydrobiologia *326/327*, 97–104.

Crepineau, F., Roscoe, T., Kaas, R., Kloareg, B., and Boyen, C. (2000). Characterisation of complementary DNAs from the expressed sequence tag analysis of life cycle stages of *Laminaria digitata* (Phaeophyceae). Plant Molecular Biology *43*, 503–513.

Davis, T., Volesky, B., and Mucci, A. (2003). A review of the biochemistry of heavy metal biosorption by brown algae. Water Research *37*, 4311–4330.

de Reviers, B., and Rousseau, F. (2007). Classification of the Phaeophyceae from past to present and current challenges. In Unravelling the Algae: the Past, Present, and Future of Algal Systematics, J. Brodie, and J. Lewis, eds. (Boca Raton: CRC Press, Taylor & Francis Group).

Deagle, B., Jarman, S., and Pemberton, D. (2005). Genetic Screening for Prey in the Gut Contents from a Giant Squid (*Architeuthis* sp.). Journal of Heredity *96*, 417–423.

Dhar, A., Dettori, A., Roux, M., Klimpel, K., and Read, B. (2003). Identification of differentially expressed genes in shrimp (*Penaeus stylirostris*) infected with *White spot syndrome virus* by cDNA microarrays. Archives of Virology *148*, 2381–2396.

Douzery, E., Snell, E., Bapteste, E., Delsuc, F., and Philippe, H. (2004). The timing of eukaryotic evolution: does a relaxed molecular clock reconcile proteins and fossils? Proceedings of the National Academy of Sciences *101*, 15386–15391.

Dupont, S., Wilson, K., Obst, M., Sköld, H., Nakano, H., and Thorndyke, M. (2007). Marine ecological genomics: when genomics meets marine ecology. Marine Ecology Progress Series *332*, 257–273.

Eichenberger, W., Araki, S., and Müller, D. (1993). Betaine lipids and phospholipids in brown algae. Phytochemistry *34*, 1323–1333.

Ekblom, R., and Galindo, J. (2010). Applications of next generation sequencing in molecular ecology of non-model organisms. Heredity *107*, 1–15.

Franssen, S., Gu, J., Bergmann, N., Winters, G., Klostermeier, U., Rosenstiel, P., Bornber-Bauer, E., and Reusch, T. (2011). Transcriptomic resilience to global warming in the seagrass *Zostera marina*, a marine foundation species. Proceedings of the National Academy of Sciences *108*, 19276–19281.

Fujita, P.A., Rhead, B., Zweig, A.S., Hinrichs, A.S., Karolchik, D., Cline, M.S., Goldman, M., Barber, G.P., Clawson, H., Coelho, A., et al. (2011). The UCSC Genome Browser database: update 2011. Nucleic Acids Research *39*, D876–D882.

Guiry, M. (2012). Algaebase.
Http://Www.Algaebase.org/Browse/Taxonomy/?Id=4360.

Hawkins, R., Hon, G., and Ren, B. (2010). Next-generation genomics: an integrative approach. Nature Reviews Genetics *11*, 476–486.

Kapp, M. (1998). Viruses infecting marine brown algae. Virus Genes *16*, 111–117.

Keeling, P., Burger, G., Durnford, D., Lang, B., Lee, R., Pearlman, R., Roger, A., and Grey, M. (2005). The tree of eukaryotes. Trends in Ecology & Evolution *20*, 670–676.

Kovalenko, I., Zdyrko, B., Magasinski, A., Hertzberg, B., Millicev, Z., Burtovyy, R., Luzinov, I., and Yushin, G. (2011). A major constituent of brown algae for use in high-capacity Li-ion batteries. Science *334*, 75–79.

Kupper, F.C., Carpenter, L.J., McFiggans, G.B., Palmer, C.J., Waite, T.J., Boneberg, E.M., Woitsch, S., Weiller, M., Abela, R., Grolimund, D., et al. (2008). Iodide accumulation provides kelp with an inorganic antioxidant impacting atmospheric chemistry. Proceedings of the National Academy of Sciences *105*, 6954–6958.

Kupper, F.C., Schweigert, N., Ar Gall, E., Legendre, J.M., Vilter, H., and Kloareg, B. (1998). Iodine uptake in Laminariales involves extracellular, haloperoxidase-mediated oxidation of iodide. Planta *207*, 163–171.

La Barre, S., Potin, P., Leblanc, C., and Delage, L. (2010). The halogenated metabolism of brown algae (Phaeophyta), its biological importance and its environmental significance. Marine Drugs *8*, 988–1010.

Lewis, R. (1996). Chromosomes of the brown algae. Phycologia *35*, 19–40.

Li, W., and Godzik, A. (2006). Cd-hit: a fast program for clustering and comparing large sets of protein or nucleotide sequences. Bioinformatics *22*, 1658–1659.

Lister, R., Pelizzola, M., Dowen, R.H., Hawkins, R.D., Hon, G., Tonti-Filippini, J., Nery, J.R., Lee, L., Ye, Z., Ngo, Q.-M., et al. (2009). Human DNA methylomes at base resolution show widespread epigenomic differences. Nature *462*, 315–322.

Manley, S. (1983). Composition of sieve tube sap from *Macrocystis pyrifera* (Phaeophyta) with emphasis on the inorganic constituents. Journal of Phycology *19*, 118–121.

Mayr, E. (1969). The biological meaning of species. Biological Journal of the Linnean Society *1*, 311–320.

McHugh, D. (2003). A guide to the seaweed industry (FAO Fisheries Technical Paper).

Michel, G., Tonon, T., Scornet, D., Cock, J., and Kloareg, B. (2010a). Central and storage carbon metabolism of the brown alga Ectocarpus siliculosus: insights into the origin and evolution of storage carbohydrates in Eukaryotes. New Phytologist *188*, 67–81.

Michel, G., Tonon, T., Scornet, D., Cock, J., and Kloareg, B. (2010b). The cell wall polysaccharide metabolism of the brown alga Ectocarpus siliculosus. Insights into the evolution of extracellular matrix polysaccharides in Eukaryotes. New Phytologist *188*, 82–97.

Moulin, P., Crepineau, F., Kloareg, B., and Boyen, C. (1999). Isolation and characterization of six cDNAs involved in carbon metabolism in *Laminaria digitata* (Phaeophyceae). Journal of Phycology *35*, 1237–1245.

Moustafa, A., Beszteri, B., Maier, U., Bowler, C., Valentin, K., and Bhattacharya, D. (2009). Genomic footprints of a cryptic plastid endosymbiosis in diatoms. Science *324*, 1724.

Neushul, P. (1989). Seaweed for war: California's World War I kelp industry. Technology and Culture *30*, 561–583.

Pagani, I., Liolios, K., Jansson, J., Chen, I., Smirnova, T., Nosrat, B., Markowitz, V., and Kyrpides, N. (2012). The Genomes Online Database (GOLD v4). Http://Www.Genomesonline.org.

Pearson, G., Serrao, E., and Cancela, M. (2001). Suppression subtractive hybridization for studying gene expression during aerial exposure and desiccation in fucoid algae. European Journal of Phycology *36*, 359–366.

Peters, A., Marie, D., Scornet, D., Kloareg, B., and Cock, J. (2004). Proposal of *Ectocarpus siliculosus* (Ectocarpales, Phaeophyceae) as a model organism for brown algal genetics and genomics. Journal of Phycology *40*, 1079–1088.

Petkau, A., Stuart-Edwards, M., Stothard, P., and Van Domselaar, G. (2010). Interactive microbial genome visualization with GView. Bioinformatics *26*, 3125–3126.

Phillips, N., Calhoun, S., Moustafa, A., Bhattacharya, D., and Braun, E. (2008). Genomic insights into evolutionary relationships among heterokont lineages emphasizing the Phaeophyceae. Journal of Phycology *44*, 15–18.

Pinori, E., Berglin, M., Brive, L., Hulander, M., Dahlström, M., and Elwing, H. (2011). Multi-seasonal barnacle (*Balanus improvisus*) protection achieved by trace amounts of a macrocyclic lactone (ivermectin) included in rosin-based coatings. Biofouling *27*, 941–953.

Qin, S., Sun, G.-Q., Jiang, P., Zou, L.-H., Wu, Y., and Tseng, C.-K. (1999). Review of genetic engineering of *Laminaria japonica* (Laminariales, Phaeophyta) in China. Hydrobiologia *398/399*, 469–472.

Radakovits, R., Jinkerson, R.E., Darzins, A., and Posewitz, M.C. (2010). Genetic engineering of algae for enhanced biofuel production. Eukaryotic Cell *9*, 486–501.

Roeder, V., Collén, J., Rousvoal, S., Corre, E., Leblanc, C., and Boyen, C. (2005). Identification of stress gene transcripts in *Laminaria digitata* (Phaeophyceae) protoplast cultures by expressed sequence tag analysis. Journal of Phycology *41*, 1227–1235.

Roesijadi, G., Jones, S., Snowden-Swan, L., and Zhu, Y. (2010). Macroalgae as a biomass feedstock: a preliminary analysis (Pacific Northwest National Laboratory).

Rokas, A., Williams, B., King, N., and Carroll, S. (2003). Genome-scale approaches to resolving incongruence in molecular phylogenies. Nature *425*, 798–804.

Sanbonsuga, Y., and Neushul, M. (1978). Hybridization of Macrocystis (Phaeophyta) with other float-bearing kelps. Journal of Phycology *14*, 214–224.

Smith, S. (1981). Marine macrophytes as a global carbon sink. Science *211*, 838–840.

Sykes, M. (1908). Anatomy and histology of *Macrocystis pyrifera* and *Laminaria saccharina*. Annals of Botany *22*, 291–325.

Towle, D., and Pearse, J. (1973). Production of the giant kelp, *Macrocystis*, estimated by in situ incorporation of ^{14}C in polyethylene bags. Limnology and Oceanography *18*, 155–159.

US Congress (1980). Energy from open ocean kelp farms (Honolulu, Hawaii: University Press of the Pacific).

Waaland, J., Stiller, J., and Cheney, D. (2004). Macroalgal candidates for genomics. Journal of Phycology *40*, 26–33.

Wargacki, A., Leonard, E., Win, M., Regitsky, D., Santos, C., Kim, P., Cooper, S., Raisner, R., Herman, A., Sivitz, AB, et al. (2012). An engineered microbial platform for direct biofuel production from brown macroalgae. Science *335*, 308–313.

Woo, J., Kitamura, E., Myouga, H., and Kamei, Y. (2002). An antifungal protein from the marine bacterium *Streptomyces* sp. strain AP77 is specific for *Pythium porphyrae*, a causative agent of Red Rot Disease in *Porphyra* spp. Applied and Environmental Microbiology *68*, 2666–2675.

Zauhar, R. (2001). University bioinformatics programs on the rise. Nature Biotechnology *19*, 285–286.

CHAPTER 3

Vertical Distribution of *Macrocystis pyrifera* Nutrient Exposure in Southern California

Abstract

We examine water-column temperature time series profiles for several years at two locations in a single kelp forest to characterize the vertical variation in temperature and nutrient exposure of *Macrocystis pyrifera* and within-bed differences in the physical environment. There is greater temperature variability during the summer months versus the winter, and at the surface versus at depth. The 14.5°C isotherm, indicating the presence of nitrate, ranged through the entire water column, and was shallowest during the winter and in the south versus the north of the kelp forest. The predicted water column integrated nitrate varies between 0 μmol NO_3^-/m^2 to 380 μmol NO_3^-/m^2 yielding a time series daily average of 0.11 gN/m^2day (North La Jolla) and 0.15 gN/m^2day (South La Jolla). Redfield conversion of these values puts the time series daily average for carbon production (upper limit) between 0.7 and 1.0 gC/m^2day for the north and south parts of the bed respectively; however, there is considerable variation at several time scales. The depth of the nutricline varied by up to 10 meters over time scales as short as hours. Variability was greatest at diurnal and semi-diurnal frequencies, with shallower water column depths showing greatest variability. These depth specific variations in temperature and nutrient exposure may have biologically important consequences for *M. pyrifera* especially during low nutrient times of the year.

Introduction

The largest algal species on earth, the giant kelp, *Macrocystis pyrifera*, has a broad geographic range and individuals that span the water column, often bridging gradients in temperature and nutrients needed for growth. A significant input of nutrients is required to support the large and rapid biological production of these forests. *M. pyrifera* productivity in California ranges from .95 – 6.8 gC/m^2day (Towle and Pearse, 1973; Mann, 2000). Using the empirical stoichiometric Redfield ratio 106:16:1 (C:N:P), this leads to estimates that 0.14 – 1.03 gN/m^2day and 0.01 – 0.06 gP/m^2day are needed to support this growth. Low nutrient conditions limit growth and survivorship as well as negatively affect adult reproductive output and juvenile recruitment (Gerard, 1982b; Graham et al., 1997; Steneck et al., 2002). Nutrients are typically stratified in the water column and linked with temperature and density (Kamykowski and Zentara, 1986), with more nutrients below the thermocline. Thus, there is variation across the alga in the opportunities for nutrient acquisition. Geographically, the stratification of nutrients increases toward the southern range of *M. pyrifera* (in North America). Temperature and nitrate concentrations can vary on multiple temporal and spatial scales with profound consequences for kelp biology.

Events occurring on time scales of tens of thousands of years such as sea level change can affect kelp communities by altering the available substrate from the rocky substrate needed for holdfast attachment and seen in southern California today to a sandy bottom (Graham et al., 2003). At the long end of human observational scales, low-frequency climate forcing (decadal to multi-decadal) can lead to marked changes in the regional-scale nutrient climate available to kelps. Low-frequency forcing can

affect the response of the kelp forest to interannual time scale events; since the 1976-1977 North Pacific climate regime shift, *M. pyrifera* canopy cover changes resulting from El Niño/Southern Oscillation (ENSO) events have been magnified (Parnell et al., 2010). ENSO is an inter-annual and Pacific wide climate pattern that involves a warming of the surface waters in the eastern Pacific relative to the long-term average. For the giant kelp in southern California, decreases in kelp stands occur with the warming temperatures. In southern California, storm and wave activity increases during ENSO years, which increases the incidence of *M. pyrifera* being detached from their substrate (Seymour et al., 1989). Loss of canopy can in turn affect the light reaching the bottom and the ability of competitors to gain ground. One of the largest ENSO events in recent history (1982 – 1984) greatly reduced *M. pyrifera* stands (Tegner and Dayton, 1991; Tegner et al., 1997; Dayton et al., 1998).

M. pyrifera has a large worldwide geographic extent. In North America, *M. pyrifera* ranges from Alaska to Baja California, Mexico. At the pole-ward extent, the species is limited by light (Stekoll and Else, 1990) and at the equator-ward extent is limited by nutrient poor warmer waters (Graham et al., 2007). The San Diego region supports two of the largest kelp beds in California, Point Loma and La Jolla. Yet unlike nutrient-replete regions to the north, the San Diego area experiences seasons (i.e. summer) when nutrients are limiting (Jackson, 1977). Internal waves are critical in "nutritionally marginal" habitats of southern California, especially during warm water events (Zimmerman and Robertson, 1985). The offshore nitracline, in addition to internal waves, can affect the availability of nitrate to the inner shelf (Lucas et al.,

2011). Sub-mesoscale coastal eddies represent another potential means of nutrient transport to kelp forests (Bassin et al., 2005).

Nitrate is the most abundant source of nitrogen for kelp and the canonical pathway for nitrate assimilation is the conversion of nitrate into nitrite by nitrate reductase, then conversion to the biologically usable form, ammonia, via nitrite reductase. Tracer studies have indicated the capacity for ammonium and nitrate assimilation on short time scales; incorporation of $^{15}NO_3^-$ into amino acids via glutamine synthetase happens within 15 min (Haxen and Lewis, 1981). Juvenile sporophytes also showed drawdown of nitrate and ammonia on time scales of minutes (Haines and Wheeler, 1978; Bray et al., 1986). Nitrate reductase activity correlates with ambient nitrate levels in other kelps (Young et al., 2007). The intertidal green alga *Ulva lactuca* showed higher tissue nitrogen in response to a higher ambient interval-wave driven nitrate environment (Pérez-Mayorga et al., 2011). Therefore, algae, including kelps, have the ability to respond quickly to nutrient input pulses at short time scales.

M. pyrifera is one of the few algae that possess sieve tube elements that allow for internal transport of metabolites such as mannitol and amino acids (Sykes, 1908; Manley, 1983). One kelp individual could be limited in both light (at depth) and nutrients (at surface) at the same time, yet still be able to grow. This sieve tube transport system, which spans the water column, means that deep-water nitrate can support growth despite low nitrate levels at the ocean surface. Principal nitrogen translocating compounds in sieve tube sap include glutamine, glutamate, and aspartate (Schmitz and Srivastava, 1979). This system may help explain why *M. pyrifera* also

can sustain growth in the absence of surface nutrients for limited periods of time. Starting with high internal nitrogen reserves, *M. pyrifera* can sustain relatively rapid growth for at least 2-3 weeks in the absence of a significant external nitrogen supply (Gerard, 1982a) though low overall nutrient availability in southern California limits this ability (Zimmerman and Kremer, 1986). Prior nutrient history can affect that response.

Nitrate is the dominant source of nitrogen, though it may not be the only source of nitrogen fueling growth. *M. pyrifera* has the ability to take up both nitrate and ammonia as nitrogen sources. Both nitrogen forms can be taken up simultaneously, though ammonia is taken up more rapidly (Haines and Wheeler, 1978). It takes additional energy to reduce nitrate to ammonia, so there may be an energetic benefit to assimilating ammonia, though it is less readily available in the environment. A recent modeling study suggested that epibionts might excrete enough ammonia to supply half the nitrogen demand in summer/fall (Fram et al., 2008) and kelp may respond opportunistically to ammonium released from fish excretion (Bray et al., 1986). It is unknown whether *M. pyrifera* is shifting its nitrogen source during the summer and fall when there is low ambient nitrate, or between sites with different nitrate concentrations. Presumably, *M. pyrifera* will utilize ammonia and other sources of organic recycled nitrogen if available, but the nitrate/m^2 ultimately limits the total nitrogen in the system.

An interesting aspect of the height of *M. pyrifera* is that water column spanning individuals may be exposed to very different nutrient opportunities within an individual. To explore water column variability in the nutrient environment at short

spatial scales (within a kelp bed; <10 km) along the length of the typical height of *M. pyrifera*, we examine a thermistor string measurements over a period of >43 months. The objectives of this study were to: (1) define the nutrient climate and the variable physical environment of *M. pyrifera* within a single kelp forest, (2) examine low frequency (seasonal) to high frequency (hourly) temperature and predicted nitrate events, focusing on depth differences, and (3) discuss them in relation to *M. pyrifera* biology.

Methods

Description of Study Sites

The La Jolla kelp forest is the second largest kelp forest in California, after Pt. Loma, with approximate dimensions of 8 km alongshore by 1.5 km cross-shelf (Figure 3.1). The bed occupies an area of mainly rocky substrate interspersed with cobble and sand patches. The northern end of the forest is located near a submarine canyon and the San Diego-La Jolla Ecological Reserve, and the southern portion of the kelp forest wraps around a headland. We chose to look at the temperature climate of two sites in this kelp bed: North La Jolla (N 32° 51.0'; W° 117 17.5') and South La Jolla (N 32° 48.6'; W 117° 17.7'). The North La Jolla site is close to the submarine canyon and has stronger currents than the South La Jolla site, which is located behind the headland. Documented biological differences include higher kelp permanence in the south as seen from aerial photos, while the north has a more dynamic canopy and more dominant understory (Parnell et al., 2006).

Temperature Data Collection

To quantify horizontal and vertical differences in temperature and hence nutrient availability at the two locations, thermistor chain data were collected from July 2007 through March 2011 at 10 minute intervals using TidBit temperature data loggers with ~0.2° resolution, and ~5 minute response time (Onset, Bourne, Massachusetts, USA). TidBits were placed on the bottom and at 2, 6, 10, 14, and 18 meters above the bottom (mab) at both sites and at the surface (21 and 22 mab) at South La Jolla (Figure 3.2).

Using Temperature as a Proxy for Nutrient Availability

There is a strong linear relationship between nitrate and temperature in the southern California nearshore at temperatures below 14.5°C, with colder waters possessing more nitrate (Kamykowski and Zentara, 1986; Zimmerman and Kremer, 1986; Dayton et al., 1999; Lucas et al., 2011). However, anomalous temperature-nitrate events have been documented in the southern part of the range (Ladah, 2003). We estimated seawater nitrate concentrations from these well-established empirically-derived temperature-nitrate relationships from offshore temperature and nitrate data from CalCOFI line 93 measurements taken from 1965-2008 for the San Diego region using the equation: -5.1 T + 72 for temperatures below 14.5°C (Lucas et al., 2011). At temperatures above 14.5°C, nitrate levels are typically insignificant (i.e. <0.1 μmol/L). We assume that this relationship is maintained inshore despite complex mixing that occurs in the nearshore. Water column integrated nitrate was calculated for a square meter of bottom at each 10 minute time step by linearly interpolating the thermistor chain data to get temperature values and calculated nitrate values (using the equation

above) throughout the water column, which were then summed in 10 cm bins. Conversions to carbon were calculated using the Redfield ratio (106 C: 16N).

Power Spectral Density

Power spectral density calculations used the Welch's averaged periodogram method with a section length of two weeks, zero overlap and application of a standard Hamming window. Power spectra were calculated at 0 mab and 18 mab at each of the two study sites and also at 6 mab for South La Jolla.

Results

During this ~4 year time series, we see periods of greater temperature variability during the summer, and lower variability during the winter months (Figures 3.2 & 3.3). This within depth variability is greater at 18 mab vs. depth (Table 3.1). In the North La Jolla time series, there is an eight-month gap resulting from the mooring being ripped from the base during a storm; only the top and bottom tidbits were recovered. Because of this gap, we chose to focus on comparisons of the 18m and bottom time series for some of our analyses (Table 3.1; Figures 3.3, 3.4, and 3.5). The mean temperatures were slightly warmer in North La Jolla compared to South La Jolla. Water column differences change predictably throughout the year; we see seasonal patterns of greater stratification in summer months and more homogenous temperatures in the winter (Figure 3.4). In North La Jolla, the dominant frequency signal is the diurnal peak, while at South La Jolla, the semi-diurnal peak is more prominent (Figure 3.5). Variance is higher at 18 mab compared to the bottom at both sites, though the difference is greater at South La Jolla. The rate of decay (slope) is

greater at the bottom, meaning that frequencies higher than semidiurnal have less power at depth compared to the surface. For our study, the Oceanic Niño Index, a measure of the occurrence and strength of El Niño/La Niña events, included the 2009-2010 El Niño event and the 2010-2011 La Niña event (Nam et al., 2011). We did not see a significant peak in the power spectra greater than diurnal. The length of our section window in the power spectra calculations precludes seeing variation longer than two weeks. Additionally, the length of this time series is limited in resolving longer time scale events such as ENSO which is recurrent on ~3-7 year time scales.

Of biological interest for *M. pyrifera* is the height in the water column of the 14.5°C isotherm at which nitrate reaches appreciable levels in this region. Depending on the depth of this isotherm, different segments of a *M. pyrifera* individual will have access to nitrate. The depth of this isotherm throughout the time series varies the entire length of the water column at both sites (Figure 3.6). There are periods when the waters surrounding an individual are likely to be completely depleted of nitrate and there are periods when waters containing nitrate bathe the entire individual. For the majority of time, the depth of nitrate coverage lies somewhere along the length of the individual. Trends are similar at both locations, although the 14.5°C isotherm is generally shallower at South La Jolla (Figure 3.6, bottom panel). The proportion of time that the 18 mab depths fall below 14.5°C is approximately 20% and at the bottom the proportion is ~80% and variable throughout the year (Table 3.1). The proportion of time is higher and the temperatures lower at South La Jolla than for North La Jolla implying that kelps at the south site spend a greater time exposed to nutrients as well as to higher nitrate levels, because at colder temperatures predicted nitrate levels

increase. Because *M. pyrifera* spans the water column, predicted water column nitrate through time may be a more appropriate measure of kelp exposure to nitrate (Figure 3.7). General temporal patterns are similar at the two sites, though the south is exposed to higher nitrate (Figure 3.7, bottom panel). Values range from 0 μmol NO_3^- /m^2 to 380 μmol NO_3^-/m^2 with a time series daily average of 0.11- 0.15 gN/m^2day; corresponding to upper limit of daily gC/m^2 of 0.7 and 1.0 gC/m^2day. On monthly, daily and even over several hours, the depth of the 14.5°C isotherm (Figure 3.8 A&B) and thus available predicted nutrients (Figure 3.8 C&D) can vary by as much as 10m (Figure 3.8).

Discussion

Environmental forcing is variable on a variety of different temporal and spatial scales; likewise, the response of kelp is likely to vary across these scales. Geographically isolated populations have exhibited environmentally consistent physiological specialization to ambient nutrient availability including growth rates, tissue nitrogen content and amino acid concentrations (Espinoza and Chapman, 1983; Kopczak et al., 1991). Kopczak et al. (1991) measured the responses of *Macrocystis* to nitrate availability from populations in Monterey Bay (high nutrients, affected by storms), Santa Barbara (a transition zone), and Santa Catalina (low wave stress, low nutrients). While maximum growth rates were similar among sites, those rates occurred at different nitrate concentrations; maximum rates occurred at lower nitrate concentrations for the algae that were acclimated to more oligotrophic conditions. The sites also differed in the amount of tissue nitrogen content with more tissue nitrogen in

algae from more oligotrophic conditions. Thus, isolated populations have evolved different responses to nitrate availability. This is in concordance with earlier work finding that growth on restricted nitrogen supply leads to an increased ability to take up NO_3^- from low concentrations (Haines and Wheeler, 1978). Nutrients may be especially important for recruitment and survival at the equatorward range limits of the species (Hernández-Carmona et al., 2001). At the southernmost extent of the North American range, Punta Eugenia, Baja California, limiting nutrient conditions are expected to be more common.

Local scale diversity patterns can be the result of processes at larger spatiotemporal scales (Witman et al., 2004). Farther north near Pt. Conception, California, diurnal-period internal waves have along-shelf coherence of >50km (Cudaback and McPhee-Shaw, 2009). Presumably, the same larger scale forcing (i.e. greater than the size of this kelp bed) could be acting on the La Jolla kelp bed; this fits with the seasonal coherence patterns at the two sites (Figures 3.2, 3.5, 3.6 and 3.7). Bight wide shifts in stratification expected with climate change would likely affect the physical forcing of the kelp bed. Alongshore winds can affect near-shore cross-shelf circulation at kilometer scale distances (Pringle and Riser, 2003). Smaller scale differences (i.e. within kelp bed) in temperature and nutrient exposure could potentially be explained by the complex undersea topography and nearby headland which may be setting up complex secondary circulation flows in the nearshore (Wolanski and Hamner, 1988). Both physical differences (i.e. shelf nearby canyon topography, currents) and biological structure (i.e. biogenic alteration of flow) may alter the physical environment kelps experience. Nutrient concentrations vary in the

alongshore direction (Jackson, 1977). The physical structure of the kelp bed itself attenuates horizontal transport and vertical mixing (Jackson and Winant, 1983; Jackson, 1998; Rosman et al., 2010) which can have effects on nutrient availability. The magnitude of this effect scales to the size of the bed (Gaylord et al., 2007). Within bed mixing has been shown to distribute zoospores released near the benthos to locations high in the water column (Cie and Edwards, 2011). Even with similar nitrate climate, growth, morphology and tissue composition can vary within a kelp bed (Stewart et al., 2008). Thus, within-bed nutrient gradients can influence morphology indicating that the nitrate climate can affect change in the regulatory mechanisms and metabolism of kelp.

Additionally, a variable temperature and nutrient environment has different biological relevance depending on depth. The majority of photosynthesis occurs in the surface canopy with half of the standing crop lying between the surface and 1.5 m as fronds reach and spread along the surface (McFarland and Prescott, 1959; Towle and Pearse, 1973; Gerard, 1986). Recruitment occurs on the kelp forest floor. Nitrate and colder temperatures are important for juvenile *M. pyrifera* growth (Dean and Jacobsen, 1984). Nutrient uptake and photosynthetic capacity of blades will vary depending on ambient conditions at a given depth. For example, nitrate uptake is higher in the dark, a factor correlated with depth in the kelp forest (Wheeler and Srivastava, 1984). Also, the nutrient/temperature history may be different at different depths: cold temperatures with warm water deviations characterize the bottom; the mid-water depths (i.e. the thermocline) have variation in both directions; and the surface warm water is punctuated by cold spikes (Figure 3.2).

While the physical environment structures kelp communities on a variety of scales, that is not the only factor affecting their persistence. Biological processes including consumption by urchins or competition with other species may also play structuring roles (Dayton et al., 1984; Dayton, 1985; Dayton et al., 1999) and these factors may have elements controlled by the physical environment. Stronger currents in the north part of the La Jolla bed, or internal tidal bores, could bring in an increased flux of urchin larvae (Pineda, 1991; 1999; Parnell et al., 2006). Alternatively, the stronger persistence of the kelp forest in South La Jolla and its potential to decrease water flow (Rosman et al., 2010), could serve to retain kelp spores within that area, acting as a positive feedback. Epibionts may actually serve a beneficial role, providing ammonium to kelp (Hepburn and Hurd, 2005). Also, with higher environmental nitrate levels, *M. pyrifera* canopy cover is expected to increase, resulting in less light reaching the benthos, making it difficult for other algae to compete.

Environmental conditions can affect the temporal dynamics of habitat-forming kelp, which in turn affects the species richness and turn over of other macroalgae (Wernberg and Goldberg, 2008). Seasonal patterns in kelp abundance and canopy cover are thought to be driven mainly via the physical environment (Jackson, 1977). Kelp tissue nitrate and total nitrogen content correspond to seasonal patterns of ambient nitrate levels (Wheeler and Srivastava, 1984). The time of year had a large impact on the relative importance of the type of nutrient delivery in the southern California Bight. Wind-driven upwelling dominates in the spring. Baroclinic motions, common during the stratified late summer months may affect the structure of

the kelp community. In the Santa Barbara Channel, diurnal internal motions are thought to provide 9-12% of the annual dissolved inorganic nitrogen supply to the kelp beds near Santa Barbara (McPhee-Shaw et al., 2007) although this percentage is expected to increase in relative importance in warmer waters further south. Storm runoff is episodic and most important in the winter and can increase dissolved inorganic nitrogen (McPhee-Shaw et al., 2007) and heavy metal loading (Fink and Manley, 2011) in kelp forests.

Daily changes in the thermocline depth are largely a function of tidal and internal wave activity. From power spectra we see the importance of diurnal and semi-diurnal tidal energy altering the depth of the thermocline and nitracline in this time series. The structure of the kelp bed can change current flow, though the semi-diurnal frequency has the least dampening (Jackson and Winant, 1983). The 14.5°C isotherm can vary by several meters over the span of minutes to hours (Figures 3.6 and 3.8) and *M. pyrifera* is able to take up nutrients on these time scales. The arrival of cold-water, high-nutrient internal waves, which can change the nutrient levels of the water surrounding kelp on the order of minutes to hours, is an especially important nutrient input mechanism during summer stratified months (McPhee-Shaw et al., 2007). It is known that kelps can take up nutrients on time scales of minutes to hours, but it is unknown exactly how kelps are reacting physiologically to these short time scale events and utilizing reserves under limiting conditions. The methods and analysis presented here are a simple, yet illuminating, way to monitor nutrient influences in kelp forests. Time series of expanded duration would allow for characterization of longer time scale events such as ENSO. Expanding this approach

by coupling telemetered thermistor chain with productivity studies and satellite imagery (e.g., Cavanaugh et al., 2010) in several kelp beds along the coast could potentially provide resource managers with predictive capabilities of changes in productivity or even collapse. Future studies should include flow measurements to resolve flux measurements. It is important to know the time and space scales of hydrographic variation in order to understand, measure and study the time and space scales of kelp biological response (Denny et al., 2004).

Acknowledgements

A National Science Foundation Graduate Research Fellowship and Mia J. Tegner Fellowship for Coastal Ecology Fieldwork provided funding support (TK). We would like to thank K. Riser and R. Darrow for help in the field. Discussion with C. Dupont, L.A. Levin, (and reviewers) significantly improved the manuscript.

Chapter 3, in full, has been submitted for publication in Estuarine, Coastal and Shelf Science. Konotchick, T., P.E. Parnell, P.K. Dayton, and J.J. Leichter. Vertical Distribution of *Macrocystis pyrifera* Nutrient Exposure in Southern California. The dissertation author was the primary investigator and author of this paper.

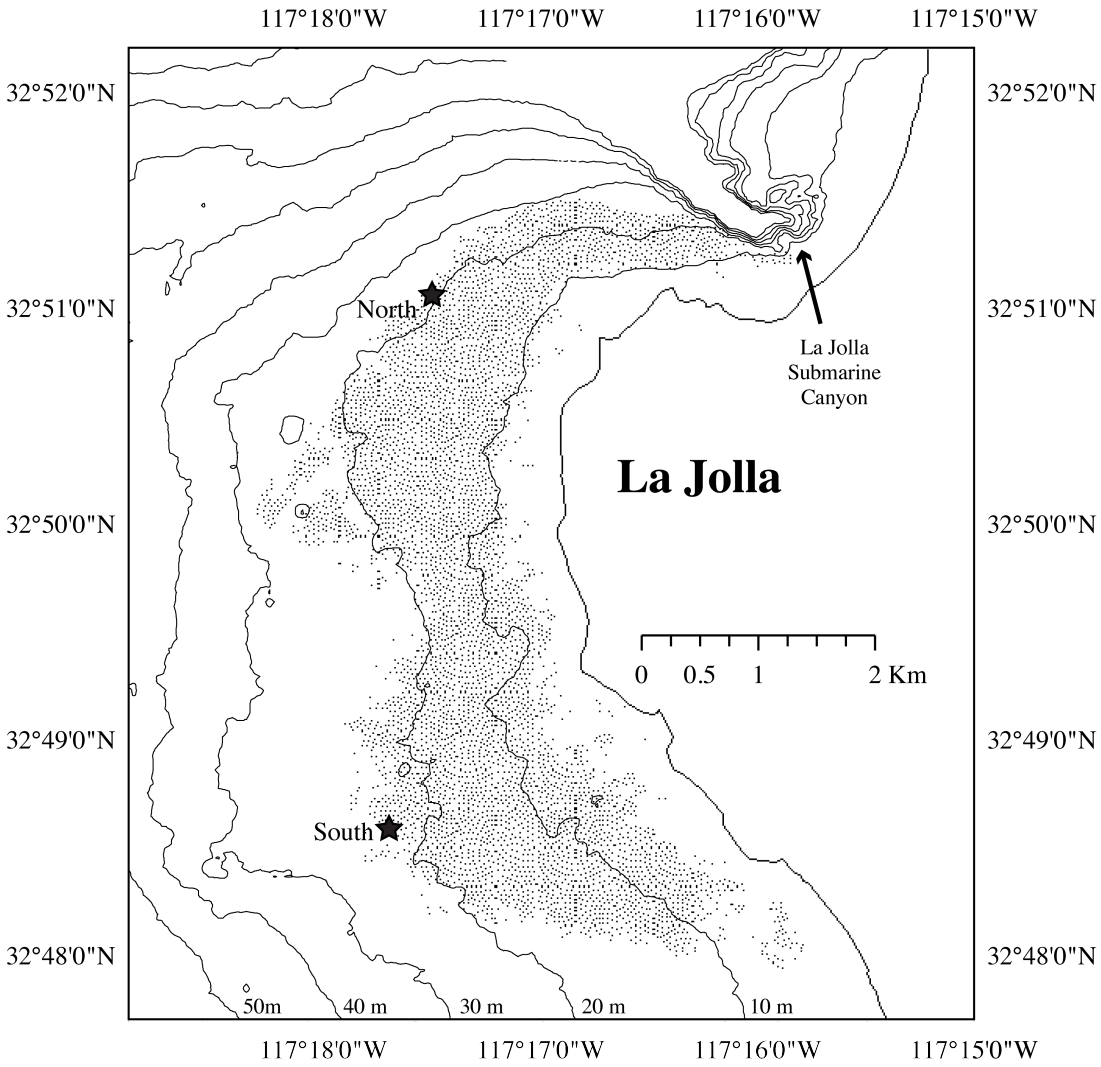

Figure 3.1: Map of the La Jolla kelp forest and nearby submarine canyon. The stippled area is where *Macrocystis pyrifera* has been observed at least once in aerial photographs taken 1967-1999). The North La Jolla and South La Jolla thermistor strings were anchored in 22m and are indicated by stars. Bathymetric contours are at 10m increments.

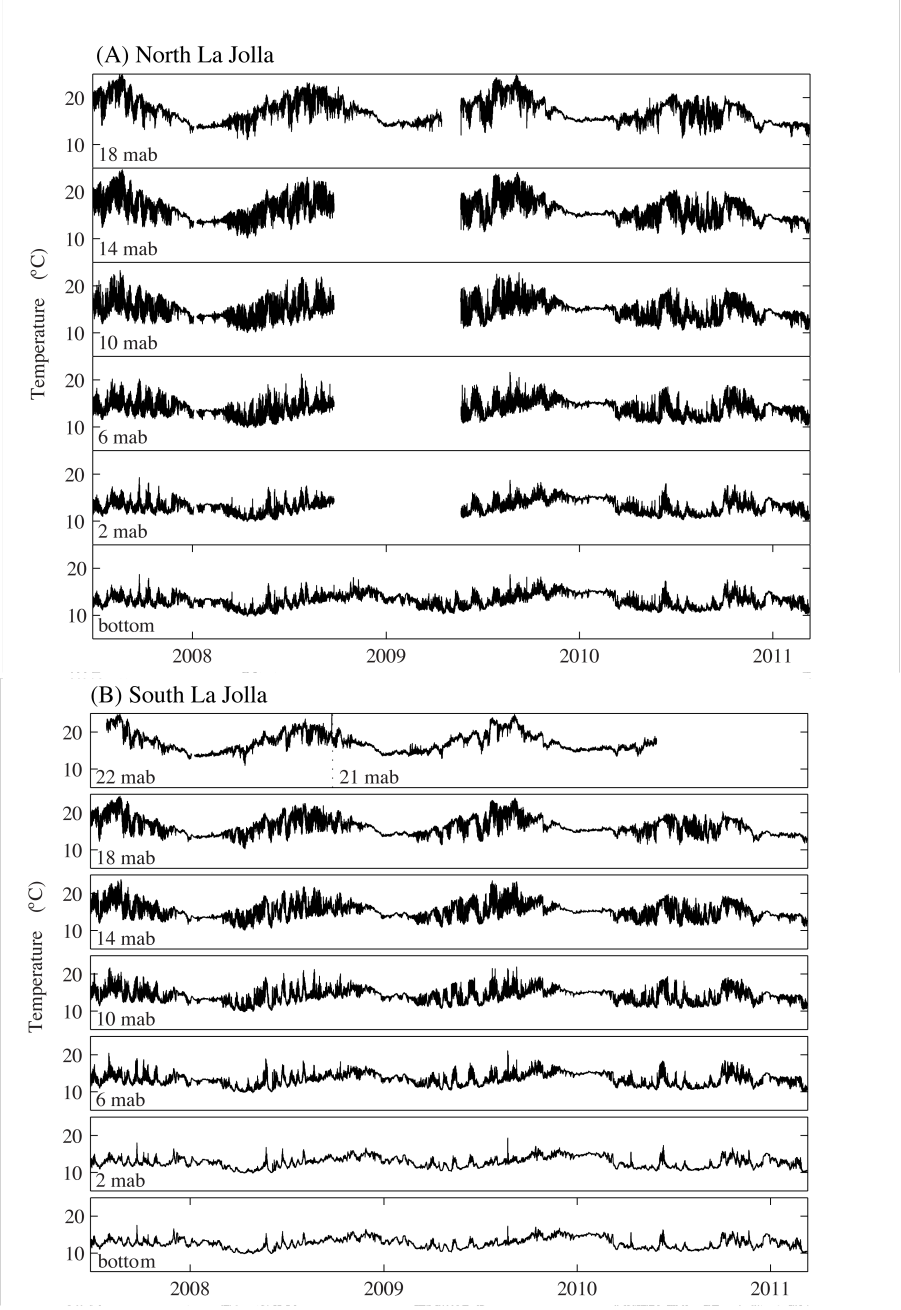

Figure 3.2: Temperature time series for North and South La Jolla. From July 2007 through March 2011, temperature was continuously recorded at depths of 0, 2, 6, 10, 14, and 18 meters above the bottom (mab) at two locations: (A) North La Jolla, and (B) South La Jolla. South La Jolla also had an additional tidbit at 22 mab from July 27th 2007 through September 24th 2008, then at 21 mab through May 30th 2010.

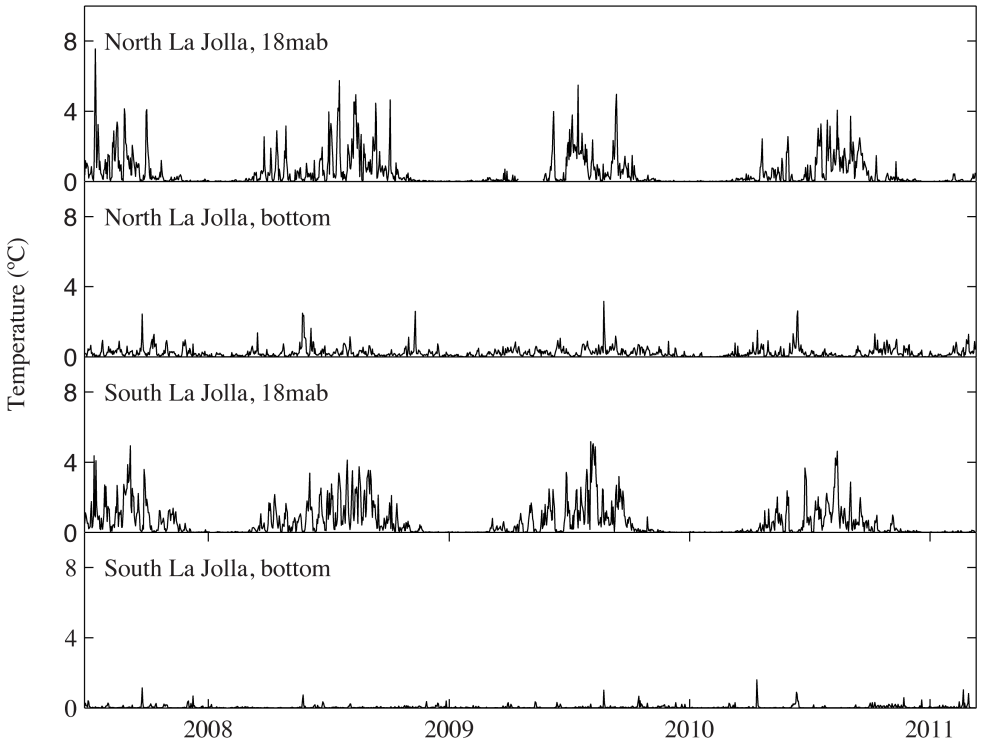

Figure 3.3: Daily averaged variance in temperature through time for 18 mab and bottom at North and South La Jolla.

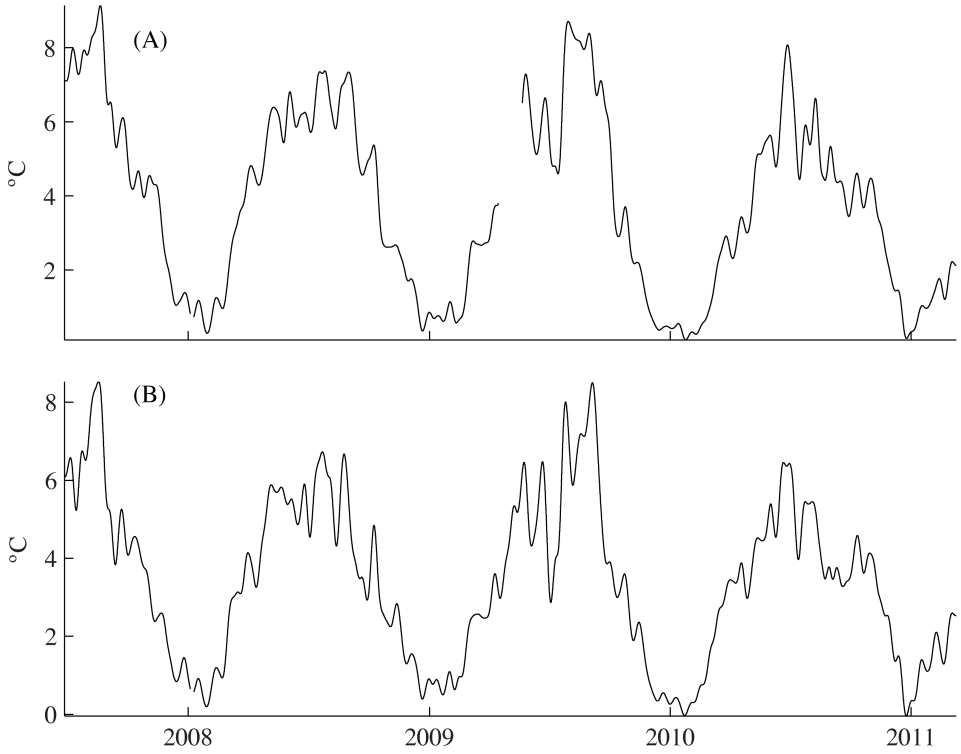

Figure 3.4: Water column differences (18 mab temperature minus 0 mab temperature) through time using one-week running mean low pass filter. (A) North La Jolla; (B) South La Jolla.

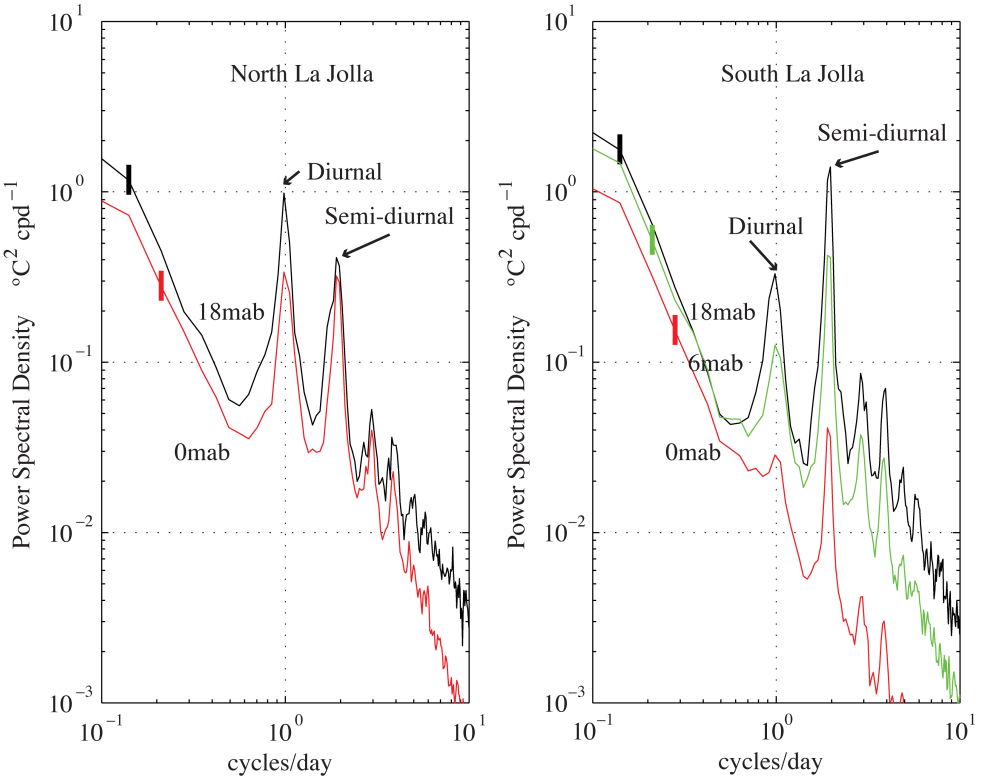

Figure 3.5: A periodogram estimating the power spectral density calculated using Welch's averaged periodogram method with a section length of two weeks, zero overlap, and a Hamming window. Vertical bars represent the 95% confidence interval for a given depth. Red line is the bottom (0mab), green is at 6 mab and black at 18 mab.

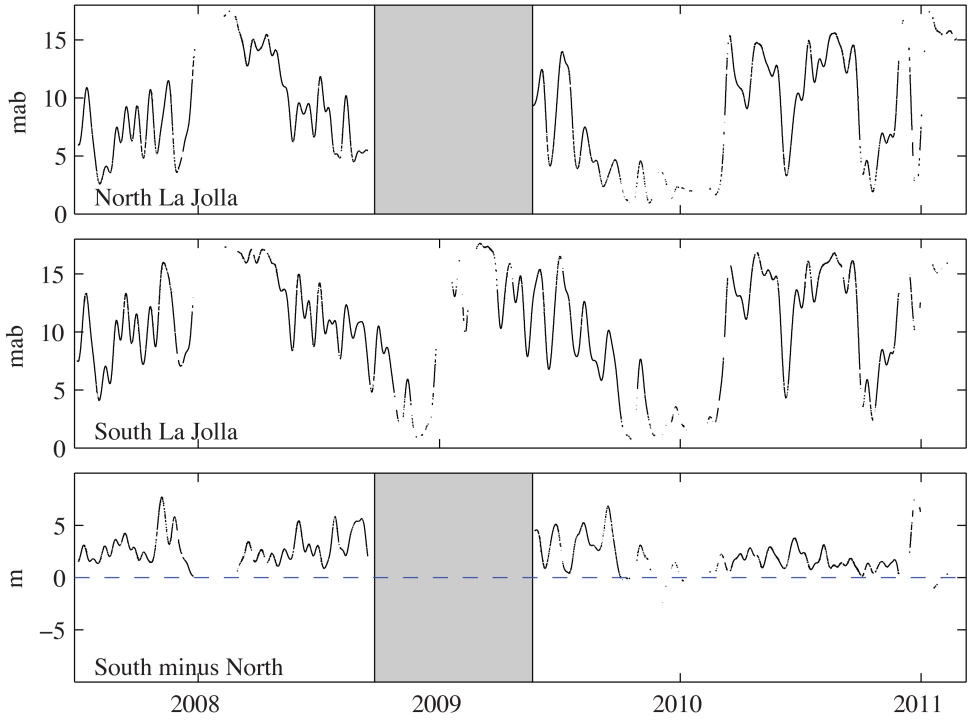

Figure 3.6: Depth (mab) of the 14.5°C isotherm through time shown for North La Jolla in the top panel and South La Jolla in the middle panel (1-week running-mean filtered data). At depths below this isotherm predicted levels of nitrate are above 0 µmol/L. The third panel shows the difference in meters of the depth of the 14.5°C isotherm between the two sites through time. Positive values indicate a shallower isotherm in the south (more of the water column bathed in nitrate) as compared to North La Jolla. Grey box indicates missing data.

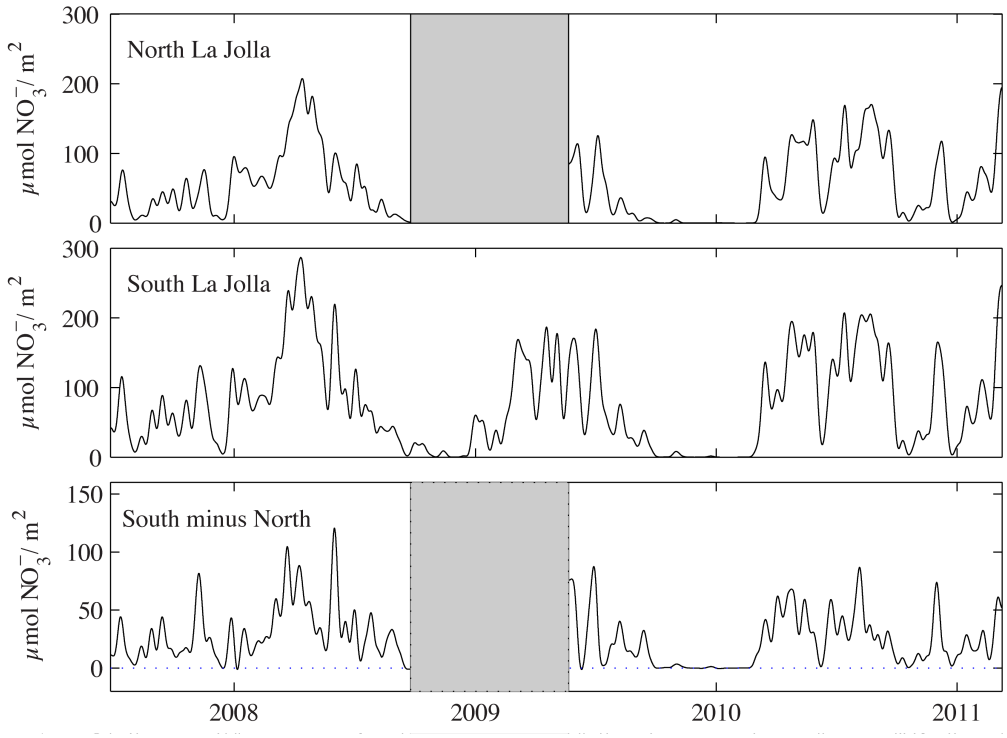

Figure 3.7*:* Predicted water column integrated nitrate through time for a m^2 of substrate calculated using the equation: nitrate = -5.1 T +72 (fit < 14.5°C) which is based on CalCOFI line 93 temperature-nitrate measurements collected from 1965-2008 (figure 6, Lucas et al., 2011). Grey box indicates missing data.

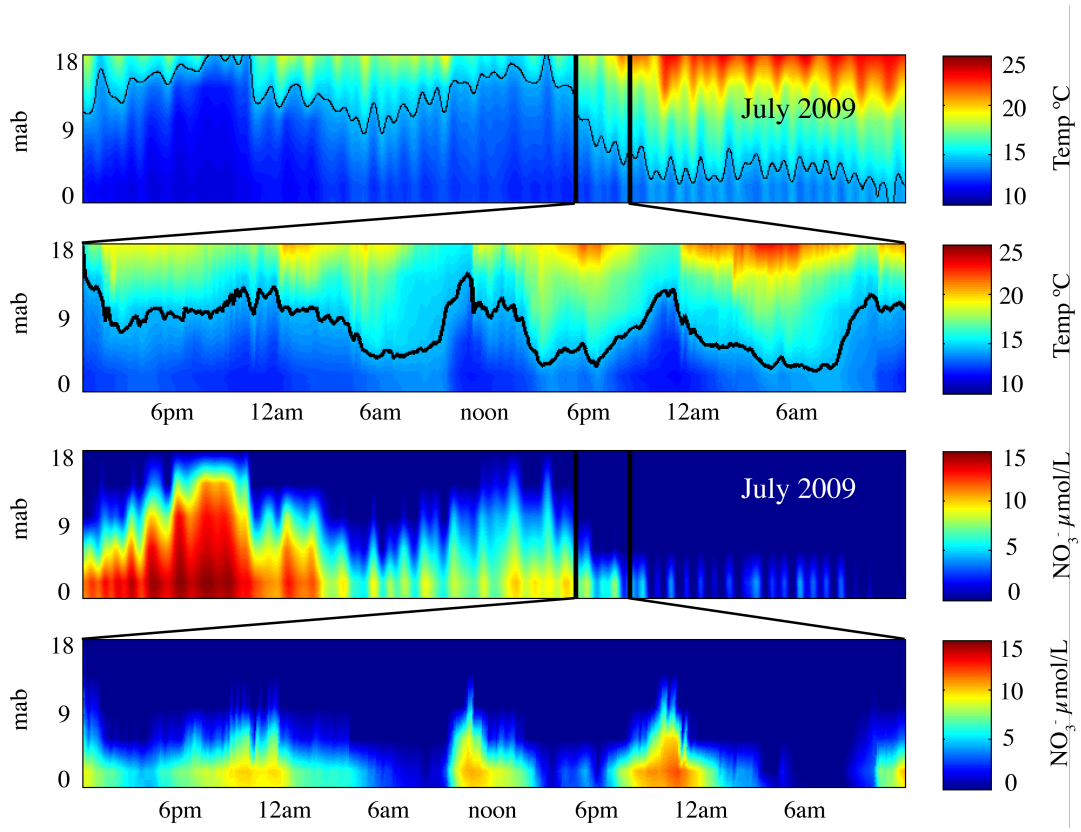

Figure 3.8: Linearly interpolated temperature and nitrate plots from July 2009 for North La Jolla. Linearly interpolated temperature plot using 6-hour running mean filtered temperature data for the month of July 2009 (top panel) and a zoomed in look at July 19-21st (second panel), as an example demonstrating that the depth of the 14.5°C isotherm can vary by several meters over the span of a few hours. Black lines represent the 14.5°C isotherm. The bottom two panels are interpolated predicted nitrate (calculated as in figure 3.7) for the same time periods as the top two panels.

Table 3.1: Temperature statistics broken down by month of year at North and South La Jolla. At the two sites, for the 18 mab and bottom temperature time series, the following statistics were calculated: mean temperature, range, variance, and the percentage of the time series that the temperature was less than or equal to 14.5°C (i.e. where predicted nitrate is greater than 0 μmol/L) and the average of those values.

		JAN	FEB	MAR	APR	MAY	JUN	JUL	AUG	SEP	OCT	NOV	DEC	mean
North	mean temp	14.34	14.47	14.64	15.47	17.69	19.02	19.06	20.14	19.02	18.20	16.85	15.04	16.99
La Jolla	range	1.58	2.09	4.00	5.35	7.31	6.16	10.00	8.17	8.84	6.21	3.88	3.04	5.55
18 mab	variance	0.06	0.10	0.40	0.71	0.85	1.30	5.16	3.13	2.42	1.19	0.66	0.55	1.38
	below 14.5C	0.67	0.63	0.28	0.14	0.04	0.01	0.06	0.04	0.03	0.01	0.03	0.23	0.18
North	mean temp	13.68	13.50	12.02	11.68	11.69	12.56	12.54	13.05	13.35	14.25	14.06	14.08	13.04
La Jolla	range	2.39	2.79	3.89	4.18	5.15	4.98	4.86	4.56	5.20	5.77	4.43	3.63	4.32
bottom	variance	0.21	0.33	0.59	0.61	0.90	1.11	0.81	0.57	0.63	0.92	0.73	0.82	0.68
	below 14.5C	0.77	0.75	0.95	0.99	0.98	0.93	0.95	0.89	0.85	0.57	0.60	0.52	0.81
South	mean temp	14.18	14.30	14.13	14.80	16.50	17.77	17.77	18.67	17.40	17.67	16.09	14.86	16.18
La Jolla	range	1.26	1.42	3.51	5.97	7.01	7.10	9.78	9.05	8.26	5.55	4.70	3.00	5.55
18 mab	variance	0.06	0.07	0.46	1.33	1.72	2.41	5.71	4.01	3.46	1.11	0.77	0.61	1.81
	below 14.5C	0.71	0.70	0.54	0.30	0.10	0.07	0.13	0.09	0.09	0.01	0.10	0.28	0.26
South	mean temp	13.56	13.20	11.37	11.20	11.30	12.20	12.17	12.54	12.96	13.92	13.71	13.98	12.68
La Jolla	range	2.08	2.64	2.38	3.19	3.42	4.35	3.03	3.39	3.54	3.49	4.05	3.75	3.28
bottom	variance	0.26	0.40	0.36	0.36	0.60	0.99	0.45	0.33	0.42	0.54	0.65	1.09	0.54
	below 14.5C	0.76	0.78	0.98	1.00	1.00	0.97	0.99	0.97	0.97	0.69	0.69	0.53	0.86

References

Bassin, C., Washburn, L., Brzezinski, M., and McPhee-Shaw, E. (2005). Sub-mesoscale coastal eddies observed by high frequency radar: a new mechanism for delivering nutrients to kelp forests in the Southern California Bight. Geophysical Research Letters *32*, L12604.

Bray, R., Purcell, L., and Miller, A. (1986). Ammonium excretion in a temperate-reef community by a planktivorous fish, *Chromis punctipinnis* (Pomacentridae), and potential uptake by young giant kelp, *Macrocystis pyrifera* (Laminariales). Marine Biology *90*, 327–334.

Cavanaugh, K., Siegel, D., Kinlan, B., and Reed, D. (2010). Scaling giant kelp field measurements to regional scales using satellite observations. Marine Ecology Progress Series *403*, 13–27.

Cie, D., and Edwards, M. (2011). Vertical distribution of kelp zoospores. Phycologia *50*, 340–350.

Cudaback, C., and McPhee-Shaw, E. (2009). Diurnal-period internal waves near point conception, California. Estuarine, Coastal and Shelf Science *83*, 349–359.

Dayton, P., Tegner, M., Edwards, P., and Riser, K. (1998). Sliding baselines, ghosts, and reduced expectations in kelp forest communities. Ecological Applications *8*, 309–322.

Dayton, P., Tegner, M., Edwards, P., and Riser, K. (1999). Temporal and spatial scales of kelp demography: The role of oceanographic climate. Ecological Monographs *69*, 219–250.

Dayton, P.K. (1985). Ecology of kelp communities. Annual Review of Ecology and Systematics *16*, 215–245.

Dayton, P.K., Currie, V., Gerrodette, T., Keller, B.D., Rosenthal, R., and Tresca, D.V. (1984). Patch dynamics and stability of some California kelp communities. Ecological Monographs *54*, 253.

Dean, T., and Jacobsen, F. (1984). Growth of juvenile *Macrocystis pyrifera* (Laminariales) in relation to environmental factors. Marine Biology *83*, 301–311.

Denny, M., Helmuth, B., Leonard, G., Harley, C., Hunt, L., and Nelson, E. (2004). Quantifying scale in ecology: lessons from a wave-swept shore. Ecological Monographs *74*, 513–532.

Espinoza, J., and Chapman, A. (1983). Ecotypic differentiation of *Laminaria longicruris* in relation to seawater nitrate concentration. Marine Biology *74*, 213–218.

Fink, L.A., and Manley, S.L. (2011). The use of kelp sieve tube sap metal composition to characterize urban runoff in southern California coastal waters. Marine Pollution Bulletin 1–14.

Fram, J., Stewart, H., Brzezinski, M., Gaylord, G., Reed, D., Williams, S., and MacIntyre, S. (2008). Physical pathways and utilization of nitrate supply to the giant kelp, *Macrocystis pyrifera*. Limnology and Oceanography *53*, 1589–1603.

Gaylord, B., Rosman, J., Reed, D., Koseff, J., Fram, J., MacIntyre, S., Arkema, K., McDonald, C., Brzezinski, M., Largier, J., et al. (2007). Spatial patterns of flow and their modification within and around a giant kelp forest. Limnology and Oceanography *52*, 1838–1852.

Gerard, V. (1982a). Growth and utilization of internal nitrogen reserves by the giant kelp *Macrocystis pyrifera* in a low-nitrogen environment. Marine Biology *66*, 27–35.

Gerard, V. (1982b). In situ rates of nitrate uptake by giant kelp, *Macrocystis pyrifera* (L.) C. Agardh: Tissue differences, environmental effects, and predictions of nitrogen-limited growth. Journal of Experimental Marine Biology and Ecology *62*, 211–224.

Gerard, V. (1986). Photosynthetic characteristics of the giant kelp (*Macrocystis pyrifera*) determined *in situ*. Marine Biology *90*, 473–482.

Graham, M., Dayton, P., and Erlandson, J. (2003). Ice ages and ecological transitions on temperate coasts. Trends in Ecology & Evolution *18*, 33–40.

Graham, M., Harrold, C., Lisin, S., Light, K., Watanabe, J., and Foster, M. (1997). Population dynamics of giant kelp *Macrocystis pyrifera* along a wave exposure gradient. Marine Ecology Progress Series *148*, 269–279.

Graham, M., Vásquez, J., and Buschmann, A. (2007). Global ecology of the giant kelp *Macrocystis* from ecotypes to ecosystems. Oceanography and Marine Biology: an Annual Review *45*, 39–88.

Haines, K., and Wheeler, P. (1978). Ammonium and nitrate uptake by the marine macrophytes *Hypnea musciformis* (Rhodophyta) and *Macrocystis pyrifera* (Phaeophyta). Journal of Phycology *14*, 319–324.

Haxen, P., and Lewis, O. (1981). Nitrate assimilation in the marine kelp, *Macrocystis angustifolia* (Phaeophyceae). Botanica Marina *24*, 631–635.

Hepburn, C., and Hurd, C. (2005). Conditional mutualism between the giant kelp *Macrocystis pyrifera* and colonial epifauna. Marine Ecology Progress Series *302*, 37–48.

Hernández-Carmona, G., Robledo, D., and Serviere-Zaragoza, E. (2001). Effect of nutrient availability on *Macrocystis pyrifera* recruitment and survival near its southern limit off Baja California. Botanica Marina *44*, 221–229.

Jackson, G. (1977). Nutrients and production in the Giant Kelp, Macrocystis pyrifera, off southern California. Limnology and Oceanography *22*, 979–995.

Jackson, G. (1998). Currents in the high drag environment of a coastal kelp stand off California. Continental Shelf Research *17*, 1913–1928.

Jackson, G., and Winant, C. (1983). Effect of a kelp forest on coastal currents. Continental Shelf Research *2*, 75–80.

Kamykowski, D., and Zentara, S.-J. (1986). Predicting plant nutrient concentrations from temperature and sigma-*t* in the upper kilometer of the world ocean. Deep Sea Research *33*, 89–105.

Kopczak, C., Zimmerman, R., and Kremer, J. (1991). Variation in nitrogen physiology and growth among geographically isolated populations of the Giant Kelp, *Macrocystis pyrifera* (Phaeophyta). Journal of Phycology *27*, 149–158.

Ladah, L.B. (2003). The shoaling of nutrient-enriched subsurface waters as a mechanism to sustain primary productivity off Central Baja California during El Niño winters. Journal of Marine Systems *42*, 145–152.

Lucas, A., Dupont, C., Tai, V., Largier, J., Palenik, B., and Franks, P. (2011). The green ribbon: Multiscale physical control of phytoplankton productivity and community structure over a narrow continental shelf. Limnology and Oceanography *56*, 611–626.

Manley, S. (1983). Composition of sieve tube sap from *Macrocystis pyrifera* (Phaeophyta) with emphasis on the inorganic constituents. Journal of Phycology *19*, 118–121.

Mann, K. (2000). Subtidal rocky shores. In Ecology of Coastal Waters, (Malden, MA: Blackwell Science), pp. 191–217.

McFarland, W., and Prescott, J. (1959). Standing crop, chlorophyll content and *in situ* metabolism of a Giant Kelp community in Southern California. Publications of the Institute of Marine Science *6*, 109–132.

McPhee-Shaw, E., Siegel, D., Washburn, L., Brzezinski, M., Jones, J., Leydecker, A., and Melack, J. (2007). Mechanisms for nutrient delivery to the inner shelf: Observations from the Santa Barbara Channel. Limnology and Oceanography *52*, 1748–1766.

Nam, S., Kim, H., and Send, U. (2011). Amplification of hypoxic and acidic events by La Niña conditions on the continental shelf off California. Geophysical Research Letters *38*.

Parnell, P., Dayton, P., Lennert-Cody, C., Rasmussen, L., and Leichter, J. (2006). Marine reserve design: optimal size, habitats, species affinities, diversity, and ocean microclimate. Ecological Applications *16*, 945–962.

Parnell, P., Miller, E., Lennert-Cody, C., Dayton, P., Carter, M., and Stebbins, T. (2010). The response of giant kelp (*Macrocystis pyrifera*) in southern California to low-frequency climate forcing. Limnology and Oceanography *55*, 2686–2702.

Pérez-Mayorga, D., Ladah, L., Zertuche-Gonzalez, J., Leichter, J., Filonov, A., and Lavin, M. (2011). Nitrogen uptake and growth by the opportunistic macroalga *Ulva lactuca* (Linnaeus) during the internal tide. Journal of Experimental Marine Biology and Ecology *406*, 108–115.

Pineda, J. (1991). Predictable upwelling and the shoreward transport of planktonic larvae by internal tidal bores. Science *253*, 548–551.

Pineda, J. (1999). Circulation and larval distribution in internal tidal bore warm fronts. Limnology and Oceanography *44*, 1400–1414.

Pringle, J., and Riser, K. (2003). Remotely forced nearshore upwelling in Southern California. Journal of Geophysical Research *108*, 3131.

Rosman, J., Monismith, S., Denny, M., and Koseff, J. (2010). Currents and turbulence within a kelp forest (*Macrocystis pyrifera*): Insights from a dynamically scaled laboratory model. Limnology and Oceanography *55*, 1145–1158.

Schmitz, K., and Srivastava, L. (1979). Long distance transport in *Macrocystis integrifolia*. I. translocation of ^{14}C-labeled assimilates. Plant Physiology *63*, 995–1002.

Seymour, R., Tegner, M., Dayton, P., and Parnell, P. (1989). Storm wave induced mortality of giant kelp, *Macrocystis pyrifera*, in Southern California. Estuarine, Coastal and Shelf Science *28*, 277–292.

Stekoll, M., and Else, P. (1990). Cultivation of *Macrocystis integrifolia* (Laminariales, Phaeophyta) in southeastern Alaskan waters. Hydrobiologia *204/205*, 445–451.

Steneck, R., Graham, M., Bourque, B., Corbett, D., Erlandson, J., Estes, J., and Tegner, M. (2002). Kelp forest ecosystems: biodiversity, stability, resilience and future. Environmental Conservation *29*, 436–459.

Stewart, H., Fram, J., Reed, D., Williams, S., Brzezinski, M., MacIntyre, S., and Gaylord, B. (2008). Differences in growth, morphology and tissue carbon and nitrogen of *Macrocystis pyrifera* within and at the outer edge of a giant kelp forest in California, USA. Marine Ecology Progress Series *375*, 101–112.

Sykes, M. (1908). Anatomy and histology of *Macrocystis pyrifera* and *Laminaria saccharina*. Annals of Botany *22*, 291–325.

Tegner, M., and Dayton, P. (1991). Sea urchins, El Niños and the long term stability of Southern California kelp forest communities. Marine Ecology Progress Series *77*, 49–63.

Tegner, M., Dayton, P., Edwards, P., and Riser, K. (1997). Large-scale, low-frequency oceanographic effects on kelp forest succession: A tale of two cohorts. Marine Ecology Progress Series *146*, 117–134.

Towle, D., and Pearse, J. (1973). Production of the giant kelp, *Macrocystis*, estimated by in situ incorporation of ^{14}C in polyethylene bags. Limnology and Oceanography *18*, 155–159.

Wernberg, T., and Goldberg, N. (2008). Short-term temporal dynamics of algal species in a subtidal kelp bed in relation to changes in environmental conditions and canopy biomass. Estuarine, Coastal and Shelf Science *76*, 265–272.

Wheeler, W., and Srivastava, L. (1984). Seasonal nitrate physiology of *Macrocystis integrifolia*. Journal of Experimental Marine Biology and Ecology *76*, 35–50.

Witman, J., Etter, R., Smith, F., and Paine, R. (2004). The relationship between regional and local species diversity in the marine benthic communities: a global perspective. Proceedings of the National Academy of Sciences *101*, 15664–15669.

Wolanski, E., and Hamner, W. (1988). Topographically controlled fronts in the ocean and their biological influence. Science *241*, 177–181.

Young, E., Dring, M., Savidge, G., Birkett, D., and Berges, J. (2007). Seasonal variations in nitrate reductase activity and internal N pools in intertidal brown algae are correlated with ambient nitrate concentrations. Plant, Cell and Environment *30*, 764–774.

Zimmerman, R., and Kremer, J. (1986). In situ growth and chemical composition of the giant kelp, *Macrocystis pyrifera*: response to temporal changes in ambient nutrient availability. Marine Ecology Progress Series *27*, 277–285.

Zimmerman, R., and Robertson, D. (1985). Effects of El Niño on local hydrography and growth of the giant kelp, *Macrocystis pyrifera,* at Santa Catalina Island, California. Limnology and Oceanography *30*, 1298–1302.

CHAPTER 4

Transcriptomic Analysis of Metabolic Function in the Giant Kelp, *Macrocystis pyrifera,* Across Depth and Season

Abstract

Macrocystis pyrifera is exposed to a range of depth-dependent light, temperature, and nitrate conditions that vary across a range of temporal and spatial scales. To understand how *M. pyrifera* reacts physiologically to this variable physical environment, we sought to increase the number of identified transcriptional units using Roche 454 pyrosequencing technology. To obtain a diversity of transcripts, we sequenced four cDNA libraries created from *M. pyrifera* samples collected in La Jolla from the sea surface and at 18m depth during the winter and summer of 2009. Assembly of filtered reads generated ~9,000 contigs. Annotations are difficult when working with a eukaryotic organism without a sequenced genome; a large portion of contigs was unannotatable via BLAST and HMM approaches. Of those that could be annotated, top hits were to *Ectocarpus siliculosus* and *Laminaria digitata*, and members of the Phaeophyceae. QPCR validation of transcripts revealed depth-related differences in function. Stress response and light harvesting genes, especially members of the LI818 family, showed high expression in the surface compared to at depth. Some nitrogen acquisition genes (e.g. nitrite reductase) were upregulated at depth compared to at the surface.

Introduction

Macrocystis pyrifera, the largest alga on earth and reaching tens of meters in length, is a dominant space competitor on temperate rocky reefs and provides a three-dimensional structure that supports many fish and invertebrate species (Dayton, 1985). Throughout its large geographic range, *M. pyrifera* is exposed to gradients of depth-dependent light, temperature, and nitrate conditions that vary on multiple temporal and spatial scales. Single individuals spanning the water column experience variations in these conditions. Despite reaching great heights, *M. pyrifera* does not possess a vascular system for metabolite transport as plants do. Instead, organic material is transported via specialized conducting cells with large pores called sieve tube cells; the composition of sieve tube sap is approximately 65% mannitol and 15% amino acids (Parker, 1966; Manley, 1983). One way that *M. pyrifera* may balance internal carbon and nitrogen under limiting conditions is through mannitol transport downward and amino acid transport upwards, especially at times of the year when upper parts of the kelp are not exposed to nitrate (e.g. during typical southern California summer stratified water column conditions) (Figure 4.1). The majority of photosynthesis occurs in the surface canopy with half of the standing crop lying between the surface and 1.5 m as fronds reach and spread along the surface (McFarland and Prescott, 1959; Towle and Pearse, 1973; Gerard, 1986). The daily increase in the dry weight of the growing tip (apical region) is greater than the products of its photosynthesis; additionally, blades further down the stipe have rates of photosynthesis that exceed their rate of growth implying likely transport of materials (Sargent and Lantrip, 1952).

Biological processes in kelp affected by nitrate include: recruitment, growth, survivorship, reproductive output, and stress tolerance (Mann, 1973; Jackson, 1977; Zimmerman and Kremer, 1986). Thus, the amount of nitrate exposure can have a large effect on the condition and existence of a kelp bed. There is a strong linear relationship between nitrate and temperature in the southern California nearshore at temperatures below 14.5°C, with colder waters possessing more nitrate (Kamykowski and Zentara, 1986; Dayton et al., 1999; Lucas et al., 2011); at temperatures above 14.5°C, nitrate levels are not generally measurable. Seasonally, in southern California, surface nitrate concentrations are low for most of the year, but increase during the winter when the water column is well mixed or upwelling occurs (Jackson, 1977). In the late summer months, when the surface temperatures rise and nutrient concentrations decrease, the surface canopy of kelp forests decline in extent (Jackson, 1977; North and Zimmerman, 1984). However, parts of kelp below the thermocline (not seen in aerial surveys) may remain healthy (North and Zimmerman, 1984). Sources of nitrate include wind-driven upwelling, upwelling from shoaling internal waves, and terrestrial sources. Nitrate is often the limiting nutrient for *M. pyrifera*, though at times phosphate may be limiting (Manley, 1985). *M. pyrifera* is also able to use ammonia as an alternate form of nitrogen though it is not as readily available as nitrate (Haines and Wheeler, 1978). Three general scenarios for kelp nutrient exposure are: (1) sufficient nitrate that is well-mixed throughout the water column (more common in the winter, during prolonged periods of wind-driven upwelling or in northern parts of the species range), (2) summer-time stratified conditions where the bottom portion of a *M. pyrifera* individual is exposed to nitrate and the upper portion

is bathed in nitrate-deplete waters, and (3) the most extreme scenario when the thermocline deepens below the shelf and the entire *M. pyrifera* is exposed to nitrate deplete water (i.e. <0.1 μmol/L) potentially for extended periods (i.e. days to weeks/months).

The photosynthetically available light for *M. pyrifera* is greatest at the surface and exponentially decreases with depth with ~1% of surface light levels typically reaching 20m in the kelp forest (Gerard, 1984). Available light shows a seasonal peak in the summer (Dean, 1985). Wavelength-specific attenuation of light in the ocean changes the spectrum of light that reaches the depths and the chlorophyll *c* and fucoxanthin pigment complex of brown algae allows for highly efficient conversion of the deepest penetrating blue-green wavelengths. Canopy shading by the kelp itself and particulate matter (both organic and inorganic) negatively affect light penetration, leading to decreased carbon fixation and growth by *M. pyrifera* blades (Towle and Pearse, 1973; Dean, 1985; Wing et al., 1993). While low light limits photosynthesis, excess light can damage photosystem II leading to oxidative stress. In response, algae have adaptations to optimize light absorption under a variable light availability through differential expression of light harvesting complexes, some of which are involved in both light capture and photoprotection (Peers et al., 2009).

Kelps respond physiologically on different temporal and spatial scales to their physical environment. For example, during summer months and El Niño years, temperatures rise, nutrients decrease, and ultimately kelp densities decrease (Jackson, 1997; Dayton et al., 1999). Outward phenotypic signs of stress may include sloughing of tissue, increased epiphytic growth, disease and ultimately senescence—the final

result of the sum of kelp physiological responses to stressors over an integrated amount of time. How *M. pyrifera* is responding on a cellular level at much shorter time scales before these conspicuous phenotypic changes manifest is unknown. Genomic information is sparse for macroalgae (Jamers et al., 2009); however, decreased sequencing costs and an increase in sequencing capabilities make it possible to examine species beyond the typical or traditional model and laboratory organisms. Additionally, the presence of both single celled and multicellular heterokont genomes (i.e. the diatoms *Phaeodactylum tricornutum*, *Thalassiosira pseudonana*, and *Aureococcus anophagefferens*, and the filamentous brown alga *Ectocarpus siliculosus*) and expressed sequence tags provides phylogenetic reference and potential model systems for detailed functional information (Armbrust et al., 2004; Bowler et al., 2008; Cock et al., 2010b). In order to be able to answer questions such as 'how do kelps regulate gene expression in response to interval-wave time-scale pulses of cold water?' we need to develop new tools. For this example, canonical pathways for nitrate uptake, reduction and incorporation into proteins are well known; however, the gene models and transcript sequences for these important enzymes in *M. pyrifera* are not. In this study, we use an RNA-Seq approach to investigate the transcripts from four *M. pyrifera* libraries spanning the water column and seasons. Objectives of this study were to: (1) increase the number of annotated transcriptional units (TUs) for *M. pyrifera,* (2) develop sequence-based tools for ecophysiological study, (3) examine physiological patterns in response to light, temperature, and nitrate.

Materials and Methods

Sample Collection

Blade tissue was sampled from *Macrocystis pyrifera* individuals in La Jolla, California, USA (N 32° 51.0; W 117° 17.5) on 7 January 2009 and 31 July 2009 using SCUBA. On each date, pieces of blade tissue were collected at the sea surface (0m) and at 18m depth, along the same stipe, for a total of four pieces of blade tissue used for transcriptomic library preparation. Surface blades were collected at least 1m away from the apical growing region and the sampling at 18m avoided the reproductive sporophylls near the base of an individual so that only one life stage was sampled. For consistency and to minimize within-blade variability, all samples were collected near the base of each blade. North (1971) reports no change in photosynthetic activity between intact and cut blades with cutting injury; any wounding effects were assumed to be consistent across samples. At the end of each dive, blades were immediately cleaned of any visible epiphytes by scrubbing with 100% ethanol and cheesecloth and then frozen on dry ice for transport to the lab.

To quantify the temperature of the water column and hence nutrient concentration, thermistor chain data were collected at 10 min intervals using TidBit temperature data loggers with ~0.2° resolution, and ~5 min response time (Onset, Bourne, Massachusetts, USA). TidBits were placed on the bottom (located in 22m water depth) and at 2, 6, 10, 14, and 18 meters above the bottom (mab). The temperature inset in Figure 4.1 is a box plot of the water temperature during the two weeks leading up to the day of collection.

Library Construction

RNA extraction followed a modified protocol (Apt et al., 1995). Frozen algal tissue was ground to a powder on liquid nitrogen then added to an extraction buffer (100mM TRIS-HCl pH 8.0, 1.5 M NaCl, 20mM EDTA, 20mM DTT and 2% CTAB) at 1:1 w/v ratio and mixed at room temperature (RT) for 15 min then heated to 65°C for 20 min. This was followed by a ½ volume chloroform extraction, 5 min at RT, then centrifugation at 10,000g for 30 min at 4°C, and collection of the supernatant. Addition of 1/3 volume ethanol was used to precipitate polysaccharides, which was followed by a second chloroform extraction. 3.0 M LiCl and 10% v/v β-mercaptoethanol was added to the aqueous phase and placed at -20°C overnight. RNA was precipitated by centrifugation at 14,000g for 30 min at 4°C and followed by two 75% ethanol washes before resuspension.

Total RNA was cleaned using RNeasy mini Kit and the optional DNase digestion (Qiagen; Valencia, CA, USA). RNA was amplified using MessageAmp II Kit (Ambion; Austin, TX, USA) with a second round of amplification. Single-strand cDNA was synthesized using SuperScript III (Invitrogen; Carlsbad, CA, USA) and oligo(dT) primers, then cleaned using RNAClean to remove salts, unincorporated primers and dNTPs (Agencourt, Beckman Coulter Genomics; Beverly, MA, USA). CloneMiner kit (Invitrogen) was used to synthesize second-strand cDNA and cleaned with AMPure (Agencourt). Size selected cDNA (.5 – 1 kb) from the four libraries was purified using QiaQuick gel extraction kit (Qiagen). A high sensitivity DNA Assay chip was used to assess quality (Agilent; Santa Clara, CA, USA).

De novo Transcriptome Assembly and Annotation Analysis

Each of the four libraries was sequenced on a ½ plate using pyrosequencing technology (454 Life Sciences, Roche; Branford, CT, USA). Reads were filtered using cd-hit-454 (Teal and Schmidt, 2010) and assembled using Newbler. Reads and isotigs were annotated using BLASTX searches conducted (cut-off 10^{-5}) against an internal JCVI database containing all completed and draft algal genomes as well as all Phaeophyceae EST libraries available in NCBI GenBank for annotation. Pairwise library comparisons of differentially expressed genes were calculated using edgeR (Robinson et al., 2010). ORFs were called from reads from all four libraries and were clustered using cd-hit at 60% identity (Li and Godzik, 2006).

qPCR Analysis of Gene Transcription

RNA was purified using RNeasy (Qiagen) and reverse transcribed using QuantiTect (Qiagen). PCR products were quantified on the same batch of cDNA to minimize experimental variation due to the cDNA synthesis process. Samples were run on 7900HT Fast Real-Time PCR system and 7500 Fast Real-Time PCR systems (Applied Biosystems; Carlsbad, CA, USA).

Using the annotations of the *M. pyrifera* ESTs to identify target TUs, we created primers for a variety of potential housekeeper genes and genes of interest (Le Bail et al., 2008). After exclusion of those with poorly amplified products, 16 potential reference genes were compared to select the most stable reference genes (Vandesompele et al., 2002). We use eukaryotic initiation factor 2 alpha subunit

(IF2A) and a protein required for 18S rRNA maturation and 40S ribosome biogenesis (18Smat) for housekeeper genes based on this analysis and their Ct range.

We chose to examine light harvesting genes because they showed obvious differences in the transcriptome and there is more knowledge about these genes compared to other genes in the Phaeophyceae class (Green et al., 1991; Green and Durnford, 1996; Dittami et al., 2010). Additionally, because of the large environmental differences in light and temperature/nutrients conditions with depth, we chose to look at various stress response, photosynthesis, carbon metabolism, and nutrient uptake genes (Table 4.1). The majority of candidate *M. pyrifera* sequences were aligned with the corresponding *E. siliculosus* sequence and primers (see Table 4.1) were created in the region of overlap using Primer 3 (Rozen and Skaletsky, 2000) with a target length of 100-150 bp and a max Tm difference < 8. RNA for qPCR came from the same extraction used to create the transcriptomic libraries. We quantified expression levels using quantitative real-time PCR via the delta-delta cycle threshold method (ΔΔCt) and report the data as fold change comparisons between the surface and depth.

Results

Transcriptomic Coverage and Annotation Results

Four libraries were sequenced with an average 118,000 reads per library after filtering artificial replicates (Gomez-Alvarez et al., 2009), an average read length of 323 bp, and GC content of 48% (Table 4.2). GC content falls within the range of reported values of 39.9 to 54 % for the Phaeophyceae (Le Gall et al., 1993). Reads

were assembled into 9184 contigs with a median size of 682 bp, and 1769 contigs of length >1000bp. For comparison, *E. siliculosus*, a small filamentous intertidal brown alga, has ~16,000 genes, of which 9,601 had EST support from 6 cDNA libraries corresponding to different developmental stages and growth conditions (Cock et al., 2010b). Approximately 68% of the total contigs were found in all four libraries (Figure 4.2) composing a large active transcriptional core across environmental gradients and giving us confidence in our ability to examine expression differences in transcripts common to all libraries.

Only 7-9% of reads in each library had a BLAST alignment using a conservative e-value cut-off of 10^{-5} because there is not much genetic data available for macroalgae and Phaeophyceae in general. Of the reads that matched: *E. siliculosus* had the highest percentage of matches (41-54%), which is encouraging because it is the only Phaeophyte with a sequenced genome. The next highest percentage of best matches was to *Laminaria digitata* (20-29%). There is a ~20 fold less genomic data available for *L. digitata* as there is for *E. siliculosus* (67106 total *Ectocarpus* reads vs. 3124 *Laminaria* reads in our EST database; Table 4.2). However, *L. digitata* is related to *M. pyrifera* at the family level, while *E. siliculosus* is related at a class level; percent similarity of orthologous proteins between *M. pyrifera* and *L. digitata* and *E. siliculosus* was 86.8% and 79.5% respectively (Figure 4.A1).

Approximately 106,000 ORF clusters were predicted at the 60% identity level and revealed the presence of several large clusters with no annotations. The main source of missing annotations appears to be from the singleton ORFans. For a cluster size of one (n=58955), only 6% had annotations. In comparison, for a cluster size of

100 or greater (n = 151), 34% had annotations for at least one member of the cluster. Many of the top size clusters did not have annotations, those that did were largely ribosomal proteins.

Physiological Patterns and Tool Demonstration

The most abundant KO transcript description in terms of read counts across all libraries were annotated as either large or small ribosomal protein (Table 4.5). Approximately half of the top 50 did not have an annotation. Patterns between surface and depth emerged in the differential expression comparisons (Tables 4.6 & 4.7). Seasonal comparisons at the same depth are listed in Tables 4.8 and 4.9. Annotated genes upregulated in the surface included photosynthesis and damage repair genes, while at depth ribosomal proteins dominated.

BLAST searches of the transcriptome assembly identified nine contigs coding for putative light harvesting complex (LHC) proteins. A phylogenetic analysis of the *M. pyrifera* LHC and the LHC from other heterokonts, grouped the *M. pyrifera* LHC isotigs into canonical LHC groups FCP, LHCR and LI818 (Table 4.3). In both seasons, all nine *Mp*LHC showed higher qPCR fold change expression at the surface compared to at depth, with the putative LI818 having the most extreme levels of up-regulation (Figure 4.3 B&C). Two of the *Mp*LHC phylogenetically lie within the LI818 group (Figure 4.3A) and showed the highest expression differences from the surface to depth of all the *Mp*LHCs.

We also examined the expression proteins known to be involved in stress response, and in carbon and nitrogen metabolism using qPCR (Table 4.1). Several

stress-related genes showed patterns of higher expression at the surface during both seasons: an antioxidant protein of the periredoxin group (ATPRX_Q); L-ascorbate peroxidase, and vanadium bromoperoxidase (Figure 4.4). ATPRX_Q showed the greatest fold change in the surface compared to depth in both seasons. Two carbon metabolism genes showed higher surface expression in both seasons: mannitol-1-phosphate 5-dehydrogenase (M1Pase) and ribose-5-phosphate isomerase (r5pi). Mannitol-1-phosphate 5-dehydrogenase is involved in metabolism of mannitol, one of the main storage carbohydrates in *M. pyrifera*. Ribose-5-phosphate isomerase, an enzyme involved in the pentose phosphate pathway producing sugars and NADPH, was upregulated in the surface. In January, several other photosynthesis-related and carbon fixation genes showed up-regulation in the surface: glycine decarboxylase complex; uroporphyrinogen decarboxylase (involved in porphyrin and chlorophyll metabolism); PsbP, the photosystem II oxygen evolution complex protein required for PSII to be fully operational; and a putative carbonic anhydrase. A spermidine/spermine synthase (thought to be a regulator in stress signaling pathways) showed higher expression in the surface (Kasukabe et al., 2004). Also, pyruvate dehydrogenase, which is involved in TCA cycle and glycolysis/gluconeogenesis, was upregulated in the surface, as was malate dehydrogenase, which is involved in carbon fixation.

In contrast, genes with higher expression at depth in both seasons included nitrite reductase and alpha-(1,2) mannosyltransferase. Nitrite reductase catalyzes the conversion of nitrite into ammonia. Nitrite reductase is usually regulated in coordination with nitrate reductase, as was the case in the January samples. There are

many factors that influence the transcription and activity of nitrate reductase including light (Crawford et al., 2000). Temperatures below 14.5°C occurring at both the surface and depth in January suggest the presence of biologically available levels of nitrate at both depths (Figure 4.1). Expression was still higher at depth, perhaps indicating regulation by light (Dohler et al., 1995) or greater nutrient accumulation at depth. Phosphofructokinase, found in glycolysis and other sugar metabolism pathways, had higher expression at depth in January.

Discussion

Contributing to the Genomic Knowledge of the Phaeophyceae

E. siliculosus is the only Phaeophyte with a sequenced genome and was chosen as a model for the Phaeophyceae because it possesses several attractive features including small genome size, short life cycle and amenability to laboratory genetic experiments (Peters et al., 2004; Cock et al., 2010b). The Phaeophyceae are a diverse group, morphologically and reproductively, and additional exploration of members of this group could yield insights into potentially unique evolutionary and physiological traits. *M. pyrifera* has evolved complex structural features such as sieve tubes for the transport of materials and may have novel genes and pathways involved in the creation and maintenance of these structures. The transcripts from this study were collected from the *M. pyrifera* sporophyte generation. The transcriptome of one life history stage will not reveal the whole gene repertoire of the species. With additional cDNA sequencing of the gametophyte generation (Roeder et al., 2005), reproductive sporophylls, the apical growing region or other morphological parts, it is reasonable to

expect that the number of annotated TUs for *M. pyrifera* will increase. Knowledge remains limited because many genes cannot be assigned a function through traditional BLAST based approaches. We employed cluster analysis to link unknown genes to known genes which provided a starting point to explore the function of unknown genes. Also, linking ecological and physiological studies with gene expression data in an iterative process can help with future annotations. Comparative approaches are aiding this process, and will become more helpful as available sequence data improves within this group.

Insights from Comparative Genomics

Macrocystis and the Phaeophyceae belong to the Stramenopile lineage which is thought to have diverged from other major eukaryotic groups over a billion years ago (Douzery et al., 2004; Yoon et al., 2004). As a result unique metabolic and developmental features have evolved (Cock et al., 2010a; 2010b). Four fully sequenced and publically available Heterokont genomes, *Thalassiosira pseudonana* (Armbrust et al., 2004), *Phaeodactylum tricornutum* (Bowler et al., 2008), *Aureococcus anophagefferens* (Gobler et al., 2011) and *Ectocarpus siliculosus* (Cock et al., 2010b), provide a new opportunity for comparative genomics and gene discovery in this group. Comparative analyses have identified transcription factors in heterokonts (Rayko et al., 2010). Transcription factors are important in the regulation of gene expression and many different families exist. Comparing the *T. pseudonana* and *P. tricornutum* TF sequences from Rayko et al. (2010) against our *M. pyrifera*

transcripts (10^{-5} E value and > 60% identity, we found 5 putative TF (3 Myb, 1 CCHH, 1 bZIP) and 4 TF (2 Myb, 1 CCHH, 1 bZIP) respectively.

The brown algae have unique carbohydrate metabolism. D-mannitol and laminarin (β-1,3-glucan) are the primary storage carbohydrates of brown algae as compared to the α-1,4-glucans (glycogen or starch) of most living organisms (Michel et al., 2010). Sucrose metabolism genes (e.g. sucrose-phosphate synthases, sucrose-phosphate phosphatase and invertases) were not found in the genome of *E. siliculosus* (or in a metabolite analysis) or diatoms or Oomycetes. We also did not find evidence in our annotation for sucrose metabolism genes. Additionally, through a comparative genomic approach with *Ectocarpus siliculosus*, we identified various carbon metabolism genes in *M. pyrifera* genes (Table 4.4). Brown algae are thought to potentially possess C4 or CAM metabolism (Kremer and Kuppers, 1977; Axelsson, 1988; Cock et al., 2010b). Genes used in other organisms in the C4 cycle and found in our *M. pyrifera* annotations include: malate dehydrogenase (NAD/NADP), aspartate aminotransferase, malate dehydrogenase (oxaloacetate-decarboxylating), alkaline transaminase, and fructoskinase (supp 21, Cock et al., 2010b).

Application of Transcriptomic Information to Develop Tools for Ecological Study

Our broad untargeted transcriptomic view allows us to begin to identify key mechanisms in the physiological and metabolic reactions to a variable environment. The identification of transcriptional units and development of primer sets for

examining expression of select metabolic genes enables targeted hypothesis testing of physiological response to environmental conditions.

At the surface, where irradiance levels are highest and the potential for oxidative damage is most intense, physiological processes are focused on protection from the damaging effects of the sun as well as the capture of light energy for photosynthesis. Several stress related proteins showed higher expression levels at the surface in both seasons including antioxidant proteins (i.e. ATPRX_Q) and peroxide proteins (i.e. L-ascorbate peroxidase and vanadium bromoperoxidase). Ascorbate peroxidases are associated with photo-oxidative stress in algae (Ishikawa and Shigeoka, 2008). Vanadium bromoperoxidases are found in several species of brown algae and are also thought to be involved in biotic and abiotic stress response (La Barre et al., 2010). The intense and variable light environment at the surface upregulates stress-response genes. Our annotation also revealed the presence of iron/manganese and copper/zinc superoxide dismutases, which protect cellular components from damage by the highly reactive superoxide.

Light appears to regulate gene expression strongly in *M. pyrifera*. The high expression at the surface of the LI818 *Mp*LHCs is consistent with a role in photoprotection (e.g. non-photochemical quenching) in a highly variable environment (Peers et al., 2009). Having multiple LHCs may indicate the importance of being able to fine-tune control of photosynthesis electron flow for blades exposed to intermittent high and low irradiances at the surface. All the light harvesting complex genes showed higher expression in the surface compared to at depth, with those in the LI818 clade having the largest fold change difference (Figure 4.4). Other studies show

functional differentiation between surface and basal blades in terms of photobiology (Gerard, 1986; Colombo Pallotta et al., 2006). Surface blades showed enhanced photoprotection, highest maximum photosynthetic rate, highest photosystem II (PSII) electron transport rate, and decreased pigment concentration, and lower photosynthetic efficiency as compared to basal blades (Colombo Pallotta et al., 2006). Other highly expressed carbon fixation genes at the surface include ribose-5-phosphate isomerase, glycine decarboxylase, and carbonic anhydrase. The photosystem II protein PsbP also showed high surface expression. Deeper blades tend to be shaded by the canopy and generally acclimated to low light conditions. Longer-term physiological adaptations of *M. pyrifera* (vs. gene expression) include higher relative amounts of chlorophyll and fucoxanthin in blades found at 20m as compared to surface blades (Smith and Melis, 1987). Blade relocation and canopy removal experiments showed that differences in light use efficiency were likely due to acclimation to light conditions rather than age (Gerard, 1986).

At the base of the kelp, where nutrient levels tend to be much higher than at the surface, especially during the stratified summer months, incorporation of nitrogen into amino acids and ultimately proteins may be a dominant process. This is evidenced by the upregulation of nitrite reductase (NiR) at depth, which catalyzes the conversion of nitrite into ammonium. However, nitrate uptake has been shown to be inversely proportional to tissue nitrogen (which varies with seasonal changes in ambient nitrate) and to be higher in subapical blades compared to older, deeper blades (Wheeler and Srivastava, 1984). *M. pyrifera* has the ability for long-term storage of C and N in excess of immediate demands, which would allow for a decoupling of growth from

immediate ambient conditions (Gerard, 1982). Thus, nitrate uptake is dependent not only on current nitrate availability, but prior nutrient exposure as well. Additionally, factors such as nutrient uptake metabolites, time of day, light, and CO_2 concentration can affect nutrient uptake. Using molecular tools developed here, future studies could examine the extent to which kelps can decouple growth from ambient conditions.

There are few genomes sequenced from ecologically relevant species in the marine environment and even fewer analyses from field studies (Dupont et al., 2007). Natural populations of *M. pyrifera* inhabit a variable physical environment and yet we were able to see strong patterns emerge. Differences in depth of dominant metabolic processes were apparent in these natural samples. Transcript levels were consistent with environment-regulated ecophysiology and this study provides a starting point for future studies coupling gene expression with finer-scale environmental measurements. Through transcriptional profiling of the giant kelp, we created a sequence-based tool kit for physiological study of this species and demonstrate differences in metabolic function across environmental gradients with depth.

Acknowledgements

The work was made possible by funding support from a Mia J. Tegner Fellowship for Coastal Ecology Fieldwork, a Sigma Xi Grant-in-Aid of Research, and a National Science Foundation Graduate Research Fellowship (TK). The BioinformaticsGent Online Genome Annotation Service (BOGAS) for *Ectocarpus siliculosus* genome annotation greatly aided analyses for *M. pyrifera*. We would like to thank C. Bowler and E. Rayko for sharing *P. tricornutum* and *T. pseudonana*

transcription factor sequence data. We thank Scripps Inst. of Oceanography's scientific diving program for diving support in the field. J. Bai and H. Zheng had helpful insights in developing laboratory protocols used in this study. Comments from and discussion with G. Peers, J. Leichter, L. Levin improved the manuscript.

Chapter 4, in full, is currently in preparation for submission. Konotchick, T., C. Dupont, J. Badger, R.E. Valas, and A.E. Allen. Transcriptomic Analysis of Metabolic Function in the Giant Kelp, *Macrocystis pyrifera*, Across Depth and Season. The dissertation author was the primary investigator and author of this paper.

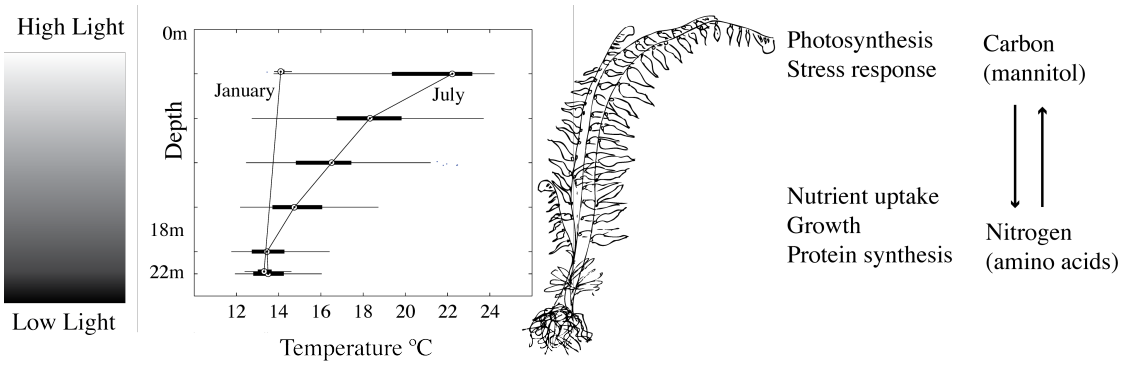

Figure 4.1: A schematic illustrating the gradients in light and temperature (and thus nutrients) that an individual *Macrocystis pyrifera* may span. Dominant physiological processes as seen in the transcript and qPCR data are shown on the right. Temperature inset is a boxplot of 10 minute sampling interval data for the two weeks leading up to the day of collection in January 2009 and July 2009 in La Jolla.

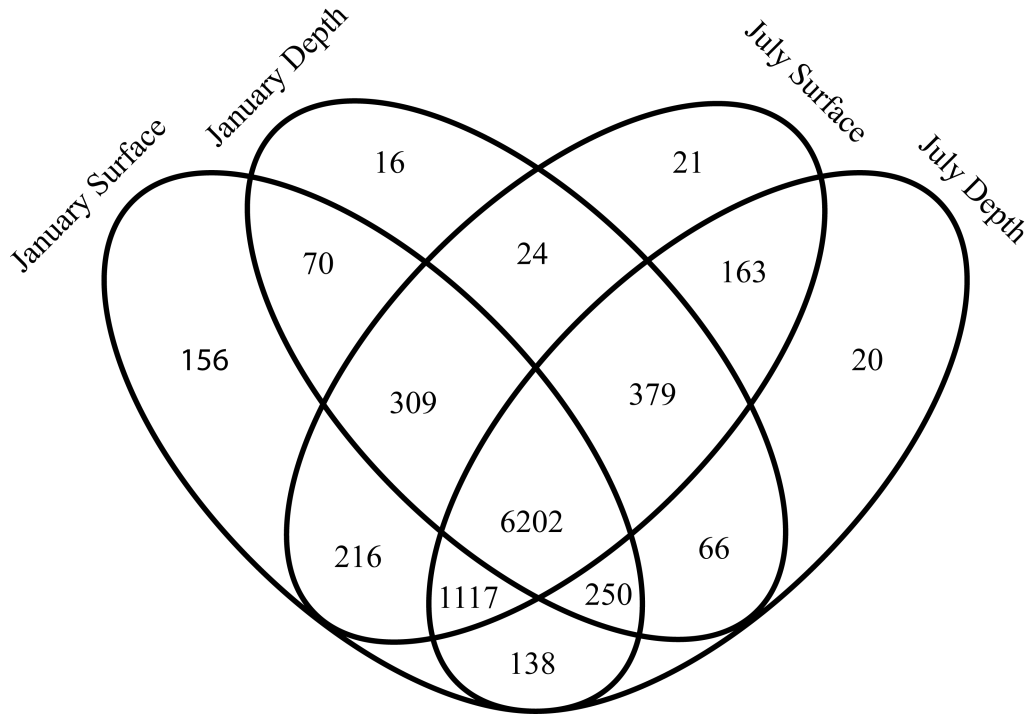

Figure 4.2: Isotig Venn diagram showing distribution of isotigs between the four *M. pyrifera* libraries (January surface, January depth, July surface, July depth) collected in La Jolla.

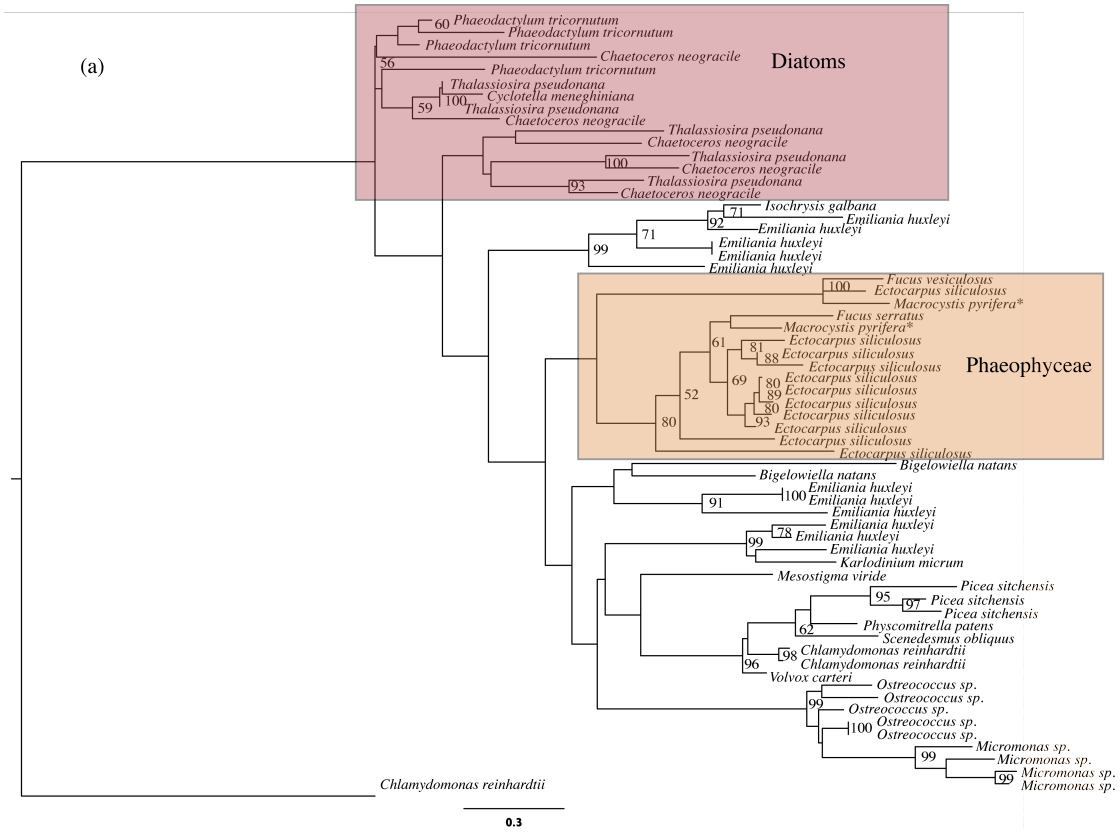

Figure 4.3: Light harvesting complexes (LHC) found in *Macrocystis pyrifera* and their expression patterns with depth. (a) Phylogenetic tree of only the LI818 light harvesting complex familiy made using all the LI818 sequences from Dittami et. al (2010) including one *Chlamydomonas reinhardtii* chlorophyll *a/b* group sequence as an outgroup. Reference sequences were aligned using MUSCLE, and then references and query sequences were aligned using HMM, PhyML with 100 bootstraps and pplacer. Two of the nine *Mp* LHCs fall within the LI818 group and are indicated with a star. The expression of the LI818 LHCs (white bars) was significantly greater than the other LHCs (dark bars) in both (b) January and (c) July (shown on next page).

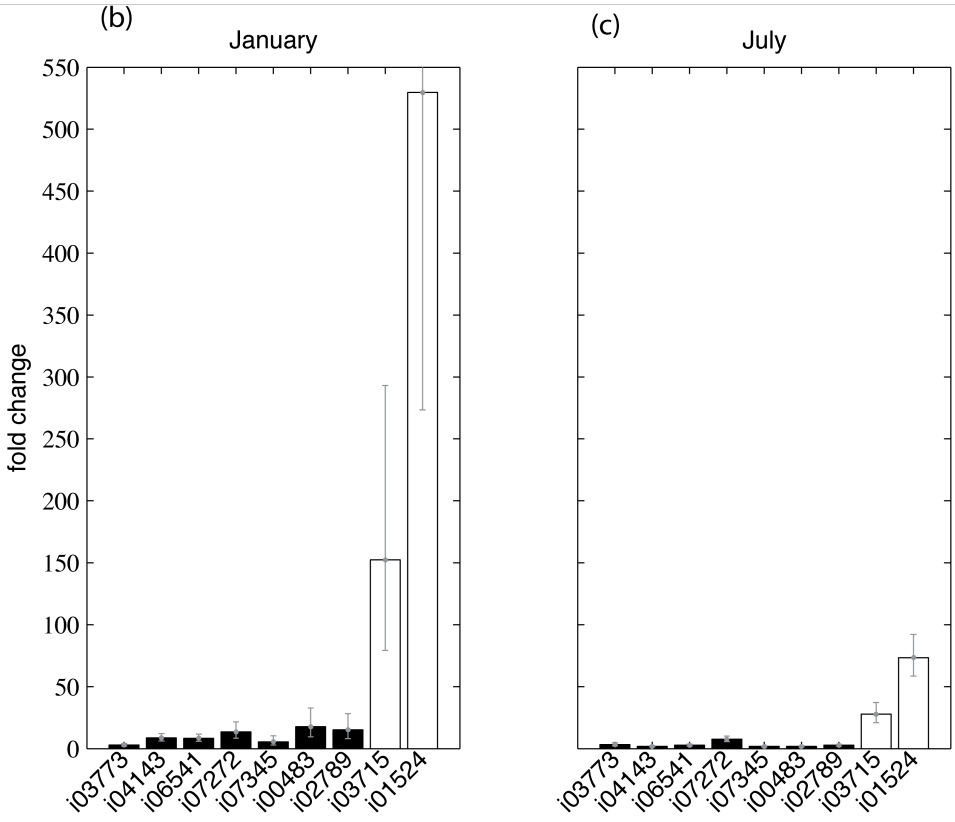

Figure 4.3, Continued: Light harvesting complexes (LHC) found in *Macrocystis pyrifera* and their expression patterns with depth. The expression of the LI818 LHCs (white bars) was significantly greater than the other LHCs (dark bars) in both (b) January and (c) July.

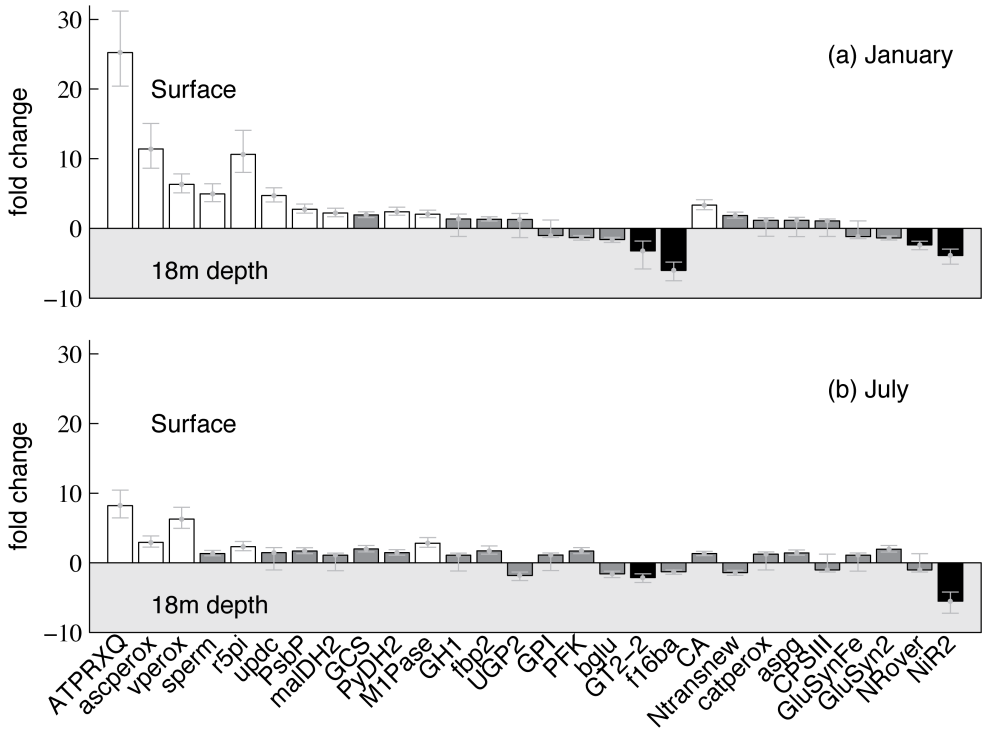

Figure 4.4: Quantitative PCR fold change expression differences between the surface (white background) and 18m depth (light grey background) for (a) January 2009 and (b) July 2009. White bars indicate greater than 2 fold expression in the surface vs. depth, black bars indicate greater than 2 fold expression at depth vs. the surface, everything else in grey. Error bars represent standard deviation. The descriptions of each primer set are listed in Table 4.1.

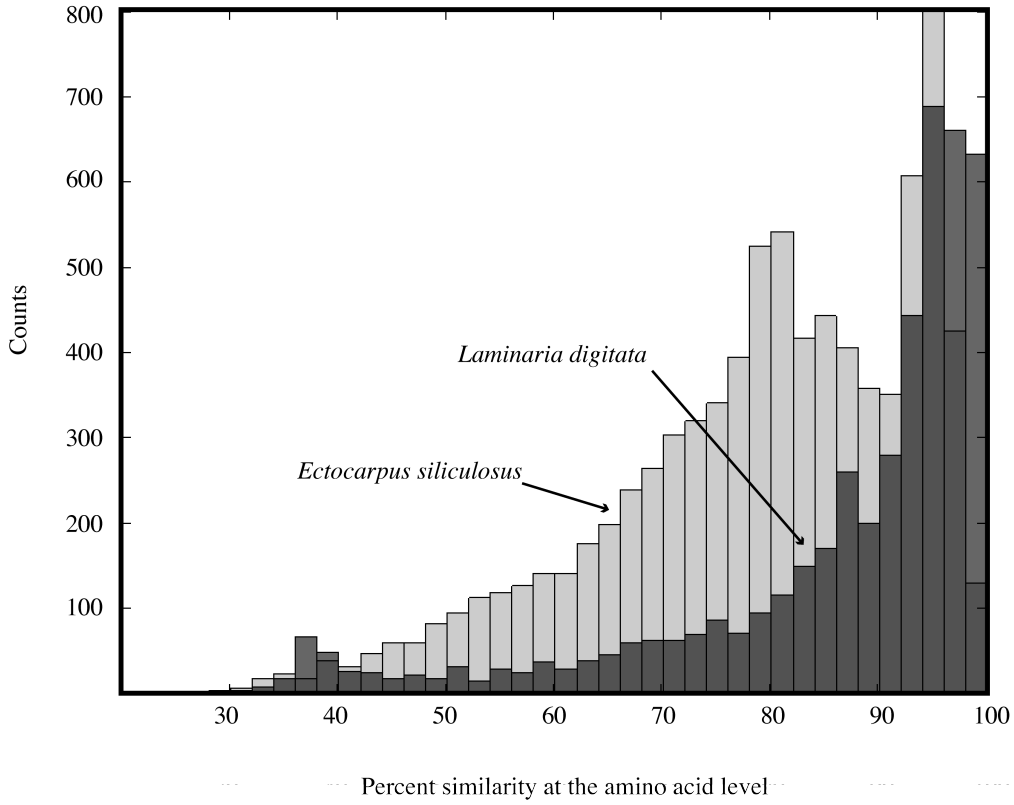

Figure 4.A1: Percent similarity at the protein level between *Macrocystis pyrifera* and *Ectocarpus siliculosus* (light grey) and *Laminaria digitata* (dark grey) using BLAST with alignments with >75% of the total read length.

Table 4.1: Quantitative PCR targets, function, and primers

ID	Name	Function	forward	reverse
18Smat	protein required for 18S rRNA maturation	housekeeper	gaacgtttaagcggttctcg	gtcacgggatttttcaccac
ascperox	(conserved unknown)	stress response	gatgaggacgatctggagga	ccctgcagctaccctctgta
aspg	Asparaginase	nitrogen metabolism	accggtgactgtaacgaagg	gtagacgccgcacctatctc
ATPRX_Q	(conserved unknown)	stress response	caggcatctgcaacttgtgt	tttcggtgaaaagcataccc
bglu	betaglucosidase	carbohydrate metabolism	cttgtccagaacatcgctga	gatgcgcagacacgagaata
CA	putative carbonic anhydrase	nitrogen metabolism	ccagcggtgtacatgagaga	gccttttccacgctgactac
catperox	catalase/peroxidase	nitrogen metabolism	agctagaacaggtggcgaag	aaagagtctgcgccatgaac
CPSIII	Carbamoyl-phosphate synthase (glutamine)	nitrogen metabolism	tatgacgacgtggtgcacat	acttgaccaggctggcatc
f16ba	fructose-1,6 bisphosphate aldolase	carbohydrate metabolism	gctggtcgagctgagaattt	aacgacgagttcccgcttat
fbp2	fructose bisphosphatase	carbohydrate metabolism	acagccgtccgagattcat	ttcttgtcaccgagttgctg
GCS	glycine decarboxylase complex	photosynthesis/carbon fixation	caacgagactttgacggaca	gtcgcagtgcttctcgtatg
GH1	glycoside hydrolase	carbohydrate metabolism	agcaatatgacgaccgaagc	gtcatcacaccagcacatcc
GluSyn2	glutamate synthase (NADH/NADPH)	nitrogen metabolism	acgaccccaagggtaacttc	tagggaagagtccgtgtgct
GluSynFe	Glutamate synthase (ferredoxin)	nitrogen metabolism	gatcgtgaaggggcttattg	ccagaatctcggcaggtact
GPI	glucose-6-phosphate isomerase	carbohydrate metabolism	gaaccacgacgaactgatga	ctgtttcccgtgaacacctt
GT2_2	alpha-(1,2) mannosyltransferase	carbohydrate metabolism	tgctcattatatggcgcaag	acctcgtttgaaaaccgttg
i00483	Light harvesting complex protein	photosynthesis/carbon fixation	cacgaggagctcaacaacaa	cacaaaagattcgacgagca
i01524	Light harvesting complex protein	photosynthesis/carbon fixation	cgcctaccagacaagaaagc	ggtcaacatcctcggctaaa
i02789	Light harvesting complex protein	photosynthesis/carbon fixation	cgtagcgtgaaaatgcagaa	accaactccctcttccacct
i03715	Light harvesting complex protein	photosynthesis/carbon fixation	agcttgtggatggcaagact	ataaaaacggtcagccaacg
i03773	Light harvesting complex protein	photosynthesis/carbon fixation	ggcagcagtctgatttcctc	ccgcgcaagcaactaataat
i04143	Light harvesting complex protein	photosynthesis/carbon fixation	agggggatacagggtctcag	ccacgtgccagctaaagact
i06541	Light harvesting complex protein	photosynthesis/carbon fixation	aggaaattgacaacgcaacc	tgcctctgcttcacataacg
i07272	Light harvesting complex protein	photosynthesis/carbon fixation	gccgagttcttcgtgtcttc	tcctaacaggcggtggtaag
i07345	Light harvesting complex protein	photosynthesis/carbon fixation	agccggatgtagatggacag	gagggtacggagaaacacca
IF2A	eukaryotic initiation factor 2 alpha subunit	housekeeper	catagcctgcttcgtctcct	accaaggtctcttggcctct
M1Pase	mannitol-1-phosphate 5-dehydrogenase	carbohydrate metabolism	ggacaaaaccgcttctacga	agaccgagcggtccttaaat
malDH2	malate dehydrogenase	photosynthesis/carbon fixation	agtgcacgtttgttgactgc	agcttgctgaatccgtgaat
NiR2	nitrite reductase	nitrogen metabolism	aagcgctacggtcaacaact	accatttgagggaccaatca
NRover	nitrate reductase	nitrogen metabolism	ccggagaaggtcgatgct	cttatccctggggtcgatct
Ntrans_new	Nitrate high affinity transporter	nitrogen metabolism	cccctcatgaaggagatcaa	cgccgataaagaaacggata
PFK	phosphofructokinase	carbohydrate metabolism	gcaacagctttcgaccagat	caccgtcctgttattgacca
PsbP	Photosystem II oxygen evolution complex protein PsbP	photosynthesis/carbon fixation	cctggctgtgaacaagaaca	cgagtcgacgagagtcttga
PyDH2	pyruvate dehydrogenase	carbohydrate metabolism	tcgcactttgttggacgtag	ggatctgatacggcaaagga
r5pi	ribose-5-phosphate isomerase	photosynthesis/carbon fixation	agggagaagatggtcgaggt	gacggtgttaagggtgtgct
sperm	spermidine/spermine synthase	stress response	aatgcctatggcttcacctg	ggtaggaaggcacggttgta
UGP2	UDP-glucose-pyrophosphorylase	carbohydrate metabolism	gtatccggcgtccacttta	atgttcggggaaaatgtcac
updc	uroporphyringoen decarboxylase	photosynthesis/carbon fixation	cgggcatatccttaaccttg	gccccctccctatctaacac
vperox	vanadium-dependent bromoperoxidase 2	stress response	gtacggcagggaagtagacg	tccatcctccagtgaacacc

Table 4.2: Pyrosequencing statistics and BLAST results.

	Total	**January Surface**	**January Depth**	**July Surface**	**July Depth**
Total # of Reads	704968	203470	112781	170598	218119
# Reads after Schmidt filtering	472063	147854	73110	123362	127737
average length of reads		337	294	296	364
%GC		48	48	49	47
% of reads with BLAST alignment		8	9	7	9
Read level BLAST alignment					
% *Ectocarpus* match[1]		49	41	51	54
% *Laminaria* match[2]		20	29	23	22
% other Phaeophyceae[3]		14	12	13	13

Total isotigs	9147
Isotigs >1000bp	1813
Median isotig (bp)	682

[1] 67106 total *Ectocarpus siliculosus* annotations in database
[2] 3124 total *Laminaria digitata* annotations in database
[3] 15230 total other Phaeophyceae annotations in database. These include ESTs from *Fucus distichus*, *F. serratus*, *F. vesciculosus*, *Sargassum binderi*, and *Saccharina japonica*.

Table 4.3: Light harvesting complexes identified from isotigs in *Macrocystis*

MpLHC	Species	bp match	GenBank	Cite	*Esi* ortholog	This tree	Dittami ID & family
i06541	*E. siliculosus*	132/182	CBN80506.1	Cock et al. 2010	Esi_0492_0004	FCP	Esi_46; FCP?
i02789	*E. siliculosus*	55/69	CBJ28877.1	Cock et al. 2010	Esi_0123_0002	FCP	Esi_24; FCP
i07272	*S. latissima*	59/71	AAG13004.1	DeMartini et al. 2000	Esi_0149_0020	FCP	N/A
i07345	*E. siliculosus*	88/117	CBN78494.1	Cock et al. 2010	Esi_0126_0039	Red?	Esi_25; Red
i03773	*E. siliculosus*	75/91	CBN74050.1	Cock et al. 2010	Esi_0012_0099	?	Esi_05; FCP
i00483	*M. pyrifera*	139/139	AAC49018.1	Apt et al. 1995	Esi_0458_0016	FCP	Esi_42; FCP
i03715	*E. siliculosus*	66/74	CBN73961.1	Cock et al. 2010	Esi_0009_0107	LI818	Esi_03; LI818
i01524	*E. siliculosus*	154/186	CBJ27804.1	Cock et al. 2010	Esi_0085_0056	LI818	Esi_19; LI818
i04143	*E. siliculosus*	28/30	CBJ30555.1	Cock et al. 2010	Esi_0199_0055	FCP	Esi_28; FCP

Table 4.4: *M. pyrifera* isotigs involved in carbon metabolism found via comparison with *E. siliculosus*

Locus ID	Name	*Mp* Isotig ID	Reference	Function
Esi0060_0128	GPI	6175	1	
Esi0080_0016	M1Pase	7727	1	
Esi0144_0004	UGP	9296	1	cytosolic isoform of UDP-glucose pyrophosphorylase
Esi0212_0019	bglu	6735	1	
Esi0013_0087	GH1	9089	1, table S2	mannosyl-oligosaccharide glucosidase, family GH63 (glycosidase hydrolase)
Esi0248_0006	GH2	01681; 01682	1, table S2	endo-1,3-beta-glucanase, family GH81 (glycosidase hydrolase)
Esi0004_0105	GT1	02050;02051	1, table S2	beta-1,3-1,4-glucan (or cellulose synthase), family GT2 (glycosyltransferase)
Esi0201_0024	GT2	5339	1, table S2	alpha-(1,2)-mannosyltranferase Alg11, GT4 (glycosyltransferase)
Esi0090_0070	GT3	3681	1, table S2	beta-1,4-galactosyltransferase, family GT7 (glycosyltransferase)
Esi0004_0179	GT4	9060	1, table S2	alpha, alpha-trehalose-phosphate synthase (UDP-forming), family GT20 (glycosyltransferase)
Esi0032_0104	GT5	7224	1, table S2	GPI mannosyltransferase, family GT22 (glycosyltransferase)
Esi0104_0037	GT6	5862	1, table S2	UDP-N-acetylglucosamine-peptide N-acetylglucosaminyltransferase, family GT41 (glycosyltransferase)
Esi0159_0022	GT7	9785	1, table S2	Dol-P-Man: dolichol pyrophosphate-Man5GlcNAc2-1,2-mannosyltranferase, Alg3, Family GT58 (glycosyltransferase)
Esi0090_0093	GT8	8187	1, table S2	alpha-1,3-xylosyltransferase, family GT77
Esi0051_0113	GMD	4129	2	GDP-mannose-6-dehydrogenase
Esi0312_0029	ST	5213	2	related to GAG sulfotranserases, good candidates to function as genuine fucan STs
Esi0004_0105	CS	02050; 02051	2	cellulose synthases
Esi0130_0079	PGP	6553	3, table S4	phosphoglycolate phosphatase (photorespiration)
Esi0046_0032	GCS	7203	3, table S4	glycine decarboxylase complex (photorespiration)
Esi0322_0005	GCS2	7173	3, table S4	glycine decarboxylase complex (photorespiration); glycine-cleavage system L-protein
Esi0003_0206	pssd	00608;00610	3, table S4	putative succinic semialdehyde dehydrogenase (potential carbon concentrating mechanisms)
Esi0006_0195	malDH2	01904; 01905	3, table S4	malate dehydrogenase (potential carbon concentrating mechanisms)
Esi0122_0080	PyDH2	7751	3, table S4	pyruvate dehydrogenase (pyruvate/alanine metabolism); E1 component alpha subunit
1 = Michel et al 2010; 2 = Michel et al. 2010b; 3 = Gravot et al. 2010				

Table 4.5: Top 40 KO descriptions across all libraries based on read counts across all libraries.

Count	Taxon	KO description
1984	*Laminaria digitata*	-
1105	*Laminaria digitata*	-
479	*Laminaria digitata*	small subunit ribosomal protein S15Ae
322	*Porphyridium purpureum*	-
270	*Laminaria digitata*	large subunit ribosomal protein L34e
199	*Laminaria digitata*	large subunit ribosomal protein L13Ae
197	*Ectocarpus siliculosus*	small subunit ribosomal protein S7e
196	*Ectocarpus siliculosus*	-
180	*Ectocarpus siliculosus*	large subunit ribosomal protein L23e
175	*Ectocarpus siliculosus*	-
162	*Laminaria digitata*	small subunit ribosomal protein S27Ae
159	*Sargassum binderi*	large subunit ribosomal protein L34e
157	*Ectocarpus siliculosus*	large subunit ribosomal protein L23e
139	*Saccharina japonica*	guanine nucleotide-binding protein subunit beta-2-like 1 protein
139	*Porphyridium purpureum*	-
138	*Ectocarpus siliculosus*	small subunit ribosomal protein S7e
134	*Saccharina japonica*	small subunit ribosomal protein S4e
117	*Ectocarpus siliculosus*	-
112	*Ectocarpus siliculosus*	-
112	*Saccharina japonica*	-
110	*Saccharina japonica*	large subunit ribosomal protein L12e
108	*Ectocarpus siliculosus*	-
108	*Ectocarpus siliculosus*	small subunit ribosomal protein S20e
107	*Ectocarpus siliculosus*	-
107	*Ectocarpus siliculosus*	-
107	*Laminaria digitata*	small subunit ribosomal protein S25e
106	*Porphyridium purpureum*	-
105	*Laminaria digitata*	small subunit ribosomal protein S25e
104	*Ectocarpus siliculosus*	small subunit ribosomal protein S5e
103	*Ectocarpus siliculosus*	large subunit ribosomal protein L23e
99	*Saccharina japonica*	-
98	*Saccharina japonica*	-
96	*Fucus serratus*	photosystem II P680 reaction center D1 protein
95	*Laminaria digitata*	-
92	*Laminaria digitata*	-
92	*Ectocarpus siliculosus*	-
92	*Laminaria digitata*	large subunit ribosomal protein L10e
90	*Saccharina japonica*	large subunit ribosomal protein L12e
83	*Ectocarpus siliculosus*	-
82	*Ectocarpus siliculosus*	-

Table 4.6: List of domains in proteins that are differentially expressed between January surface and January 18m using criteria of a $\log_2$ fold change (logFC) of at least one or greater (a doubling) and p-value <0.05 as calculated using EdgeR. For comparisons with zero count in one library, data are reported only if counts in the other library count were 10 or greater; in those cases logFC is reported as >10. For domain description, n/a = no annotation, GAP indicates a region of at least 30 amino acids that does not hit an HMM annotation.

Higher Expression in January surface vs. January 18m

Domain Description	log FC
Photosynthetic reaction centre protein	>10
Bacteriophage lambda integrase, N-terminal domain ||_GAP_||Phage integrase family	>10
Bacteriophage lambda integrase, N-terminal domain ||Phage integrase, N-terminal SAM-like domain||Phage integrase family	>10
GAP||Chlorophyll A-B binding protein	>10
Excisionase-like protein	>10
GcpE protein	>10
GAP||short chain dehydrogenase	>10
n/a	>10
Excisionase-like protein||Bacteriophage lambda integrase, N-terminal domain	>10
Excisionase-like protein||Bacteriophage lambda integrase, N-terminal domain	>10
GAP||Ribosome recycling factor	>10
n/a	>10
Oxidoreductase family, NAD-binding Rossmann fold||Oxidoreductase family, C-terminal alpha/beta domain	>10
n/a	>10
Mitochondrial carrier protein||Mitochondrial carrier protein||Mitochondrial carrier protein	>10
YgbB family	>10
Ribosomal protein S13/S18	>10
GAP||haloacid dehalogenase-like hydrolase	>10
GAP||Domain of unknown function (DUF1995)	>10
n/a	>10
Ribosomal protein S13/S18	>10
GAP||Phosphoglycerate kinase	>10
Photosynthetic reaction centre protein	>10
Hsp70 protein||_GAP_||Hsp70 protein	>10
n/a	>10
COP9 signalosome, subunit CSN8	>10
Photosynthetic reaction centre protein	4
Bacteriophage lambda integrase, N-terminal domain ||Phage integrase, N-terminal SAM-like domain||Phage integrase family	4

Table 4.6: List of domains in proteins that are differentially expressed between January surface and January 18m depth, Continued.

Higher Expression in January surface vs. January 18m, Continued

Domain Description	log FC
Chlorophyll A-B binding protein	4
GAP||PAP_fibrillin	4
n/a	3
GAP||alpha/beta hydrolase fold	3
n/a	3
RNA polymerase Rpb3/RpoA insert domain	3
n/a	3
n/a	3
n/a	3
n/a	3
n/a	2
GAP||NifU-like domain	2
n/a	2
n/a	2
Fructose-1-6-bisphosphatase	2
n/a	2
n/a	2
Hsp70 protein||_GAP_||Hsp70 protein	2
GAP||PsbP	2
Mitochondrial carrier protein||Mitochondrial carrier protein||Mitochondrial carrier protein	2
n/a	2
n/a	2
GAP||3-beta hydroxysteroid dehydrogenase/isomerase family	2
Ribosomal protein L18e/L15	1

Higher Expression in January 18m vs. January surface

Domain Description	log FC
n/a	>10
n/a	4
GAP||Uncharacterized ACR, COG1678	4
GAP||Ribosomal protein S7e	4
Ribosomal protein S9/S16	3
Ribosomal protein L31e	3
GAP||Pex19 protein family	3
n/a	3
Ribosomal protein L14p/L23e	3
n/a	3
n/a	3

Table 4.6: List of domains in proteins that are differentially expressed between January surface and January 18m depth, Continued.

Higher Expression in January 18m vs. January surface, Continued

Domain Description	log FC
Ribosomal family S4e	3
Dephospho-CoA kinase	3
GAP||Ribosomal protein S13/S18	3
n/a	3
S25 ribosomal protein	3
Ribosomal protein S19e	3
n/a	3
S25 ribosomal protein	2
Ribosomal protein S10p/S20e	2
GAP||Complex I intermediate-associated protein 30 (CIA30)	2
n/a	2
Ribosomal protein L34e	2
DNA directed RNA polymerase, 7 kDa subunit	2
GAP||Exportin 1-like protein	2
n/a	2
Ribosomal protein L22p/L17e	2
Ribosomal protein S7e	2
Hsp70 protein	2
n/a	2
Ribosomal protein L31e	2
Ribosomal protein S24e	2
Ribosomal protein L34e	2
S25 ribosomal protein	2
GAP||G-patch domain	2
GAP||Ribosomal protein L14	2
Ribosomal protein L1p/L10e family	2
GAP||Ribosomal L27e protein family	1
GAP||Ribosomal protein S7p/S5e	1
Ribosomal protein S10p/S20e	1
Ribosomal S17	1
GAP||Ribosomal protein S7e	1
Ribosomal protein L16p/L10e	1
Ribosomal protein L13e	1
Ribosomal protein L14p/L23e	1

Table 4.7: List of domains in proteins that are differentially expressed between July surface and July18m using criteria of a fold change of a $\log_2$ fold change (logFC) of at least one or greater (a doubling) and p-value <0.05 as calculated using EdgeR. For comparisons with zero count in one library, data are reported only if counts in the other library count were 10 or greater; in those cases logFC is reported as >10. For domain description, n/a = no annotation, GAP indicates a region of at least 30 amino acids that does not hit an HMM annotation.

Higher expression in July surface vs. July 18m

Domain Description	logFC
n/a	>10
Photosynthetic reaction centre protein	4
GAP||Domain of unknown function DUF59||CobQ/CobB/MinD/ParA nucleotide binding domain||ParA/MinD ATPase like||_GAP_||Protein of unknown function (DUF971)	4
Bacteriophage lambda integrase, N-terminal domain ||Phage integrase, N-terminal SAM-like domain||Phage integrase family	4
Phosphotyrosyl phosphate activator (PTPA) protein	3
n/a	3
Putative carnitine deficiency-associated protein||_GAP_||Putative carnitine deficiency-associated protein	3
GAP||tRNA synthetases class I (C) catalytic domain||_GAP_||DALR domain	3
GAP||FKBP-type peptidyl-prolyl cis-trans isomerase	3
n/a	3
Mitochondrial carrier protein||Mitochondrial carrier protein||Mitochondrial carrier protein	3
S-adenosylmethionine-dependent methyltransferase	3
n/a	3
n/a	3
GAP||Ankyrin repeat||Ankyrin repeat||Ankyrin repeat	3
n/a	3
GAP||Protein of unknown function (DUF1336)	2
n/a	2
Mitochondrial carrier protein||Mitochondrial carrier protein||Mitochondrial carrier protein	2
GAP||Ribosomal protein S15	2
Domain of unknown function (DUF1995)	2
Ran-interacting Mog1 protein	2
GAP||Protein of unknown function (DUF1336)	2
GAP||Fe-S metabolism associated domain||_GAP_||BolA-like protein	2
GAP||tRNA synthetases class I (W and Y)	2
Asparagine synthase	2
n/a	2

Table 4.7: List of domains in proteins that are differentially expressed between July surface and July18m, Continued.

Higher expression in July surface vs. July 18m, Continued

Domain Description	logFC
n/a	1
n/a	1
n/a	1
3-beta hydroxysteroid dehydrogenase/isomerase family	1
n/a	1
n/a	1
GAP||2Fe-2S iron-sulfur cluster binding domain	1
GAP||Tetratricopeptide repeat||_GAP_||Tetratricopeptide repeat	1
GAP||PAP_fibrillin||_GAP_||PAP_fibrillin	1
GAP||Eukaryotic porin	1

Higher expression in July 18m vs. July surface

Domain Description	logFC
GAP||Spt4/RpoE2 zinc finger	>10
GAP||3'-5' exonuclease	>10
Ribosomal S3Ae family	>10
Ribosomal L15	3
Enoyl-CoA hydratase/isomerase family||_GAP_||3-hydroxyacyl-CoA dehydrogenase, NAD binding domain||3-hydroxyacyl-CoA dehydrogenase, C-terminal domain||_GAP_||3-hydroxyacyl-CoA dehydrogenase, C-terminal domain	3
Ribosomal protein L11, N-terminal domain||Ribosomal protein L11, RNA binding domain	3
Ribosomal protein L4/L1 family	3
Proteasome subunit	3
n/a	3
Ribosomal S3Ae family	3
Ribosomal protein S24e	3
Ribosomal protein S24e	2
GAP||Ribosomal protein L14	2
Ribosomal protein L11, N-terminal domain||Ribosomal protein L11, RNA binding domain	2
GAP||Uncharacterized ACR, COG1678	2
Proteasome subunit	2
Ribosomal protein S24e	2
Ribosomal L15	2
n/a	2
Ribosomal protein L16p/L10e	2
Ubiquitin family||Ribosomal protein S27a	2

Table 4.7: List of domains in proteins that are differentially expressed between July surface and July18m, Continued.

Higher expression in July 18m vs. July surface, Continued.

Domain Description	logFC
GAP||Ribosomal protein S7e	1
Glutathione S-transferase, N-terminal domain||Glutathione S-transferase, C-terminal domain||_GAP_||Elongation factor 1 gamma, conserved domain	1
GAP||Ribosomal protein S7e	1
Ribosomal protein L18e/L15	1
Ribosomal protein L34e	1
n/a	1
Ribosomal protein L1p/L10e family	1

Table 4.8: List of domains in proteins that are differentially expressed between January surface and July surface using criteria of a $\log_2$ fold change (logFC) of at least one or greater (a doubling) and p-value <0.05 as calculated using EdgeR. For comparisons with zero count in one library, data are reported only if counts in the other library count were 10 or greater; in those cases logFC is reported as >10. For domain description, n/a = no annotation, GAP indicates a region of at least 30 amino acids that does not hit an HMM annotation.

Greater expression in January surface vs. July surface

Domain Description	log FC
Excisionase-like protein	>10
n/a	>10
Excisionase-like protein||Bacteriophage lambda integrase, N-terminal domain	>10
Glutathione S-transferase, N-terminal domain||Glutathione S-transferase, C-terminal domain||_GAP_||Elongation factor 1 gamma, conserved domain	>10
PT repeat||PT repeat||TonB-dependent Receptor Plug Domain||_GAP_||TonB dependent receptor	>10
GAP||Peptidase family M20/M25/M40	>10
Photosynthetic reaction centre protein	>10
Ribosomal protein S13/S18	>10
GAP||haloacid dehalogenase-like hydrolase	>10
GAP||Phosphoglycerate kinase	>10
Photosynthetic reaction centre protein	>10
Bacteriophage lambda integrase, N-terminal domain ||Phage integrase, N-terminal SAM-like domain||Phage integrase family	4
n/a	4
Bacteriophage lambda integrase, N-terminal domain ||_GAP_||Phage integrase family	4
Excisionase-like protein||Bacteriophage lambda integrase, N-terminal domain	4
n/a	3
Oxidoreductase family, NAD-binding Rossmann fold||Oxidoreductase family, C-terminal alpha/beta domain	3
n/a	3
Proteasome subunit	3
n/a	3
Photosynthetic reaction centre protein	3
Photosynthetic reaction centre protein	3
n/a	3
GAP||RimM N-terminal domain	3
n/a	3
n/a	3
GAP||Phosphoglucose isomerase	3
Ribosomal protein L11, N-terminal domain||Ribosomal protein L11, RNA binding domain	3
n/a	3

Table 4.8: List of domains in proteins that are differentially expressed between January surface and July surface, Continued

Greater expression in January surface vs. July surface, Continued.

Domain Description	log FC
KH domain||Ribosomal protein S3, C-terminal domain	3
GAP||FabA-like domain	3
Oxidoreductase family, NAD-binding Rossmann fold||Oxidoreductase family, C-terminal alpha/beta domain	3
GAP||Aldo/keto reductase family	3
GAP||PAP_fibrillin	3
n/a	3
n/a	3
GAP||short chain dehydrogenase	3
GAP||Phosphoglucose isomerase	2
Chlorophyll A-B binding protein	2
Ribosomal protein S24e	2
GAP||Ribosomal protein S7e	2
GAP||Ribosomal protein S17	2
GAP||Bacterial trigger factor protein (TF)	2
Ribosomal S3Ae family	2
GAP||DNA methylase	2
n/a	2
n/a	2
n/a	2
GAP||Ribosome recycling factor	2
n/a	2
Ribosomal protein L18e/L15	2
Photosynthetic reaction centre protein	2
n/a	2
GAP||Chlorophyll A-B binding protein	2
GAP||3-beta hydroxysteroid dehydrogenase/isomerase family	2
n/a	2
Glutathione S-transferase, N-terminal domain||Glutathione S-transferase, C-terminal domain||_GAP_||Elongation factor 1 gamma, conserved domain	2
GcpE protein	1
Ribosomal protein S8	1

Greater expression in July surface vs. January surface

Domain Description	log FC
n/a	4
GAP||SET domain	4
Ribosomal protein S9/S16	4
n/a	4

Table 4.8: List of domains in proteins that are differentially expressed between January surface and July surface, Continued

Greater expression in July surface vs. January surface, Continued.

Domain Description	log FC
GAP||Ribosomal protein S7e	4
GAP||Ribosomal protein S15	4
GAP||Ankyrin repeat||Ankyrin repeat||Ankyrin repeat	3
GAP||Protein of unknown function (DUF1336)	3
Asparagine synthase	3
Tetratricopeptide repeat	3
GAP||2Fe-2S iron-sulfur cluster binding domain	3
S-adenosylmethionine-dependent methyltransferase	3
GAP||Leucine carboxyl methyltransferase	3
GAP||WD domain, G-beta repeat||WD domain, G-beta repeat||WD domain, G-beta repeat||WD domain, G-beta repeat||WD domain, G-beta repeat||WD domain, G-beta repeat||WD domain, G-beta repeat||WD domain, G-beta repeat	3
n/a	3
n/a	3
GAP||Rhomboid family	3
GAP||PAP_fibrillin||_GAP_||PAP_fibrillin	3
Proteasome subunit	3
3-beta hydroxysteroid dehydrogenase/isomerase family	3
Ran-interacting Mog1 protein	3
GAP||HEAT repeat	3
n/a	3
GAP||3' exoribonuclease family, domain 1||3' exoribonuclease family, domain 2	3
n/a	2
GAP||Domain of unknown function DUF59||CobQ/CobB/MinD/ParA nucleotide binding domain||ParA/MinD ATPase like||_GAP_||Protein of unknown function (DUF971)	2
GAP||Protein of unknown function (DUF1336)	2
n/a	2
GAP||NnrU protein	2
GAP||Tetratricopeptide repeat||_GAP_||Tetratricopeptide repeat	2
WD domain, G-beta repeat||WD domain, G-beta repeat||WD domain, G-beta repeat||WD domain, G-beta repeat	2
Domain of unknown function (DUF1995)	2
Ribosomal protein L14	2
GAP||GWT1	2
Tetratricopeptide repeat	2
Ribosomal protein L13e	2
GAP||G-patch domain	2
GAP||Uncharacterised P-loop hydrolase UPF0079	2
n/a	2

Table 4.8: List of domains in proteins that are differentially expressed between January surface and July surface, Continued

Greater expression in July surface vs. January surface, Continued.

Domain Description	log FC
Ribosomal protein S10p/S20e	2
n/a	2
GAP||Protein of unknown function (DUF1077)	2
GAP||Eukaryotic porin	2
n/a	2
n/a	1
GAP||PAP_fibrillin	1
GAP||Ribosomal protein S13/S18	1
GAP||G-patch domain	1
Ribosomal S17	1

Table 4.9: List of domains in proteins that are differentially expressed between January 18m and July 18m using criteria of a $\log_2$ fold change (logFC) of at least one or greater (a doubling) and p-value <0.05 as calculated using EdgeR. For comparisons with zero count in one library, data are reported only if counts in the other library count were 10 or greater; in those cases logFC is reported as >10. For domain description, n/a = no annotation, GAP indicates a region of at least 30 amino acids that does not hit an HMM annotation.

Higher expression in January 18m vs. July 18m

Domain Description	log FC
n/a	>10
n/a	4
n/a	4
n/a	3
Ribosomal family S4e	3
n/a	3
GAP||T5orf172 domain	3
Ribosomal protein L34e	3
GAP||Exportin 1-like protein	3
n/a	3
n/a	3
n/a	2
n/a	2
PT repeat||PT repeat||TonB-dependent Receptor Plug Domain||_GAP_||TonB dependent receptor	2
KH domain||Ribosomal protein S3, C-terminal domain	2
n/a	2
n/a	2
S25 ribosomal protein	2
GAP||Ribosomal protein S17	2
n/a	1
S25 ribosomal protein	1
TFIIS helical bundle-like domain||_GAP_||Transcription factor S-II (TFIIS), central domain||Transcription factor S-II (TFIIS)	1
Ribosomal protein S10p/S20e	1

Table 4.9: List of domains in proteins that are differentially expressed between January 18m and July 18m, Continued.

Higher expression in July 18m vs. January 18m

Domain Description	log FC
GAP||3'-5' exonuclease	>10
GAP||PAP_fibrillin||_GAP_||PAP_fibrillin	>10
GcpE protein	>10
n/a	4
n/a	3
n/a	3
GAP||NifU-like domain	3
n/a	3
3-beta hydroxysteroid dehydrogenase/isomerase family	3
n/a	3
Enoyl-CoA hydratase/isomerase family||_GAP_||3-hydroxyacyl-CoA dehydrogenase, NAD binding domain||3-hydroxyacyl-CoA dehydrogenase, C-terminal domain||_GAP_||3-hydroxyacyl-CoA dehydrogenase, C-terminal domain	3
n/a	2
n/a	2
Proteasome subunit	2
GAP||Initiation factor 2 subunit family	2
n/a	2
n/a	2
Ribosomal protein S9/S16	1
n/a	1
Proteasome subunit	1
n/a	1
GAP||S1 RNA binding domain||S1 RNA binding domain||S1 RNA binding domain	1
n/a	1

Table 4A.1: List of potential housekeeper genes tested for *M. pyrifera* quantitative PCR

18S	18S ribosomal RNA gene
18Smat	protein required for 18S rRNA maturation and 40S ribosome biogenesis
actin	actin
atub2	alpha tubulin
betatub	beta tubulin
DHC	dynein heavy chain
elong	eukaryotic elongation factor-1 B gamma
elonga	eukaryotic translation elongation factor 1 alpha
Fzinc	F-box, zinc finger protein
GAPDH	Glyceraldehyde 3-phosphate dehydrogenase
IF2A	eukaryotic initiation factor 2 alpha subunit
pepcyc	peptidyl-prolyl cis-trans isomerase
R26S	40S ribosomal protein S26
RPS7	ribosomal protein S7
ubi2	ubiquitin
ubiA	ubiquitin

References

Apt, K., Clendennen, S., Powers, D., and Grossman, A. (1995). The gene family encoding the fucoxanthin chlorophyll proteins from the brown alga *Macrocystis pyrifera*. Molecular and General Genetics *246*, 455–464.

Armbrust, E.V., Berges, J.A., Bowler, C., Green, B., Martinez, D., Putnam, N.H., Zhou, S., Allen, A.E., Apt, K.E., Bechner, M., et al. (2004). The genome of the diatom *Thalassiosira pseudonana*: ecology, evolution, and metabolism. Science *306*, 79–86.

Axelsson, L. (1988). Changes in pH as a measure of photosynthesis by marine macroalgae. Marine Biology *97*, 287–294.

Bowler, C., Allen, A.E., Badger, J.H., Grimwood, J., Jabbari, K., Kuo, A., Maheswari, U., Martens, C., Maumus, F., Otillar, R.P., et al. (2008). The *Phaeodactylum* genome reveals the evolutionary history of diatom genomes. Nature *456*, 239–244.

Cock, J., Coelho, S., Brownlee, C., and Taylor, A. (2010a). The *Ectocarpus* genome sequence: insights into brown algal biology and the evolutionary diversity of the eukaryotes. New Phytologist *188*, 1–4.

Cock, J., Sterck, L., Rouzé, P., Scornet, D., Allen, A., Amoutzias, G., Anthouard, V., Artiguenave, F., Aury, J.-M., Badger, J., et al. (2010b). The *Ectocarpus* genome and the independent evolution of multicellularity in brown algae. Nature *465*, 617–621.

Colombo Pallotta, M., García Mendoza, E., and Ladah, L. (2006). Photosynthetic performance, light absorption, and pigment composition of Macrocystis pyrifera (Laminariales, Phaeophyceae) blades from different depths. Journal of Phycology *42*, 1225–1234.

Crawford, N., Kahn, M., Leustek, T., and Long, S. (2000). Nitrogen and sulfur. In Biochemistry & Molecular Biology of Plants, B. Buchanan, W. Gruissem, and R. Jones, eds. (American Society of Plant Physiologists).

Dayton, P., Tegner, M., Edwards, P., and Riser, K. (1999). Temporal and spatial scales of kelp demography: The role of oceanographic climate. Ecological Monographs *69*, 219–250.

Dayton, P.K. (1985). Ecology of kelp communities. Annual Review of Ecology and Systematics *16*, 215–245.

Dean, T. (1985). The temporal and spatial distribution of underwater quantum irradiation in a southern California kelp forest. Estuarine, Coastal and Shelf Science *21*, 835–844.

Dittami, S., Michel, G., Collén, J., Boyen, C., and Tonon, T. (2010). Chlorophyll-binding proteins revisited- a multigenic family of light-harvesting and stress proteins from a brown algal perspective. BMC Evolutionary Biology *10*, 365–378.

Dohler, G., Hagmeier, E., and David, C. (1995). Effects of solar and artificial UV irradiation on pigments and assimilation of ^{15}N ammonium and ^{15}N nitrate by macroalgae. Journal of Photochemistry and Photobiology B *30*, 179–187.

Douzery, E., Snell, E., Bapteste, E., Delsuc, F., and Philippe, H. (2004). The timing of eukaryotic evolution: does a relaxed molecular clock reconcile proteins and fossils? Proceedings of the National Academy of Sciences *101*, 15386–15391.

Dupont, S., Wilson, K., Obst, M., Sköld, H., Nakano, H., and Thorndyke, M. (2007). Marine ecological genomics: when genomics meets marine ecology. Marine Ecology Progress Series *332*, 257–273.

Gerard, V. (1982). Growth and utilization of internal nitrogen reserves by the giant kelp *Macrocystis pyrifera* in a low-nitrogen environment. Marine Biology *66*, 27–35.

Gerard, V. (1984). The light environment in a giant kelp forest: influence of *Macrocystis pyrifera* on spatial and temporal variability. Marine Biology *84*, 189–195.

Gerard, V. (1986). Photosynthetic characteristics of the giant kelp (*Macrocystis pyrifera*) determined *in situ*. Marine Biology *90*, 473–482.

Gobler, C., Berry, D., Dyhrman, S., Wilhelm, S., Salamov, A., Lobanov, A., Zhang, Y., Collier, J., and Wurch, L. (2011). Niche of harmful alga *Aureococcus anophagefferens* revealed through ecogenomics. In Proceedings of the National Academy of Sciences, pp. 4352–4357.

Gomez-Alvarez, V., Teal, T.K., and Schmidt, T.M. (2009). Systematic artifacts in metagenomes from complex microbial communities. The ISME Journal *3*, 1314–1317.

Green, B., and Durnford, D. (1996). The chlorophyll-carotenoid proteins of oxygenic photosynthesis. Annual Review of Plant Physiology and Plant Molecular Biology *47*, 685–714.

Green, B., Pichersky, E., and Kloppstech, K. (1991). Chlorophyll *a/b*-binding proteins: an extended family. Trends in Biochemical Sciences *16*, 181–186.

Haines, K., and Wheeler, P. (1978). Ammonium and nitrate uptake by the marine macrophytes *Hypnea musciformis* (Rhodophyta) and *Macrocystis pyrifera* (Phaeophyta). Journal of Phycology *14*, 319–324.

Ishikawa, T., and Shigeoka, S. (2008). Recent advances in ascorbate biosynthesis and the physiological significance of ascorbate peroxidase in photosynthesizing rganisms. Bioscience, Biotechnology and Biochemistry *72*, 1143–1154.

Jackson, G. (1977). Nutrients and production in the Giant Kelp, Macrocystis pyrifera, off southern California. Limnology and Oceanography *22*, 979–995.

Jackson, G. (1997). Currents in the high drag environment of a coastal kelp stand off California. Continental Shelf Research *17*, 1913–1928.

Jamers, A., Blust, R., and De Coen, W. (2009). Omics in algae: Paving the way for a systems biological understanding of algal stress phenomena? Aquatic Toxicology *92*, 114–121.

Kamykowski, D., and Zentara, S.-J. (1986). Predicting plant nutrient concentrations from temperature and sigma-*t* in the upper kilometer of the world ocean. Deep Sea Research *33*, 89–105.

Kasukabe, Y., He, L., Nada, K., Misawa, S., Ihara, I., and Tachibana, S. (2004). Overexpression of spermidine synthase enhances tolerance to multiple environmental stresses and up-regulates the expression of various stress-regulated renes in transgenic *Arabidopsis thaliana*. Plant and Cell Physiology *45*, 712–722.

Kremer, B.P., and Kuppers, U. (1977). Carboxylating enzymes and pathway of photosynthetic carbon assmilation in different marine algae-Evidence for the C_4-pathway? Planta *133*, 191–196.

La Barre, S., Potin, P., Leblanc, C., and Delage, L. (2010). The halogenated metabolism of brown algae (Phaeophyta), its biological importance and its environmental significance. Marine Drugs *8*, 988–1010.

Le Bail, A., Dittami, S., De Franco, P., Rousvoal, S., Cock, M., Tonon, T., and Charrier, B. (2008). Normalisation genes for expression analyses in the brown alga model *Ectocarpus siliculosus*. BMC Molecular Biology 2011 12:2 *9*, 75–83.

Le Gall, Y., Brown, S., Marie, D., Mejjad, M., and Kloareg, B. (1993). Quantification of nuclear DNA and G-C content in marine macroalgae by flow cytometry of isolated nuclei. Protoplasma *173*, 123–132.

Li, W., and Godzik, A. (2006). Cd-hit: a fast program for clustering and comparing large sets of protein or nucleotide sequences. Bioinformatics *22*, 1658–1659.

Lucas, A., Dupont, C., Tai, V., Largier, J., Palenik, B., and Franks, P. (2011). The green ribbon: Multiscale physical control of phytoplankton productivity and community structure over a narrow continental shelf. Limnology and Oceanography *56*, 611–626.

Manley, S. (1983). Composition of sieve tube sap from *Macrocystis pyrifera* (Phaeophyta) with emphasis on the inorganic constituents. Journal of Phycology *19*, 118–121.

Manley, S.L. (1985). Phosphate Uptake by Blades of *Macrocystis pyrifera*(Phaeophyta). Botanica Marina *28*, 237–244.

Mann, K. (1973). Seaweeds: their productivity and strategy for growth. Science *182*, 975–981.

McFarland, W., and Prescott, J. (1959). Standing crop, chlorophyll content and *in situ* metabolism of a Giant Kelp community in Southern California. Publications of the Institute of Marine Science *6*, 109–132.

Michel, G., Tonon, T., Scornet, D., Cock, J., and Kloareg, B. (2010). Central and storage carbon metabolism of the brown alga Ectocarpus siliculosus: insights into the origin and evolution of storage carbohydrates in Eukaryotes. New Phytologist *188*, 67–81.

North, W., and Zimmerman, R. (1984). Influences of macronutrients and water temperatures on summertime survival of *Macrocystis* canopies. Hydrobiologia *116/117*, 419–424.

Parker, B. (1966). Translocation in *Macrocystis*. III. Composition of sieve tube exudate and identification of the major C^{14}-labeled products. Journal of Phycology *2*, 38–41.

Peers, G., Truong, T., Ostendorf, E., Busch, A., Elrad, D., Grossman, A., Hippler, M., and Niyogi, K. (2009). An ancient light-harvesting protein is critical for the regulation of algal photosynthesis. Nature *462*, 518–522.

Peters, A., Marie, D., Scornet, D., Kloareg, B., and Cock, J. (2004). Proposal of *Ectocarpus siliculosus* (Ectocarpales, Phaeophyceae) as a model organism for brown algal genetics and genomics. Journal of Phycology *40*, 1079–1088.

Rayko, E., Maumus, F., Maheswari, U., Jabbari, K., and Bowler, C. (2010). Transcription factor families inferred from genome sequences of photosynthetic stramenopiles. New Phytologist *188*, 52–66.

Robinson, M., McCarthy, D., and Smyth, G. (2010). edgeR: a Bioconductor package for differential expression analysis of digital gene expression data. Bioinformatics *26*, 139–140.

Roeder, V., Collén, J., Rousvoal, S., Corre, E., Leblanc, C., and Boyen, C. (2005). Identification of stress gene transcripts in *Laminaria digitata* (Phaeophyceae) protoplast cultures by expressed sequence tag analysis. Journal of Phycology *41*, 1227–1235.

Rozen, S., and Skaletsky, H. (2000). Primer3 on the WWW for general users and for biologist programmers. In Bioinformatics Methods and Protocols: Methods in Molecular Biology, S. Krawetz, and S. Misener, eds. (Humana Press, Totowa, NJ), pp. 365–386.

Sargent, M., and Lantrip, L. (1952). Photosynthesis, growth and translocation in Giant Kelp. American Journal of Botany *39*, 99–107.

Smith, B., and Melis, A. (1987). Photosystem stoichiometry and excitation distribution in chloroplasts from surface and minus 20 meter blades of *Macrocystis pyrifera*, the giant kelp. Plant Physiology *84*, 1325–1330.

Teal, T.K., and Schmidt, T.M. (2010). Identifying and removing artificial replicates from 454 pyrosequencing data. Cold Spring Harbor Protocols *2010*, pdb.prot5409.

Towle, D., and Pearse, J. (1973). Production of the giant kelp, *Macrocystis*, estimated by in situ incorporation of ^{14}C in polyethylene bags. Limnology and Oceanography *18*, 155–159.

Vandesompele, J., De Preter, K., Pattyn, F., Poppe, B., Van Roy, N., De Paepe, A., and Speleman, F. (2002). Accurate normalization of real-time quantitative RT-PCR data by geometric averaging of multiple internal control genes. Genome Biology *3*, 1–12.

Wheeler, W., and Srivastava, L. (1984). Seasonal nitrate physiology of *Macrocystis integrifolia*. Journal of Experimental Marine Biology and Ecology *76*, 35–50.

Wing, S., Leichter, J., and Denny, M. (1993). A dynamic model for wave-induced light fluctuations in a kelp forest. Limnology and Oceanography *38*, 396–407.

Yoon, H., Hackett, J., Ciniglia, C., Pinto, D., and Bhattacharya, D. (2004). A Molecular Timeline for the Origin of Photosynthetic Eukaryotes. Molecular Biology and Evolution *21*, 809–818.

Zimmerman, R., and Kremer, J. (1986). In situ growth and chemical composition of the giant kelp, *Macrocystis pyrifera*: response to temporal changes in ambient nutrient availability. Marine Ecology Progress Series *27*, 277–285.

CHAPTER 5

Transcriptional Profiling of the Giant Kelp, *Macrocystis pyrifera*, Spanning Water Column Gradients in Light, Temperature and Nutrients

Abstract

The Giant Kelp, *Macrocystis pyrifera*, spans biologically relevant gradients in light, temperature and nutrients. We used an RNA-Seq approach to examine global transcriptional changes across these environmental gradients. From a single water-column spanning individual, RNA was extracted from blades collected every 3m from the surface to 18m depth. Three technical replicates for each of the seven depth samples were prepared for cDNA library construction and sequenced on the Illumina Genome Analyzer IIx. 45 Gbp of raw sequence across the 21 libraries assembled into 371,000 transcripts, greatly expanding the number of annotated transcriptional units for this species and enabling sequence-based tool creation for future studies of the molecular physiology of *M. pyrifera*. We saw high reproducibility between the technical replicates and distinct grouping by depth from expression profile clustering. Carbon assimilation is concentrated in the upper canopy of the individual, while genetic information processing and degradation are dominant processes at depth. This work creates a genomic resource for future study of the ecologically important *Macrocystis pyrifera*.

Introduction

There are few sequenced genomes from ecologically important species in the marine environment and even fewer analyses from field studies (Dupont et al., 2007). Early sequencing efforts have been directed towards representative laboratory model organisms which possess various attractive features including ease of genetic manipulation, small nuclear genome size, and short life cycle (Peters et al., 2004). Ecologically important species may not share these same features. For example, the sporophyte generation of the giant kelp, *Macrocystis pyrifera,* is very large and not amenable to large-scale genetic experiments. *M. pyrifera* supports a wide range of fish and invertebrate species in the rocky subtidal temperate environment.

The water column-spanning *M. pyrifera* sporophyte is a unique system with which to explore physiological response to measured physical environmental gradients (light, temperature, nutrients). All parts of the kelp (e.g. blades, stipe, holdfast) are able to photosynthesize and take up nutrients; however the availability of nutrients surrounding the kelp changes based on depth and is variable across a range of different spatiotemporal scales (e.g. Chapter 3). *M. pyrifera* possesses a sieve-tube system with the ability to transport metabolites such as mannitol and amino acids, which allows for allocation of resources and functional separation of various metabolisms. The unique sieve system used to support such a large size, may not be represented in laboratory organisms, and provide a reason for genome or transcriptome exploration. To date, publically available sequence information for the Phaeophyceae includes ESTs from a handful of members and one sequenced genome (i.e. *Ectocarpus siliculosus*).

Challenges to working with non-model organisms include lack of a reference for assembly and functional annotation. To begin to explore the functional separation within *M. pyrifera* at a physiological level, we needed to develop the tools to do so. The Illumina platform provides very deep sequencing coverage, which gives power for gene expression comparisons regardless of annotation. Recent studies also demonstrate that Illumina reads provide ample coverage for *de novo* assembly despite their short length (Collins et al., 2008; Birzele et al., 2010). We used an RNA-Seq approach to examine global transcriptional changes across environmental gradients. From a single water-column spanning individual, RNA was extracted from blades collected every 3m from the surface to 18m depth. Three technical replicates for each of the seven depth samples were prepared for cDNA library construction and sequenced on the Illumina Genome Analyzer IIx. Objectives of this study were to: (1) expand the number of identified transcriptional units for this ecologically-important species, (2) generate functional and taxonomic annotation for kelp transcripts, and (3) characterize the depth-distribution of gene expression of transcripts within functionally-annotated pathways at seven depths in a *M. pyrifera* individual spanning the thermocline.

Materials and Methods

Sample Collection

Blade tissue was sampled from a *Macrocystis pyrifera* sporophyte in La Jolla, California, USA (N 32° 51.0; W 117° 17.5) on 3 August 2010 using SCUBA. Blades were collected from the surface (0m), and every 3m down the length of one stipe to

18m depth, for a total of seven depth samples. Three technical replicates for each of the seven depths were prepared for cDNA library construction (Auer and Doerge, 2010). Surface blades were collected at least 1m away from the apical growing region and the samples from 18m avoided the reproductive sporophylls near the base of an individual. For consistency and to minimize within-blade variability, all samples were collected near the base of each blade. North (1971) reports no change in photosynthetic activity between intact and cut blades; any wounding effects were assumed to be consistent across samples. At the end of each dive, blades were immediately cleaned of any visible epiphytes using 100% ethanol and cheesecloth and then frozen on dry ice for transport to the lab.

Characterizing the Physical Environment

To quantify the temperature of the water column, thermistor chain data were collected at 10 min intervals using TidBit temperature data loggers with ~0.2° resolution, and ~5 min response time (Onset, Bourne, Massachusetts, USA). TidBits were placed on the bottom and at 2, 6, 10, 14, and 18 meters above the bottom (mab) in 22m water depth. The temperature inset in Figure 5.2 is a box plot of the water temperature during the 24 hours leading up to time of collection. Nutrient samples were collected at depth on SCUBA in previously acid cleaned bottles, syringe filtered (0.22 μm) in the lab into 20 ml acid cleaned bottles, then frozen and sent for analysis at the Marine Science Institute Analytical Laboratory at the University of California, Santa Barbara via Flow Injection Analysis. For a secchi disc reading of 5.5m, the

attenuation coefficient of quanta was calculated to be 0.27 based on the equation $\log k_Q = 0.14 - 0.95 \log D$ (Walker, 1982).

Library Construction

RNA extraction followed a modified protocol (Apt et al., 1995). Frozen algal tissue was ground to a powder on liquid nitrogen then added to an extraction buffer (100mM TRIS-HCl pH 8.0, 1.5 M NaCl, 20mM EDTA, 20mM DTT and 2% CTAB) at 1:1 w/v ratio and mixed at room temperature (RT) for 15 min then heated to 65°C for 20 min. This was followed by a ½ volume chloroform extraction, 5 min at RT, then centrifugation at 10,000g for 30 min at 4°C, and collecting the supernatant. Addition of 1/3 volume ethanol was used to precipitate polysaccharides, which was followed by a second chloroform extraction. 3.0 M LiCl and 10% v/v β-mercaptoethanol was added to the aqueous phase and placed at -20°C overnight. RNA was precipitated by centrifugation at 14,000g for 30 min at 4°C and followed by two 75% ethanol washes before resuspension.

Sequencing preparation followed the Illumina TruSeq mRNA Sequencing Sample Preparation guide (Illumina, San Diego, CA, USA). Starting with 0.67 – 1 µg of total RNA for each of the 21 libraries (7 depths x 3 technical replicates), I purified the poly-A containing mRNA molecules, and fragmented mRNA for 8.5 – 9 minutes. After first and second strand cDNA synthesis, end repair, adapter ligation, and purification, I used PCR enrichment of 12-14 cycles. A High Sensitivity DNA Assay chip was used to assess quality (Agilent; Santa Clara, CA, USA); the average size of cDNA sent for sequencing ranged from 510 – 558 bp.

De novo Transcriptome Assembly and Annotation Analysis

Three lanes with seven multiplexed samples in each lane were run on the Illumina Genome Analyzer IIx platform (San Diego, CA, USA) generating 508 million reads for a total of 45 Gbp of sequence for this analysis. Reads were assembled using CLC Workbench. Contigs were annotated using BLASTX searches conducted (cut-off 10^{-5}) against an internal JCVI database containing all completed and draft algal genomes as well as all Phaeophyceae EST libraries available in NCBI GenBank for annotation. ORFs were predicted with FragGeneScan (Rho et al., 2010). We used the edgeR package to analyze count data and test for differential expression (Robinson et al., 2010).

Pathway Analysis

For all the KO terms in a given KEGG pathway, the number of reads mapping to a given ORF with that KO designation were summed. The three technical replicates for each depth were averaged before clustering. Hierarchical clustering was performed using Matlab's clustergram function using the Euclidean distance metric to calculate pair-wise distances across the KO term dimension. KEGG pathways examined include photosynthesis, porphyrin and chlorophyll metabolism, carotenoid biosynthesis, terpenoid backbone biosynthesis, carbon fixation in photosynthetic organisms, oxidative phosphorylation, photosynthesis/antenna proteins, lipopolysaccharide biosynthesis, peptidoglycan biosynthesis, fatty acid biosynthesis,

ABC transporter, protein export, spliceosome, RNA transport, proteosome, lysosome, and ubiquitin-mediated proteolysis.

Results & Conclusions

Three lanes of multiplexed Illumina sequencing yielded 508 million reads for a total of 45Gbp of sequence. Statistics broken down by depth (average of the three technical replicates) are shown in Table 5.1. Approximately 8-14% of the contigs were assigned either KO or pfam annotations using alignment based annotations (Table 5.1).

Expression profile clustering shows high reproducibility between technical replicates (Figure 1). Expression profile clustering groups similar profiles from different samples together and implies related function. This process utilizes all sequences, regardless of whether an annotation can be assigned or not. Depth is an important factor affecting transcription; the shallow depths cluster together (0m, 3m, 6m, and 9m) and the deeper depths (12m, 15m, and 18m) form a second major cluster. With increasing depth-distance between samples, the number of differentially expressed genes in pair-wise comparisons increases. 3m and 6m are more similar to each other than to the surface. 9m may represent a transition zone as seen in the clustering of transcripts as well as in the physical environmental data. In the temperature profile, at 9m depth and deeper, temperatures decreased below 14.5°C indicating the presence of nitrate (Figure 5.2a). This is reflected in the actual nutrient measurements as well (Figure 5.2 b, d-g).

Estimated light attenuation based on secchi measurements indicates almost complete extinction of surface illumination at 20m depth. The photosynthesis pathway was extremely upregulated in the surface and 3m (Figure 5.3). Top expressed proteins in the surface (e.g. 0m) were Photosystem II (PSII) Psb27 protein which is involved in PSII repair, as well as PSII PsbU which is crucial for thermal tolerance (Nishiyama et al., 1999), indicating potentially stressful or damaging conditions at the surface. Interestingly, the majority of photosynthesis pathway proteins showed highest expression at 3m, indicating perhaps photo-inhibition at the surface. Other photosynthesis-associated pathways showed upregulation at shallow depths, including porphyrin and chlorophyll metabolism (Figure 5.4), carotenoid biosynthesis (Figure 5.5), terpenoid backbone biosynthesis (Figure 5.6), carbon fixation in photosynthetic organisms (Figure 5.7) and oxidative phosphorylation (Figure 5.8). The photosynthesis-antenna protein pathway (Figure 5.9) showed high surface upregulation, but several proteins had their highest expression at other depths as well, indicating perhaps the specialization of different light harvesting complexes for different depths (i.e. light levels). With an increase in these photosynthetic processes, we also see an increase in lipopolysaccharide (Figure 5.10), peptidoglycan (Figure 5.11), and fatty acid (Figure 5.12) biosynthesis. The ABC transporter pathway (Figure 5.13), is a ubiquitous system in eukaryotes for the translocation of substrates across a membrane; the up-regulation of this pathway may be related to photosynthetic ATP creation in shallow depths. The protein export pathway (Figure 5.14) showed high expression in shallow depths, indicating possible production of outer membrane or organelle proteins.

Genetic information processing and degradation processes appear to be highly expressed at the deeper depths (i.e. 12-18m). Transcription pathways including the spliceosome (Figure 5.15), which is involved in the removal of pre-mRNA introns, and RNA transport (Figure 5.16) had high expression at depth. Degradation pathways upregulated at depth include the proteosome pathway (Figure 5.17), lysosome pathway (Figure 5.18), and ubiquitin-mediated proteolysis (Figure 5.19).

We applied next generation sequencing to characterize the transcriptome of *M. pyrifera* and explore gene expression in relation to gradients in the physical environment. We greatly expanded the number of annotated transcriptional units for *M. pyrifera*, creating a valuable genomic resource for future studies of this ecologically important species. Examining gene expression patterns in relation to the environment also provides empirical support for identified TUs. Potential applications of this sequence-based dataset include as a reference for the assessment of genetic variation, SNP discovery, microsatellite discovery and construction, and candidate gene finding (Ekblom and Galindo, 2010). Microarrays can now be constructed for this non-model organism or molecular markers for ecological and population genetic studies. Combined *in situ* field measurements (including gene expression analysis) with physical data such as t-strings and satellite data (Cavanaugh et al., 2010) could be combined to create a very useful and potentially predictive tool for coastal resource managers.

Acknowledgements

The work was made possible by funding support from a Mia J. Tegner Fellowship for Coastal Ecology Fieldwork, a Sigma Xi Grant-in-Aid of Research, a National Science Foundation Graduate Research Fellowship (TK); and the J. Craig Venter Institute. We thank Scripps Institution of Oceanography's scientific diving program for diving support in the field.

Chapter 5, in full, is currently in preparation for submission. Konotchick, T., C. Dupont, R.E. Valas, and A.E. Allen. Transcriptional Profiling of the Giant Kelp, *Macrocystis pyrifera*, Spanning Water Column Gradients in Light, Temperature, and Nutrients. The dissertation author was the primary investigator and author of this paper.

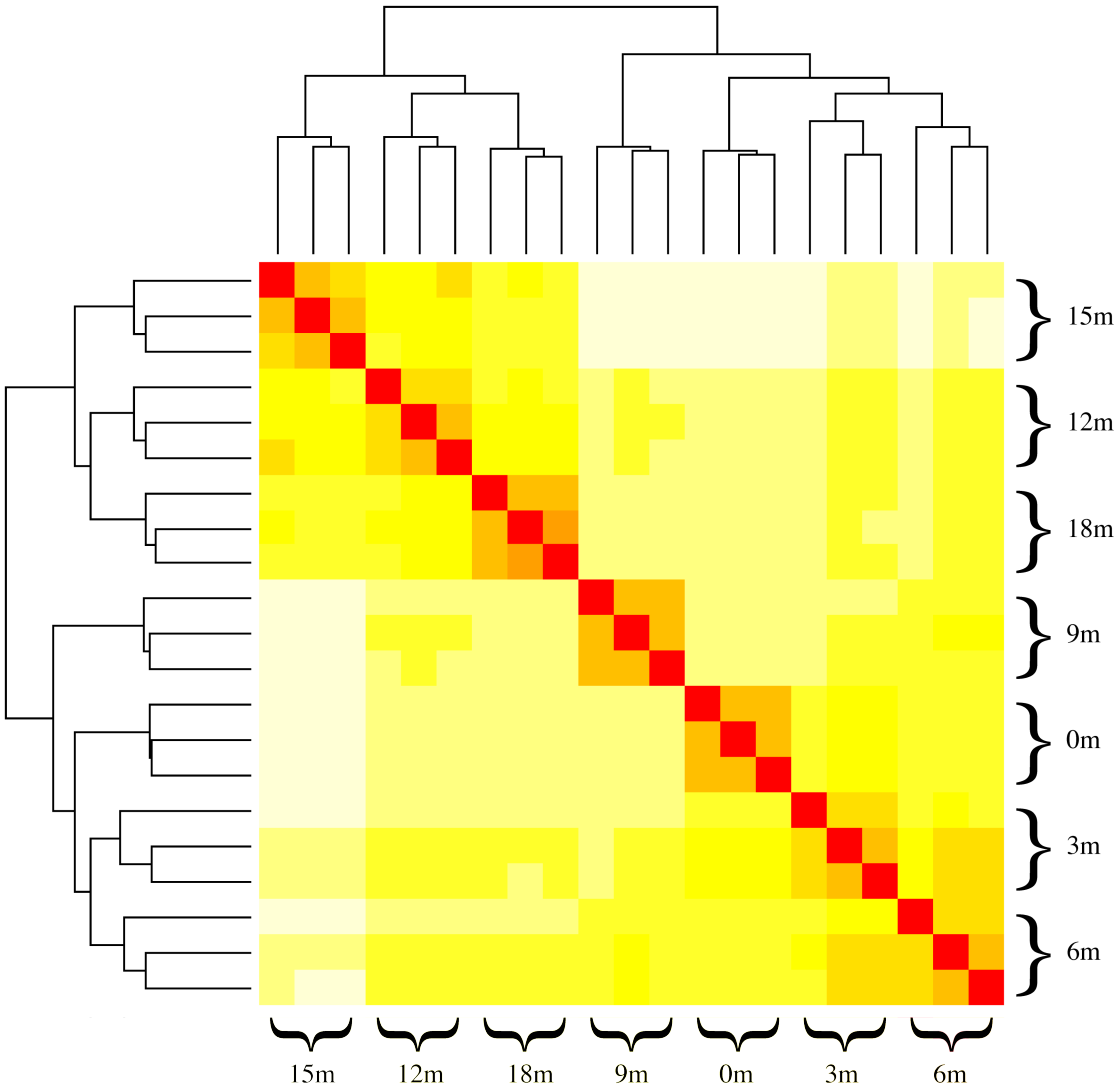

Figure 5.1: Expression profile clustering of the contigs from the 21 sequenced libraries.

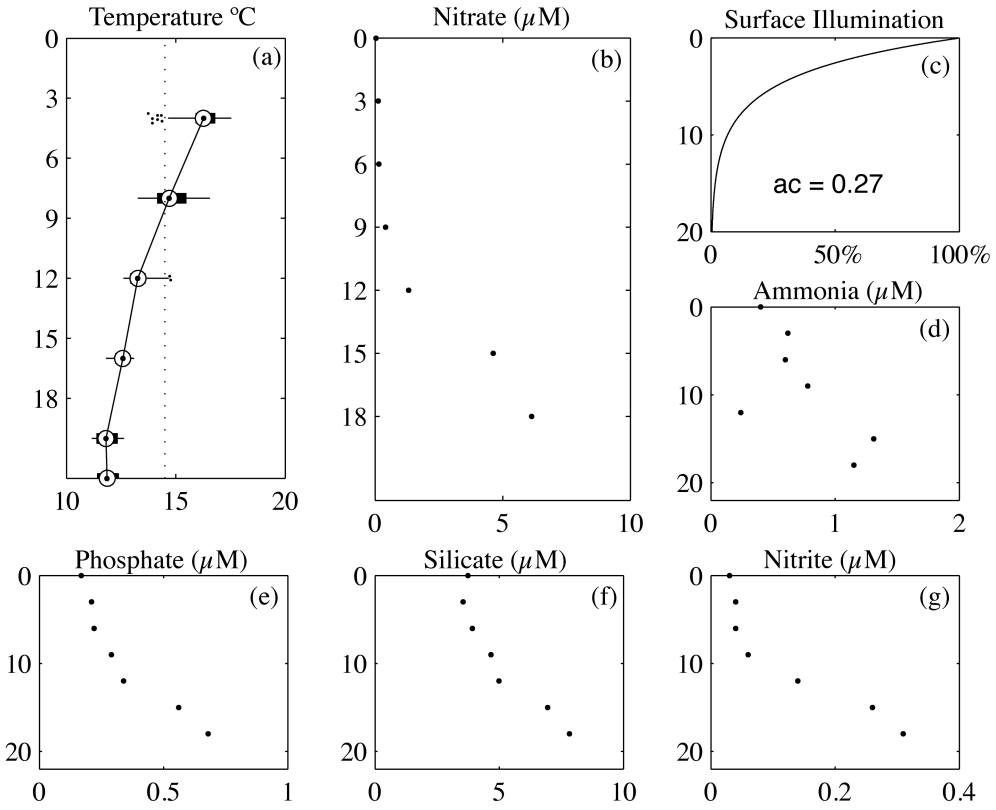

Figure 5.2: Characterization of the physical environment in the La Jolla kelp forest on 3 August 2010 when *M. pyrifera* samples were collected. (a) vertical dotted line indicates the 14.5°C isotherm, temperatures below which indicate the presence of nutrients, (b) , (c) light profile based on attenuation coefficient calculated from secchi depth, (d) , (e) , (f) , (g)

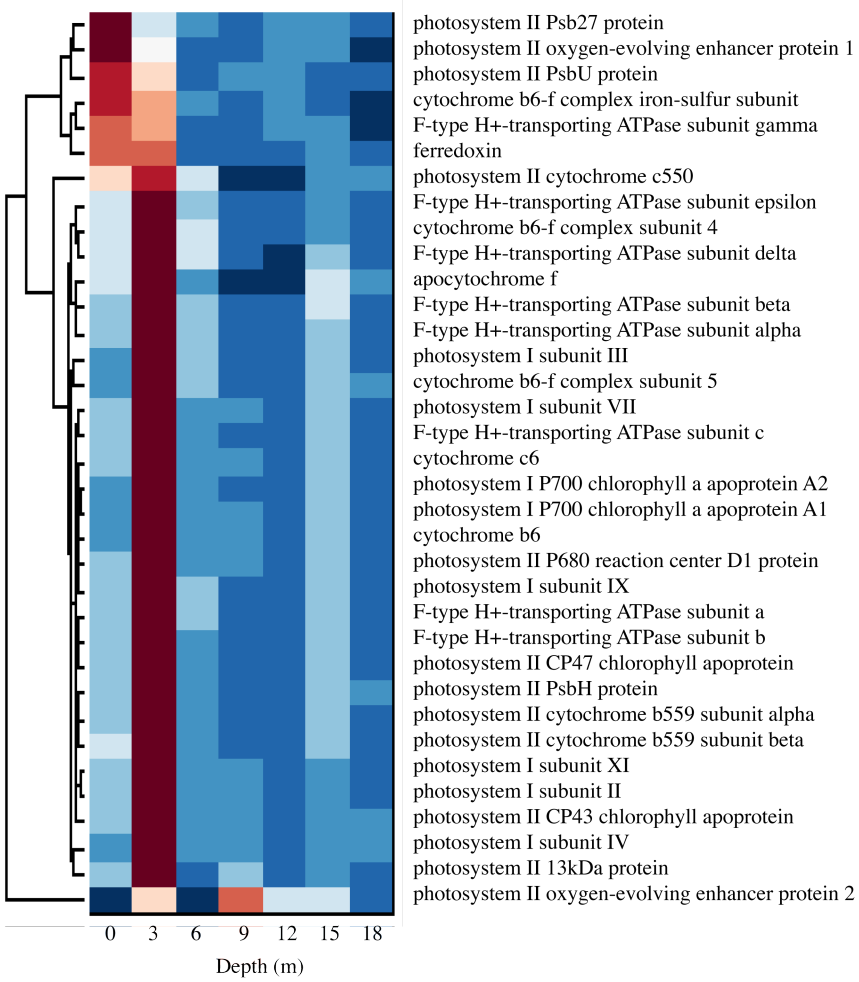

Figure 5.3: Hierarchical clustering of the read counts that map to a given ORF with a KO annotation in the photosynthesis KEGG pathway.

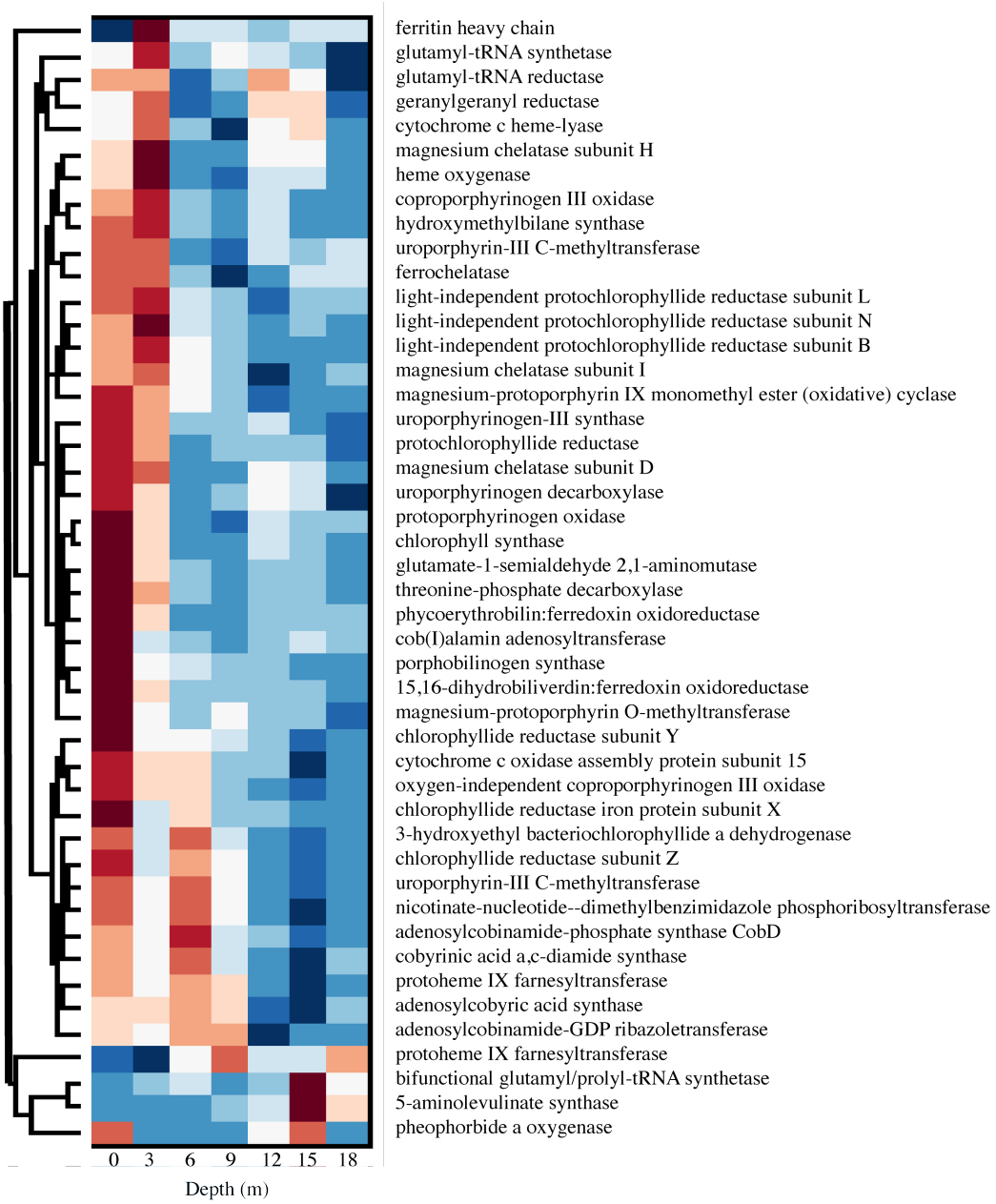

Figure 5.4: Hierarchical clustering of the read counts that map to a given ORF with a KO annotation in the porphyrin and chlorophyll metabolism KEGG pathway.

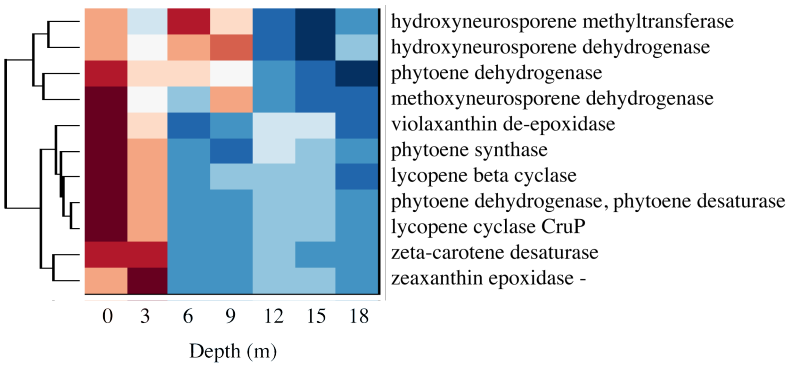

Figure 5.5: Hierarchical clustering of the read counts that map to a given ORF with a KO annotation in the carotenoid biosynthesis KEGG pathway.

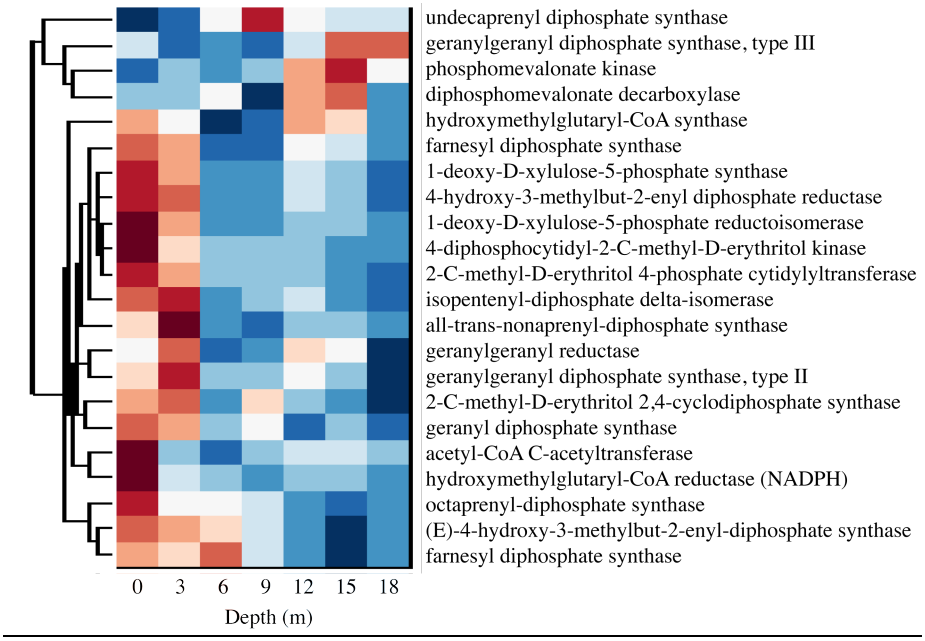

Figure 5.6: Hierarchical clustering of the read counts that map to a given ORF with a KO annotation in the terpenoid backbone biosynthesis KEGG pathway.

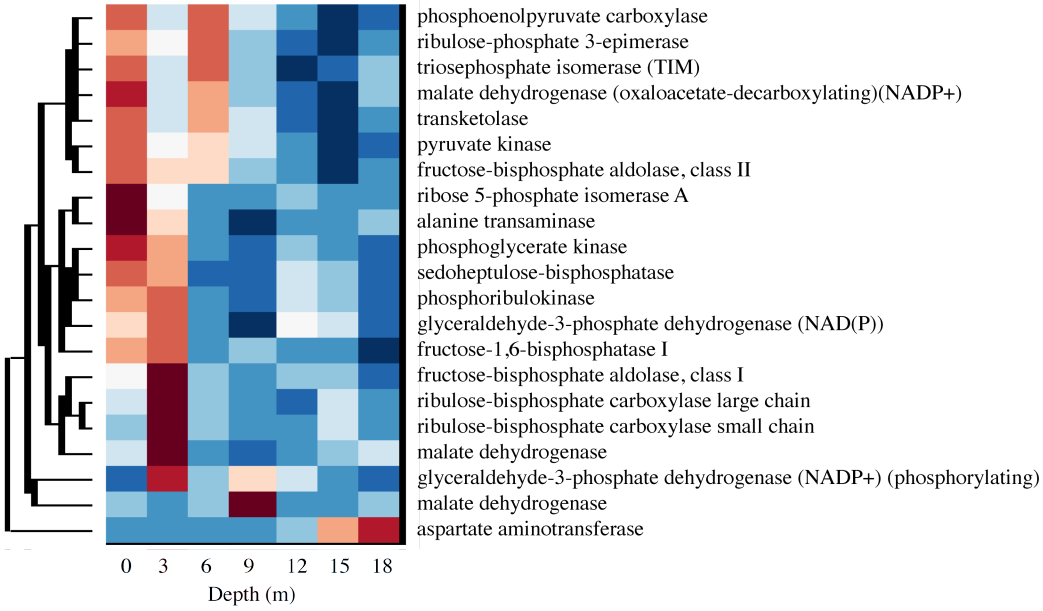

Figure 5.7: Hierarchical clustering of the read counts that map to a given ORF with a KO annotation in the carbon fixation in photosynthetic organisms KEGG pathway.

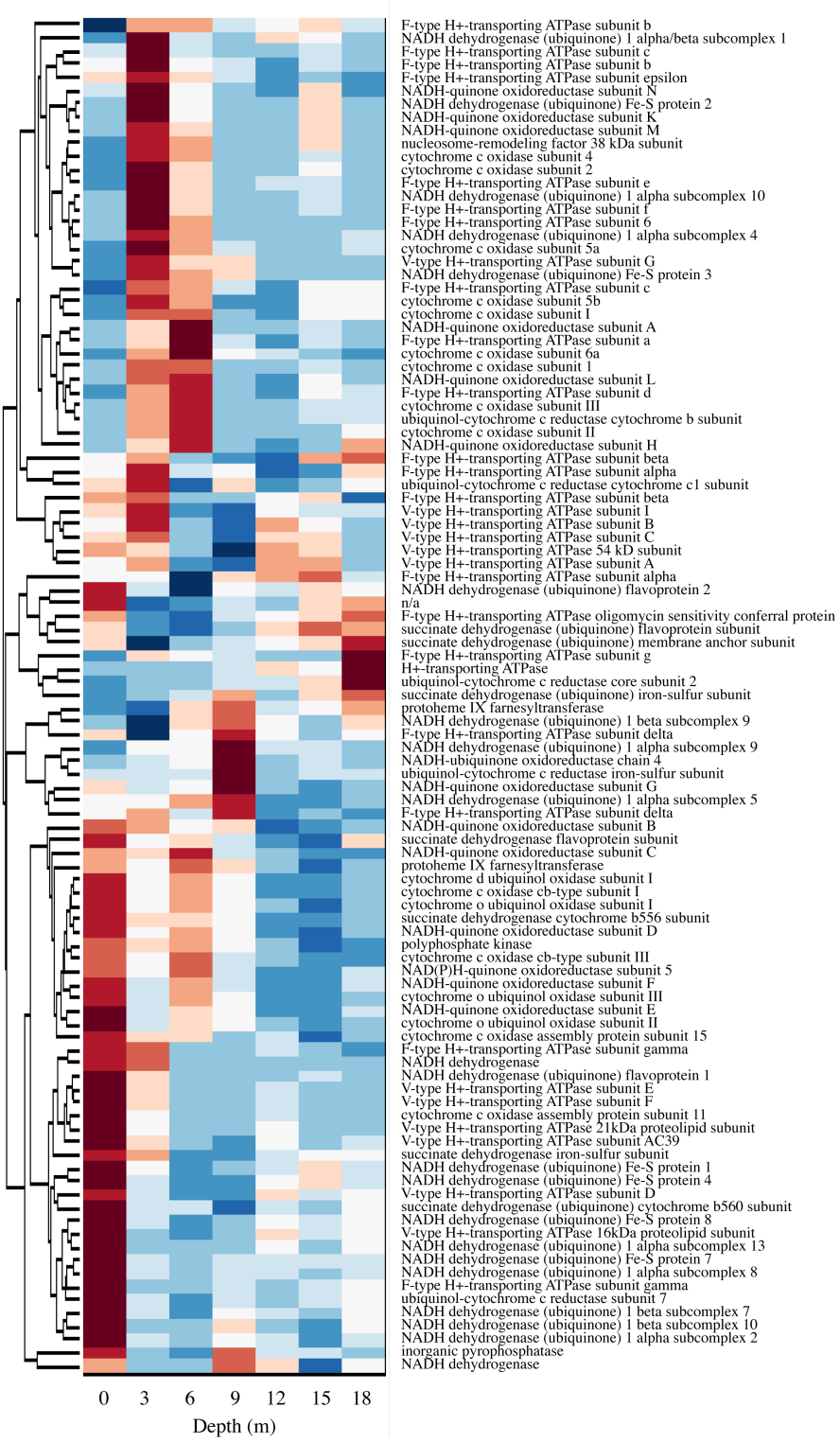

Figure 5.8: Hierarchical clustering of the read counts that map to a given ORF with a KO annotation in the oxidative phosphorylation KEGG pathway.

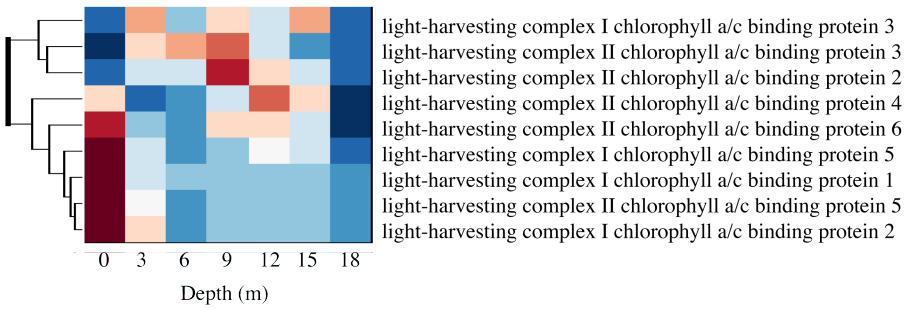

Figure 5.9: Hierarchical clustering of the read counts that map to a given ORF with a KO annotation in the photosynthesis-antenna protein KEGG pathway.

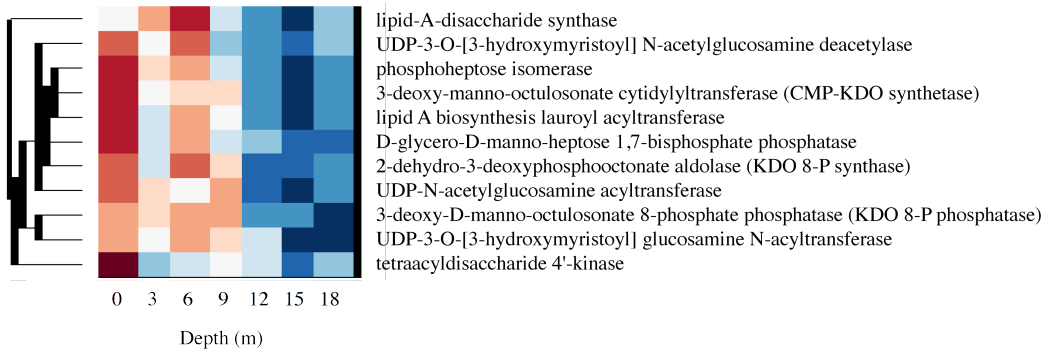

Figure 5.10: Hierarchical clustering of the read counts that map to a given ORF with a KO annotation in the lipopolysaccharide biosynthesis KEGG pathway.

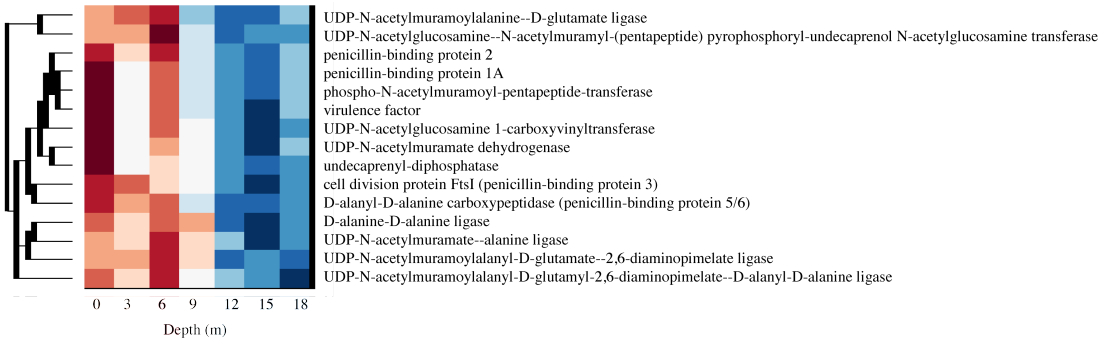

Figure 5.11: Hierarchical clustering of the read counts that map to a given ORF with a KO annotation in the peptidoglycan biosynthesis KEGG pathway.

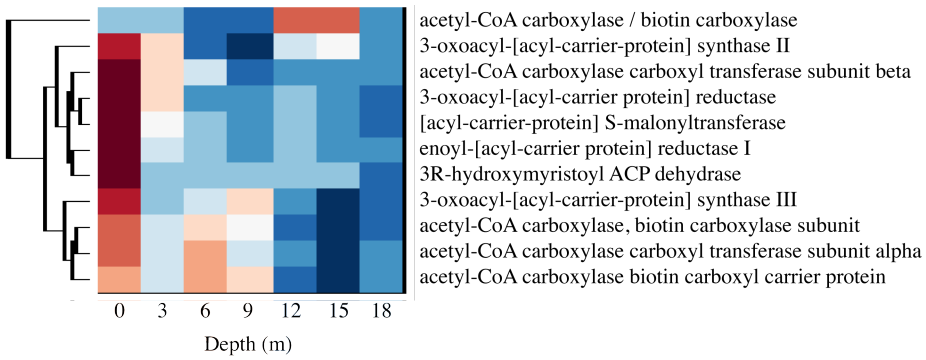

Figure 5.12: Hierarchical clustering of the read counts that map to a given ORF with a KO annotation in the fatty acid biosynthesis KEGG pathway.

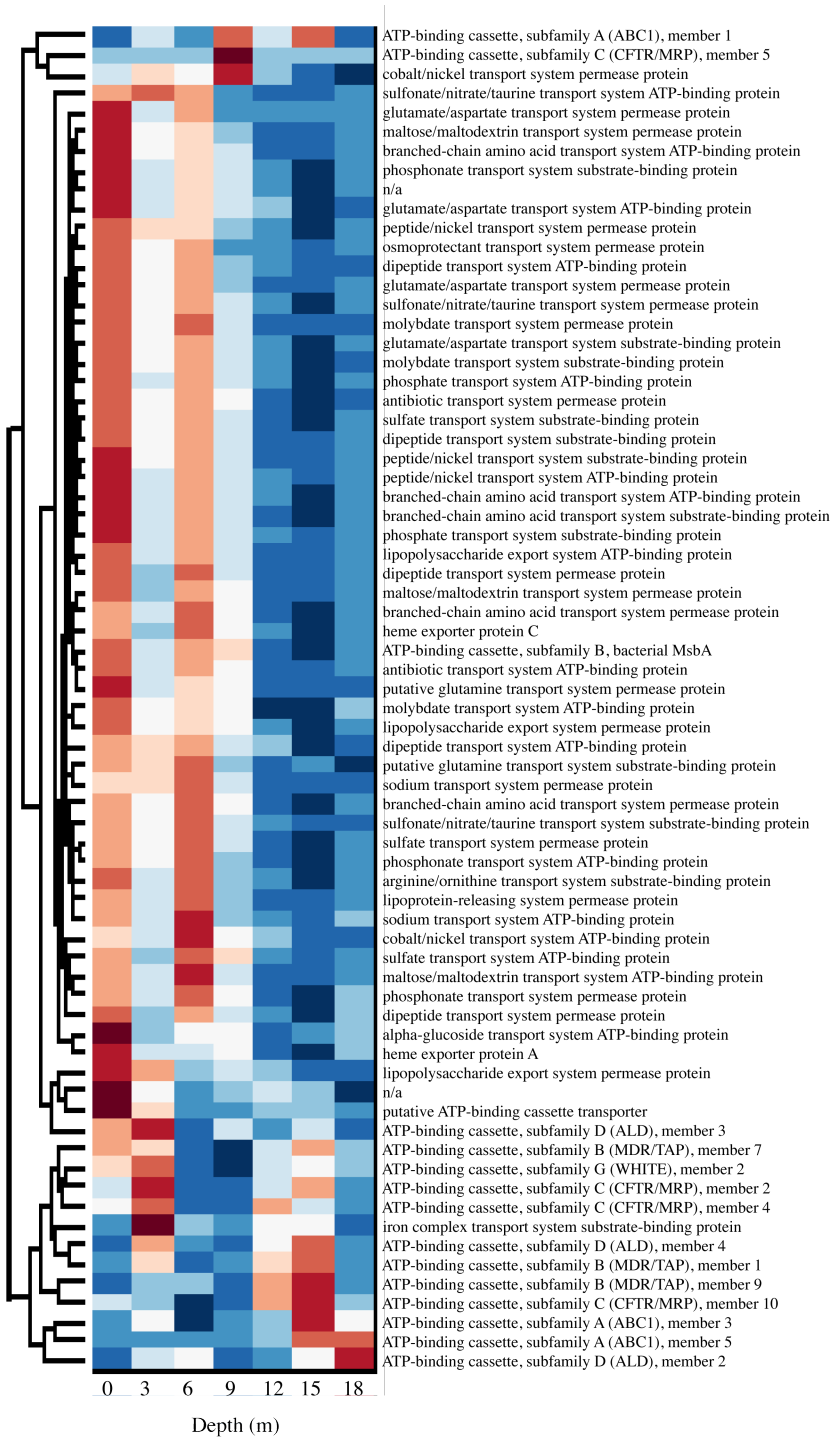

Figure 5.13: Hierarchical clustering of the read counts that map to a given ORF with a KO annotation in the ABC transporter KEGG pathway.

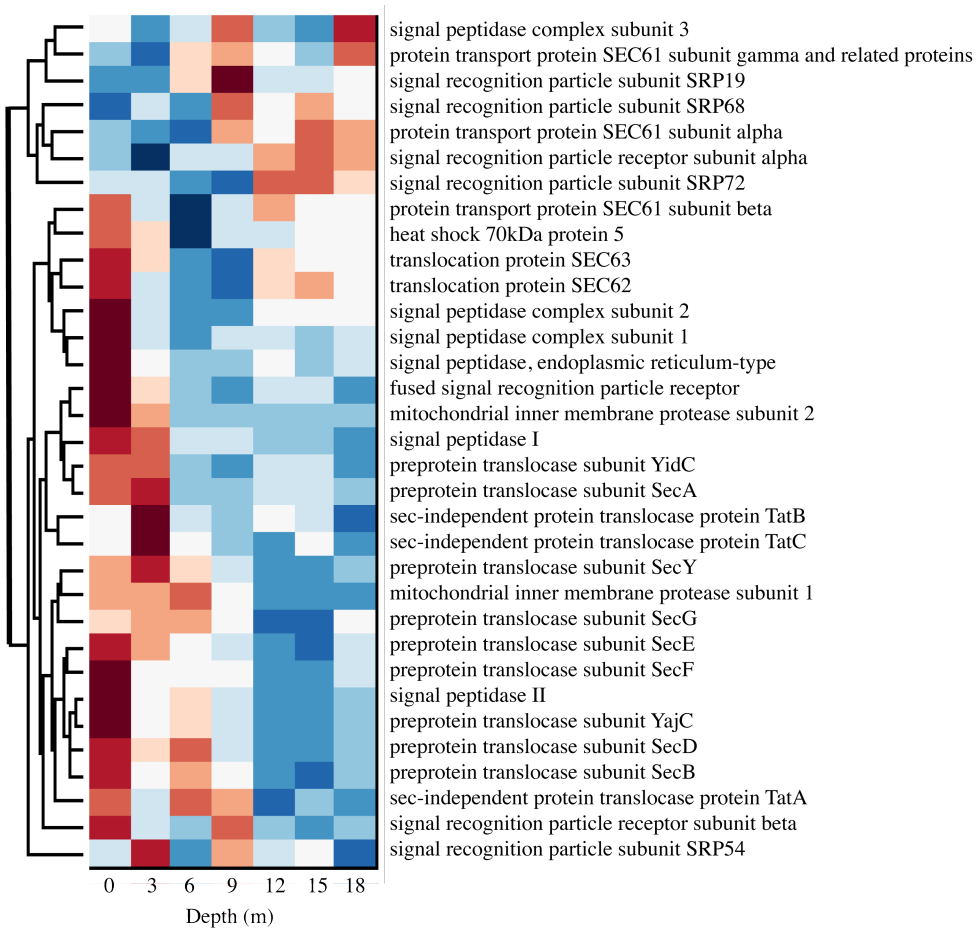

Figure 5.14: Hierarchical clustering of the read counts that map to a given ORF with a KO annotation in the protein export KEGG pathway.

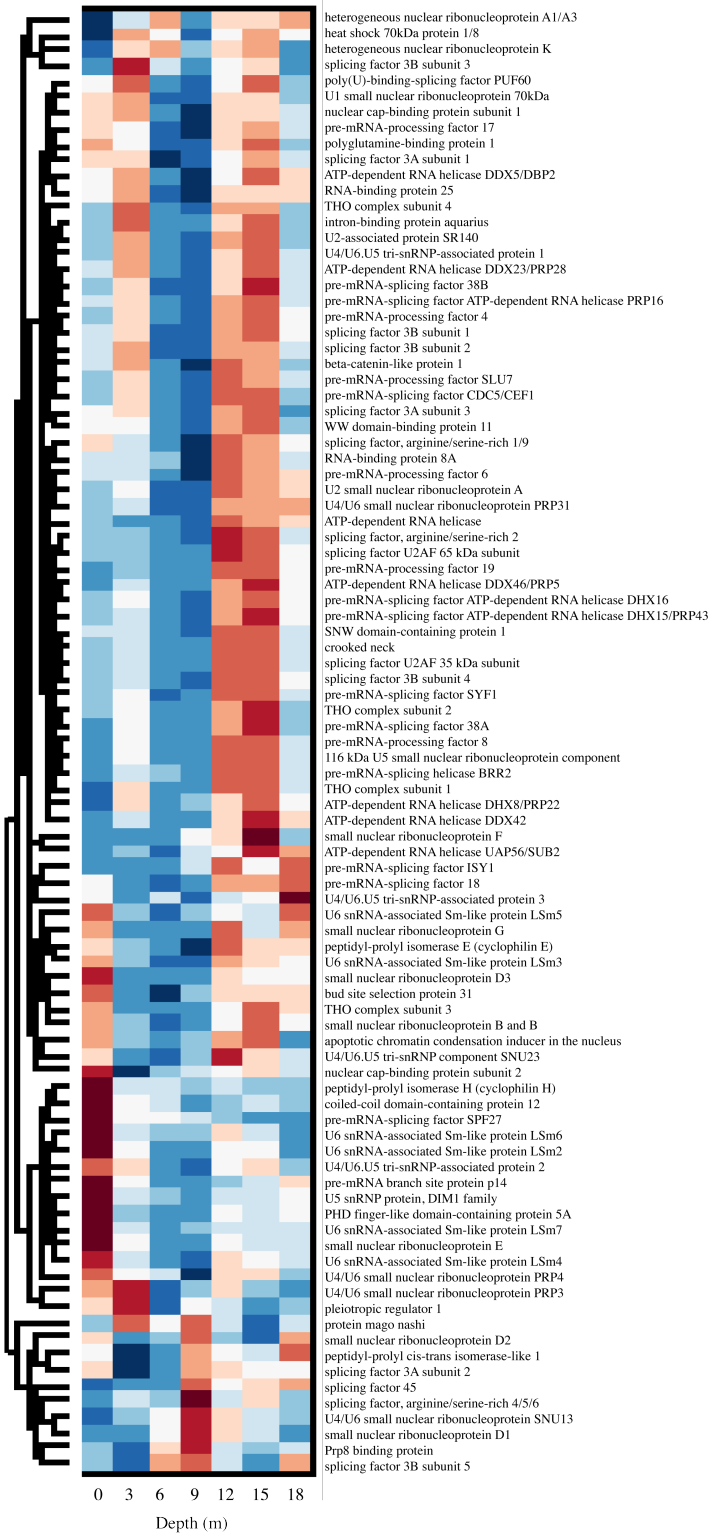

Figure 5.15: Hierarchical clustering of the read counts that map to a given ORF with a KO annotation in the spliceosome KEGG pathway.

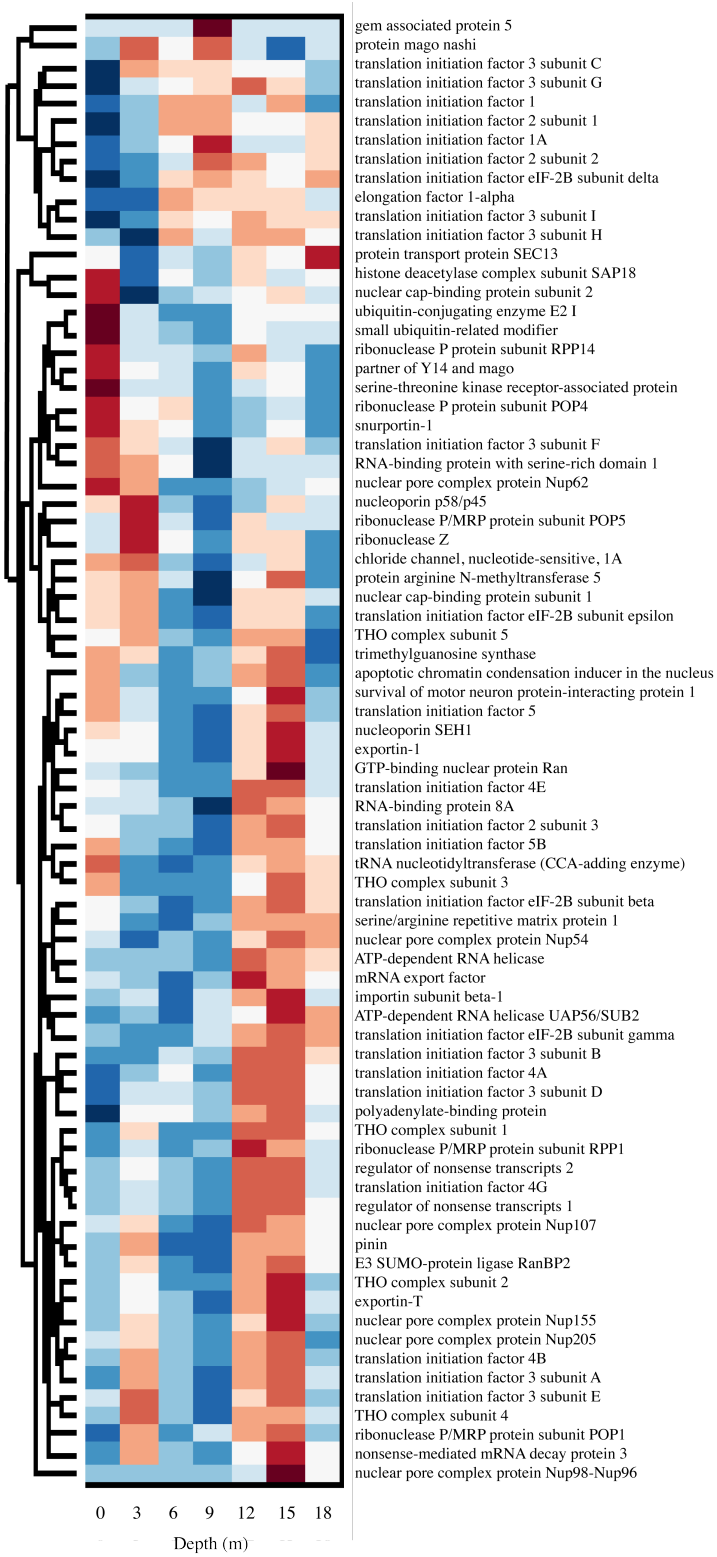

Figure 5.16: Hierarchical clustering of the read counts that map to a given ORF with a KO annotation in the RNA transport KEGG pathway.

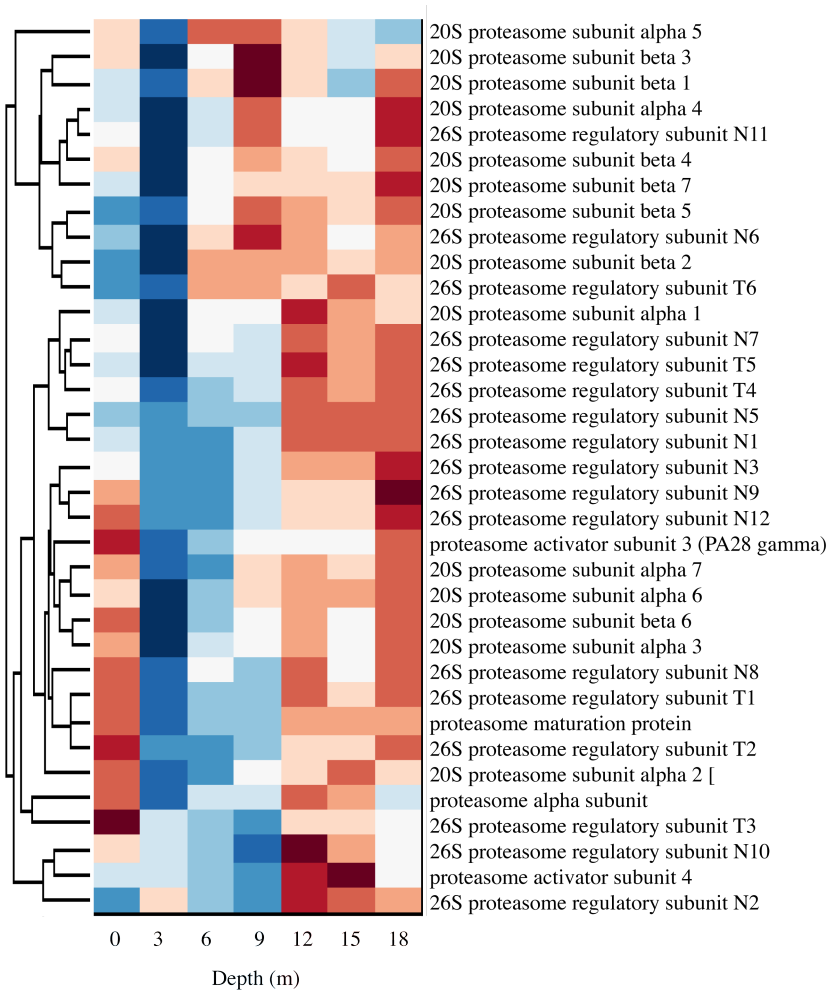

Figure 5.17: Hierarchical clustering of the read counts that map to a given ORF with a KO annotation in the proteosome KEGG pathway.

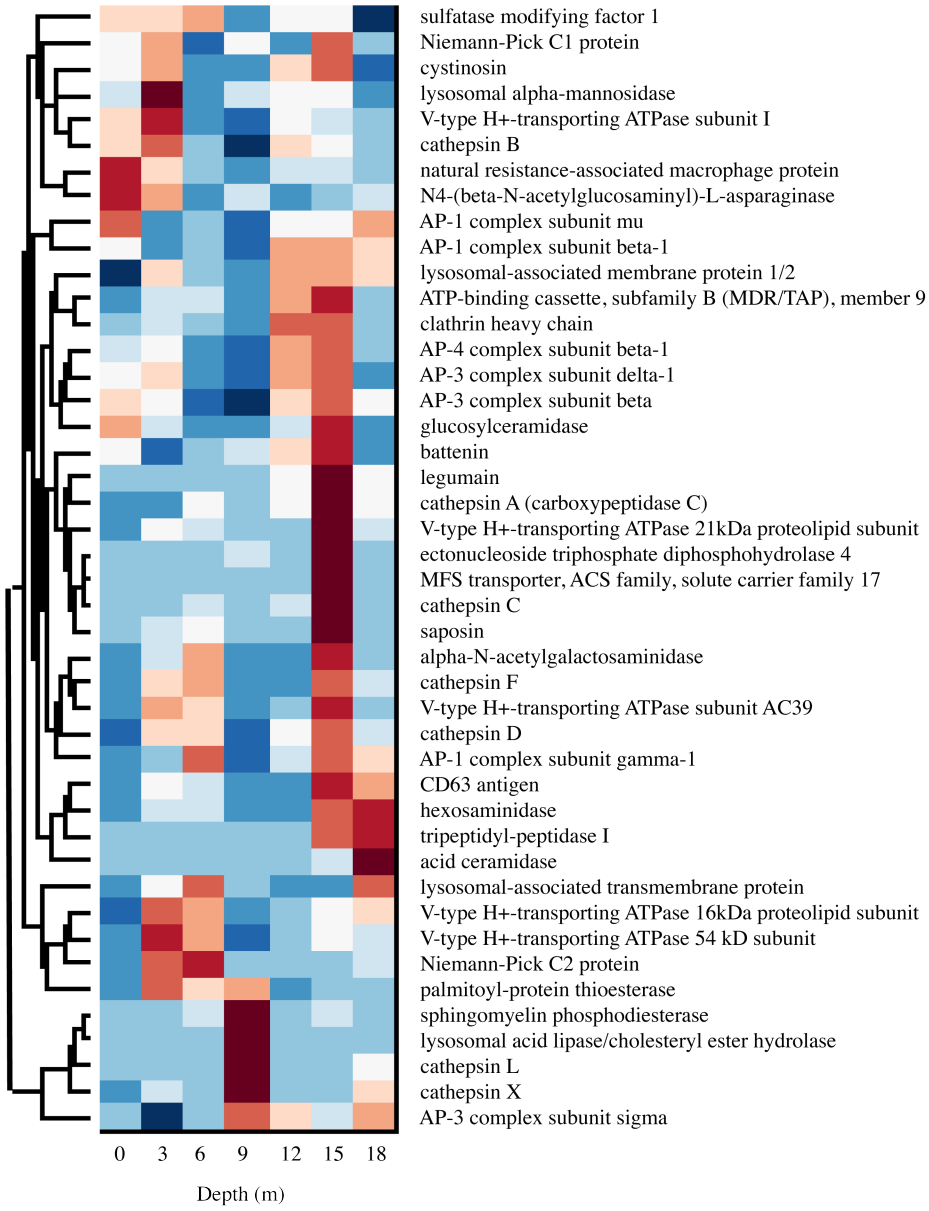

Figure 5.18: Hierarchical clustering of the read counts that map to a given ORF with a KO annotation in the lysosome KEGG pathway.

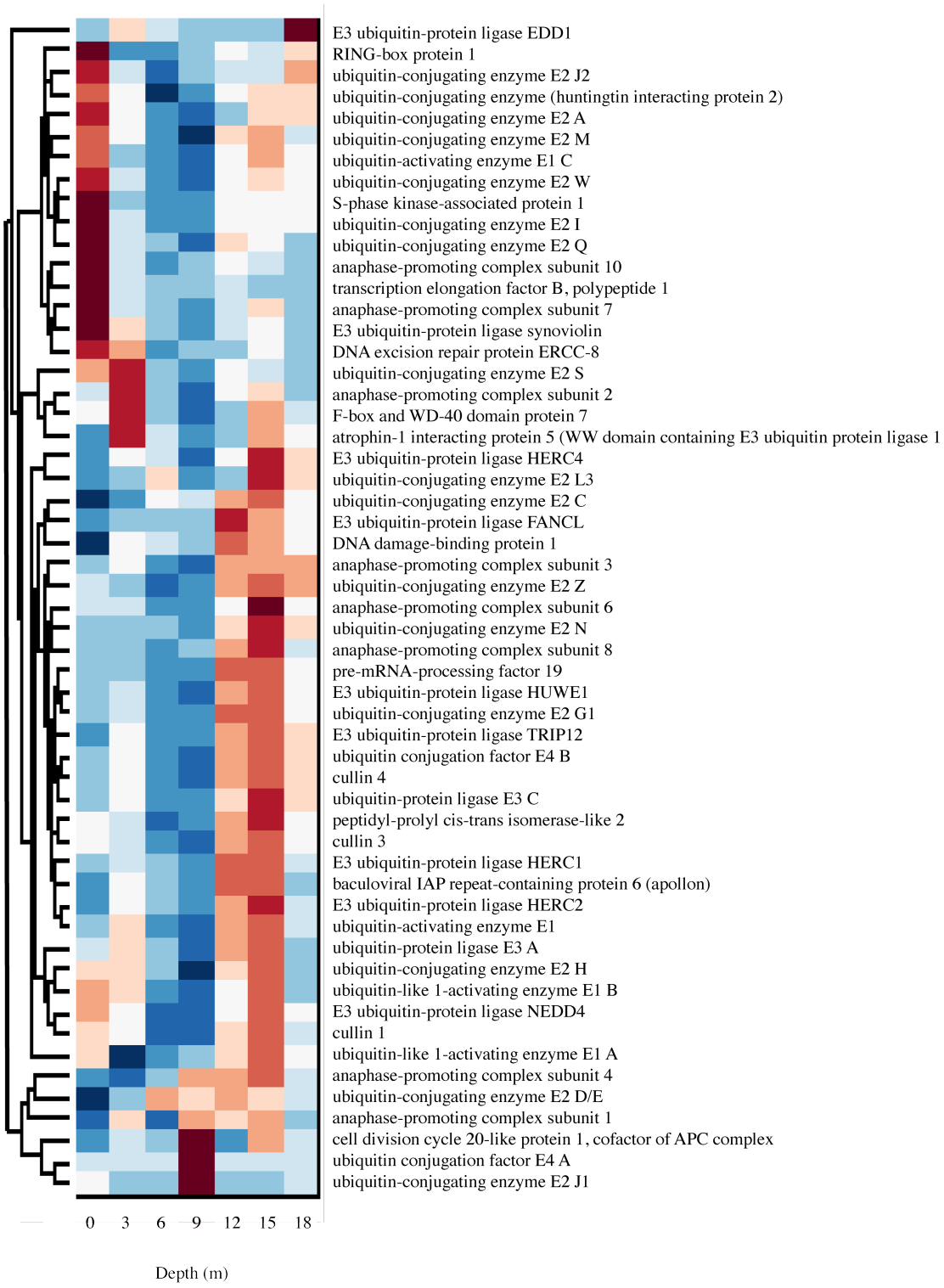

Figure 5.19: Hierarchical clustering of the read counts that map to a given ORF with a KO annotation in the ubiquitin-mediated proteolysis KEGG pathway.

Table 5.1: Sequencing statistics

Total Transcripts (10^3)	371
Transcript (Mbp)	122

	0m	3m	6m	9m	12m	15m	18m
average library size (Gbp)	1.72	2.53	1.68	1.97	1.94	2.33	2.82
average # reads (10^6)	19.5	28.6	19.0	22.2	21.9	26.3	31.9
average # of assembled reads (10^6)	16.1	25.3	16.7	19.6	18.8	22.8	27.3
average # transripts (10^3)	192	231	208	218	273	301	286
average % w/ KO annotation	8.2	9.0	10.3	9.7	8.1	8.0	8.6
average % with pfam annotation	11.3	12.1	13.8	13.3	11.2	11.3	12.1

References

Apt, K., Clendennen, S., Powers, D., and Grossman, A. (1995). The gene family encoding the fucoxanthin chlorophyll proteins from the brown alga *Macrocystis pyrifera*. Molecular and General Genetics *246*, 455–464.

Auer, P., and Doerge, R. (2010). Statistical design and analysis of RNA sequencing data. Genetics *185*, 405–416.

Birzele, F., Schaub, J., Rust, W., Clemens, C., Baum, P., Kaufmann, H., Weith, A., Schulz, T.W., and Hildebrandt, T. (2010). Into the unknown: expression profiling without genome sequence information in CHO by next generation sequencing. Nucleic Acids Research *38*, 3999–4010.

Cavanaugh, K., Siegel, D., Kinlan, B., and Reed, D. (2010). Scaling giant kelp field measurements to regional scales using satellite observations. Marine Ecology Progress Series *403*, 13–27.

Collins, L., Biggs, P., Voelckel, C., and Joly, S. (2008). An approach to transcriptome analysis of non-model organisms using short-read sequences. Genome Informatics *21*, 3–14.

Dupont, S., Wilson, K., Obst, M., Sköld, H., Nakano, H., and Thorndyke, M. (2007). Marine ecological genomics: when genomics meets marine ecology. Marine Ecology Progress Series *332*, 257–273.

Ekblom, R., and Galindo, J. (2010). Applications of next generation sequencing in molecular ecology of non-model organisms. Heredity *107*, 1–15.

Nishiyama, Y., Los, D., and Murata, N. (1999). PsbU, a protein associated with photosystem II, is required for the acquisition of cellular thermotolerance in *Synechococcus* species PCC 7002. Plant Physiology *120*, 301–308.

Peters, A., Marie, D., Scornet, D., Kloareg, B., and Cock, J. (2004). Proposal of *Ectocarpus siliculosus* (Ectocarpales, Phaeophyceae) as a model organism for brown algal genetics and genomics. Journal of Phycology *40*, 1079–1088.

Rho, M., Tang, H., and Ye, Y. (2010). FragGeneScan: predicting genes in short and error-prone reads. Nucleic Acids Research *38*, e191.

Robinson, M., McCarthy, D., and Smyth, G. (2010). edgeR: a Bioconductor package for differential expression analysis of digital gene expression data. Bioinformatics *26*, 139–140.

Walker, T. (1982). Use of a secchi disc to measure attentuation of underwater light for photosynthesis. Journal of Applied Ecology *19*, 539–543.

CONCLUDING REMARKS

The giant kelp, *Macrocystis pyrifera*, is the largest alga on earth and also has a large geographic distribution. It is a member of the brown algae (Phaeophyceae), a complex multicellular group divergent from other eukaryotes with interesting evolutionary and ecological features and biotechnological applications (Chapter 2). Due to its large height, *M. pyrifera* possesses some interesting structural features including sieve tubes that allow for metabolite transfer between different parts of an individual allowing for physical separation of processes such as photosynthesis and nutrient acquisition. All parts of *M. pyrifera* are photosynthetic, yet different sections of one individual may inhabit very different environmental conditions, making the giant kelp a unique organism to explore physiological variation within the environment.

M. pyrifera lives in a variable environment. In order to understand, measure and study the temporal and spatial scales of kelp biological response, it is important to understand the spatiotemporal scales of hydrographic variation. Thermistor chain data was used to examine depth-specific variations in temperature, and therefore nutrients, on a variety of time scales (Chapter 3). These vertical distribution patterns were shown to vary spatially within a kelp bed, with biologically important consequences for *M. pyrifera*. The variable temperature and nutrient environment has different biological relevance depending on depth; for example, the majority of photosynthesis occurs in the surface canopy, while recruitment processes take place on the kelp forest floor. This time series was also used to calculate water-column integrated nitrate

through time and which was used to estimate an upper bound of productivity. The dominant time scales of temperature variations were diurnal and semidiurnal. The time series showed evidence of rapid variation in the depth of the nutricline, as much as 10m vertical change over the span of a few hours. These abrupt changes in the nitrate climate may affect change in regulatory mechanisms and the metabolism of kelp. Evidence of short time scale environmental events, such as nutrient pulses delivered with internal waves, provide a natural setting to look at short-time scale physiological responses of *M. pyrifera* to these events. Kelps can take up nutrients on time scales of minutes to hours, but it is unknown exactly how kelps are reacting physiologically to these short time scale inputs.

Phaeophyceae are evolutionarily distant from other photoautotrophs, thus, the applicability of information learned from species such as the model plant *Arabidopsis* remain somewhat limited for the Phaeophyceae. Chapter 2 assesses the current state of genomic knowledge for the Phaeophyceae and reviews examples of sequence-based data being applied to evolutionary and ecological questions. *E. siliculosus* is the only member of the Phaeophyceae with a sequenced genome, and there are only a handful of other Phaeophyceae members with EST data. Yet, even this limited data provide information on novel proteins (Chapter 2). The current increasing trend in genomic information linked with decreasing sequencing costs provides an opportunity to expand our sequenced-based knowledge of non-model, but ecologically important, organisms such as *M. pyrifera*.

Through next-generation transcriptional profiling of the giant kelp, *M. pyrifera,* we greatly increased the number of identified transcriptional units and

created a sequence-based tool kit for future ecophysiological study of this species. A RNA extraction protocol was optimized to consistently obtain high quality RNA for downstream qPCR and sequencing efforts. This dissertation represents one of the few examples of large-scale expression sequence analysis of an organism without an appropriate reference genome. Challenges included assigning functional annotations to transcripts through traditional alignment based approaches because of the lack of related organisms with annotated genomes. The broad untargeted transcriptomic view that next generation sequencing provides allowed us to begin to identify key mechanisms of the physiological and metabolic response to a changing environment.

In exploring variability in gene expression with depth across natural environmental gradients, we saw some interesting patterns emerge. Chapter 4 compares gene expression in *M. pyrifera* blades collected at the surface and at 18m depth in two seasons; Chapter 5 examines blades every 3m through the water column to explore depth-related patterns in the global transcriptome in the giant kelp across biologically relevant gradients in light, temperature and nutrients. At the surface, where irradiance levels are highest and the potential for oxidative damage is most intense, physiological processes are focused on the capture of light energy for photosynthesis as well as protection from the damaging effects of the sun. *M. pyrifera* has multiple light harvesting complexes, which may indicate the importance of being able to adjust photosynthetic electron flow in a variable environment. Genes involved in nutrient acquisition, genetic information processing and degradation tended to be more highly expressed at depth.

In addition to *M. pyrifera* gene expression patterns with depth, I saw patterns in *M. pyrifera* tissue stable isotopes with depth (Appendix 1) that warrant further investigation. Stable isotopes represent the physiological response of kelp to environmental conditions integrated over longer time scales than that of gene expression and provide another way to examine kelp response on longer time scales. Consistent patterns of negative correlations of both $\delta^{13}C$ and $\delta^{15}N$ values with depth in *Macrocystis pyrifera* blades along a stipe were seen at three locations along the California coastline during the summer. Values did not vary with depth during the winter in La Jolla. Higher $\delta^{13}C$ values near the surface may be a result of increased rates of photosynthesis due to higher light availability, thus altering the balance of CO_2 vs. HCO_3^- incorporation. The lower $\delta^{15}N$ values at depth likely reflect oceanic nitrate values and higher values in the surface may be due to recycling of nitrogen or an alternate nitrogen source.

Symbioses can also affect the kelp physiology, either negatively or positively. Appendix 2 is a brief exploration of the bacteria associated with *M. pyrifera* blades. Scanning electron micrographs revealed the presence of several different bacterial morphotypes living on the blades of *M. pyrifera*. I taxonomically identified bacteria isolated from *M. pyrifera* blades that were capable of growing on a mannitol-based carbon source. Future studies using culture-independent techniques will be able to examine the biodiversity and begin to explore the complex ecology of these symbiotic interactions in the ecologically important giant kelp, *M. pyrifera*. This appears to be a rich area for future research, especially with rapid advances in molecular tools and approaches for both algal and microbial genomics.

This dissertation provides the first transcriptomic characterization of *M. pyrifera* and places the findings in the context of its natural and variable environment. Just as the development of the microscope and SCUBA allowed for exploration of unknown and previously unseen aspects of biology, sequencing technology also provides an opportunity for the generation of new hypotheses and a tool to extend biological studies. These transcriptomic data represent a valuable genomic resource for future study of *M. pyrifera*. As with much of science, attempting to address one question, opens the doors to many others.

APPENDIX 1

Carbon and Nitrogen Stable Isotope Patterns with Depth in *Macrocystis pyrifera*

Abstract

Consistent patterns of negative correlations of both $\delta^{13}C$ and $\delta^{15}N$ values with depth in *Macrocystis pyrifera* blades along a stipe were seen in three locations along the California coastline during the summer; depth-dependent variation was not observed during the winter in La Jolla. $\delta^{13}C$ with $\delta^{15}N$ were positively correlated, as were percent tissue N with percent C. Higher $\delta^{13}C$ values near the surface may be due to increased rates of photosynthesis due to higher light availability, thus altering the balance of CO_2 vs. HCO_3^- incorporation. The lower $\delta^{15}N$ values at depth likely reflect oceanic nitrate values and higher values in the surface may be due to the recycling of nitrogen or an alternate nitrogen source. The observed patterns warrant further investigation.

Introduction

An understanding of the variability in carbon and nitrogen natural abundance ratios at the base of the food web (i.e. primary producers) is useful for understanding food web dynamics as these values will be reflected in the consumers. Stable isotope values of primary producers vary in time and space and reflect the time-integrated nutrient and carbon exposure and source. I examined within-individual variation of carbon and nitrogen stable isotope values in the primary producer *Macrocystis pyrifera*, at three locations in California: La Jolla, Del Mar, and Monterey, during the summer and winter of 2009.

Methods

Sampling sites included La Jolla (N 32° 51; W 117° 18) and Del Mar (N 32° 58; W 117° 17), San Diego County; Hopkins Marine Station, Monterey (N 36° 37; W 121° 54). The Monterey site was chosen as a location where nitrate should be more readily available for the kelp; however, temperatures were anomalously warm on the sampling days in Monterey. Blades of *M. pyrifera* were collected on SCUBA at depths ranging from the surface to 21 m depth depending on the site, on several sampling dates in 2009 (Table A1.1) and cleaned of any epiphytes. Samples were then dried to a constant mass at 60°C and ground to a fine powder using a mortar and pestle. Approximately 5 mg *M. pyrifera* powder (weighed with precision to .001g) was placed in tin capsules and sent to the UC Davis Stable Isotope Facility where they were analyzed for $\delta^{13}C$ and $\delta^{15}N$ isotopes and total amount of tissue carbon and nitrogen using a PDZ Europa ANCA-GSL elemental analyzer interfaced to a PDZ

Europa 20-20 isotope ratio mass spectrometer (Sercon Ltd., Cheshire, UK). Some samples had three replicates sent for analysis; if that was the case, these were averaged before analysis. Samples collected in January were considered 'winter'; samples collected in June – August were considered 'summer.'

Results & Discussion

The range and mean of all *M. pyrifera* samples collected during 2009 at the three locations were: $\delta^{13}C$ (-20.6 to -11.6; -16.0), $\delta^{15}N$ (5.3 to 12.2; 9.8), %C (18.6 to 40.8; 33.6), and %N (0.7 to 5.0; 2.7). These values are consistent with other *M. pyrifera* values reported in the literature (Table A1.2). In Table A1.1, these parameters are reported by sampling day and location.

There was a positive correlation between $\delta^{15}N$ and $\delta^{13}C$; and for %N & %C (Figures 1-4, a & b). In central California, $\delta^{13}C$ and $\delta^{15}N$ showed seasonal patterns; lowest values occurred in the spring and the highest in the Fall (Foley and Koch, 2010). In that study, temporal variation in $\delta^{15}N$ was most strongly related to the strength of upwelling and nitrate concentration. At locations where my sampling was conducted in both summer and winter (La Jolla and Del Mar), summer $\delta^{15}N$ values were lower than winter values (Figures A1.2 – A1.3, a). In La Jolla, percent N also was lower in summer compared to winter (Figure A1.2b). There was no apparent correlation between C:N and depth, though the spread of data points was greater at the surface (Figures A1.1-A1.4, e). In Monterey, $\delta^{15}N$ and percent nitrogen had a positive correlation ($R^2 = 0.3618$, Figure A1.4f).

A consistent pattern of decreasing $\delta^{15}N$ with depth along a kelp stipe was seen at all three locations (Figures A1.1-A1.4, c) except for the La Jolla individual collected during the winter (Figure A1.2c). Lower $\delta^{15}N$ values at deeper depths may be reflective of upwelled nitrate. Values of 5-7 ‰ are found in subthermocline waters of the North Pacific (Wada et al., 1975; Casciotti et al., 2002; Wankel et al., 2007). Ocean $\delta^{15}N$ values for nitrate ranged from 2.6 – 14.5 ‰ in Monterey Bay, with higher values in the euphotic zone due to phytoplankton uptake (Wankel et al., 2007). Algae discriminate between heavy and light isotopes when nutrients are abundant (Ostrom et al., 1997). If nitrate were the only source of nitrogen being incorporated, surface blades would not be able to fractionate isotopically (because nitrate levels can be limiting near the surface) so they would be expected to have values approximately equal to those of the available to nitrate. However, we are seeing the opposite pattern: higher $\delta^{15}N$ values where we suspect there is less available nitrate from upwelling. Thus, additional nitrogen sources besides nitrate are likely being utilized. Enriched $\delta^{15}N$ values are associated with processes associated with the microbial loop and regeneration of nitrogen so there may be a higher level of nitrogen recycling in the surface waters. Fractionation occurs with both nitrate and ammonium uptake and assimilation because $\delta^{14}N$ is preferentially taken up compared to $\delta^{15}N$ (Evans, 2001). Terrestrial sources of nitrogen along the Big Sur coastline were considered to contribute little due to their episodic nature and their signal was swamped by the more consistent upwelling (Foley and Koch, 2010). Perhaps the seasonal difference in slope of $\delta^{15}N$ with depth is reflective of upwelling conditions. Southern California has even less storm activity and river input than farther up the coast, so here too we expect

terrestrial nitrogen to have minimal contributions, though we cannot rule out the possibility that the enriched values at the surface represent a source other than oceanic nitrate or recycled nitrogen.

There was also a consistent pattern of decreasing $\delta^{13}C$ with depth (Figures A1.1-A1.4, d), with the exception of the La Jolla individual collected in winter (Figure A1.2, d). The range of $\delta^{13}C$ values for macroalgae correlates with taxonomic group and carbon concentrating mechanisms related to photosynthesis, with higher $\delta^{13}C$ values potentially resulting from increased use of bicarbonate (Raven et al., 2002). Additionally, pelagic phytoplankton drawdown of CO_2 in the surface may be forcing the kelp to increase its use of HCO_3^-. If blades near the surface had a higher rate of aqueous CO_2 drawdown compared to depth (as would be expected with higher rates of photosynthesis near the surface), they would have higher $\delta^{13}C$ values compared to at depth (Simenstad et al., 1993). This pattern of higher $\delta^{13}C$ values in shallower samples is also seen by Foley & Koch (2010) during the spring and early summer. $\delta^{13}C$ enrichment at high irradiance may be related to increased rates of photosynthesis and uptake of bicarbonate, an enriched source of carbon (Cornelisen et al., 2007). Perhaps the seasonal differences in slope with depth in La Jolla relate to seasonal CO_2 stratification in the water. The conversion of photosynthate into lipids can cause a decrease in $\delta^{13}C$ (Raven et al., 2002), which may be another factor in the depth differences seen in *M. pyrifera.*

The patterns seen in this study and elsewhere should be examined in further detail with higher sample numbers and on different space and time scales. Some

potential hypotheses to test with a statistically rigorous experimental design in the future include:

H_1: *M.* pyrifera $\delta^{15}N$ values are reflecting their ambient nitrate concentration, which differs along the length of the stipe. To test, fine scale measurements of water column nitrate and dissolved organic nitrogen should be taken in conjunction with kelp tissue nitrogen stable isotope sampling through time. Seasonal differences, such as the loss of depth-dependent variation in the winter in La Jolla, would be worth exploring in the context of seasonal upwelling.

H_2: Carbon and nitrogen isotope values may change with age of blade tissue (Page et al., 2008). Surface blades along a given stipe are younger because the stipes grow toward the surface from depth. Differences in age could potentially lead to differences in uptake needs and abilities. Transplant experiments that take blades of the same age and place at different depths could isolate the effects of age from other factors.

H_3: $\delta^{13}C$ values are correlated with irradiance levels and photosynthetic activity. To assess this hypothesis, blades acclimated to the same conditions could be placed in experimentally manipulated light level conditions (perhaps with mesh screens in the natural environment) while CO_2 saturation state of the water and the $\delta^{13}C$ and photosynthetic parameters of the kelp, and perhaps physiological activity such as gene expression of bicarbonate transporters, are measured.

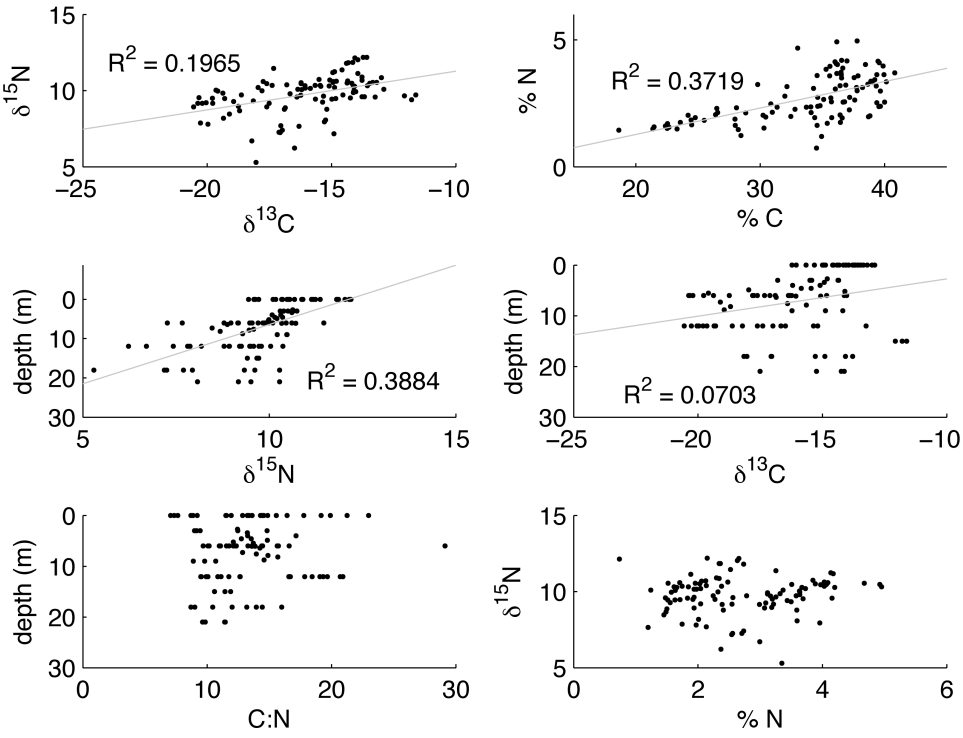

Figure A1.1: *Macrocystis pyrifera* stable isotope and percent carbon and nitrogen data aggregated from all sites. R^2 values shown if p-value < 0.01

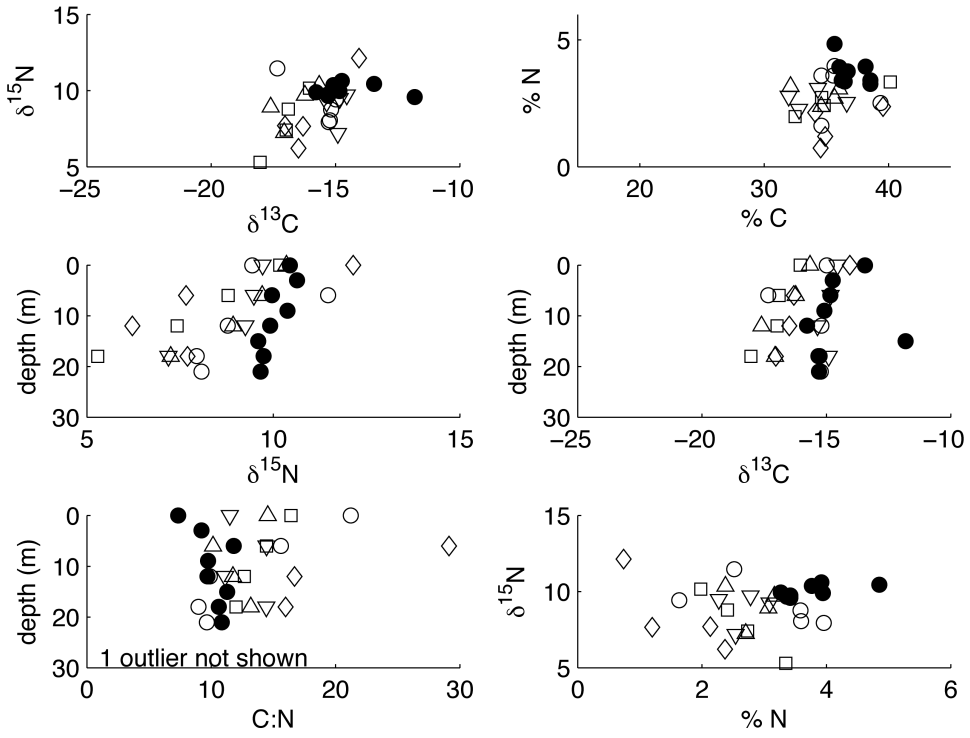

Figure A1.2: La Jolla *Macrocystis pyrifera* stable isotope and percent carbon and nitrogen with depth. Each symbol represents a different individual, n = 6. Solid symbols indicate samples collected in winter and open symbols indicate samples collected in summer.

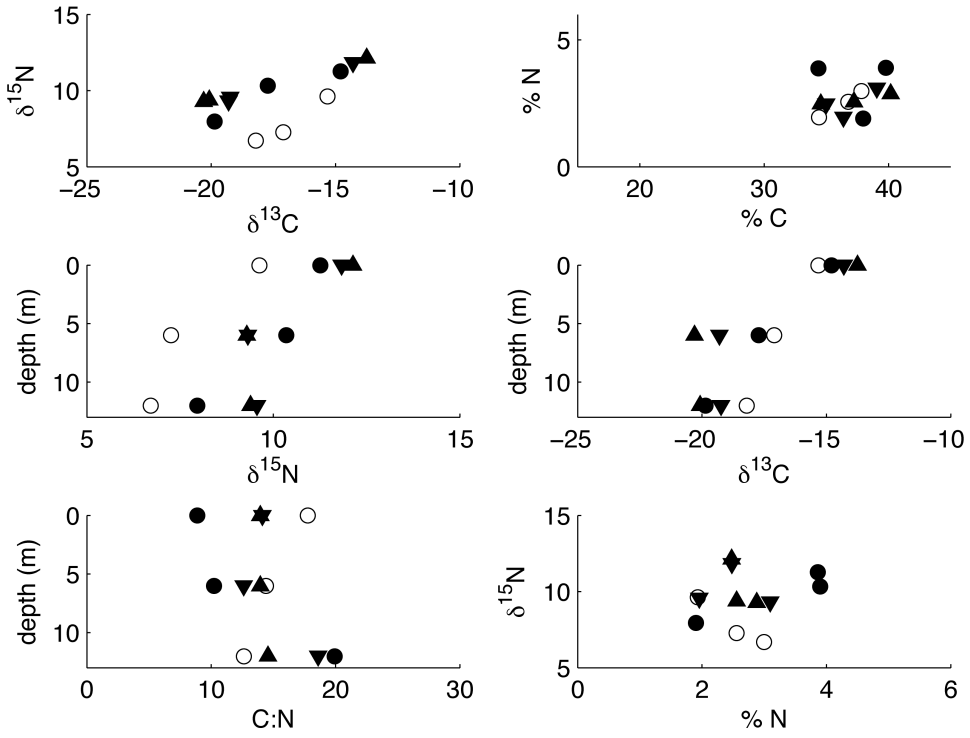

Figure A1.3: Del Mar *Macrocystis pyrifera* stable isotope and percent carbon and nitrogen with depth. Each symbol represents a different individual, n = 4. Solid symbols indicate samples collected during the winter and open symbols indicate samples collected during the summer.

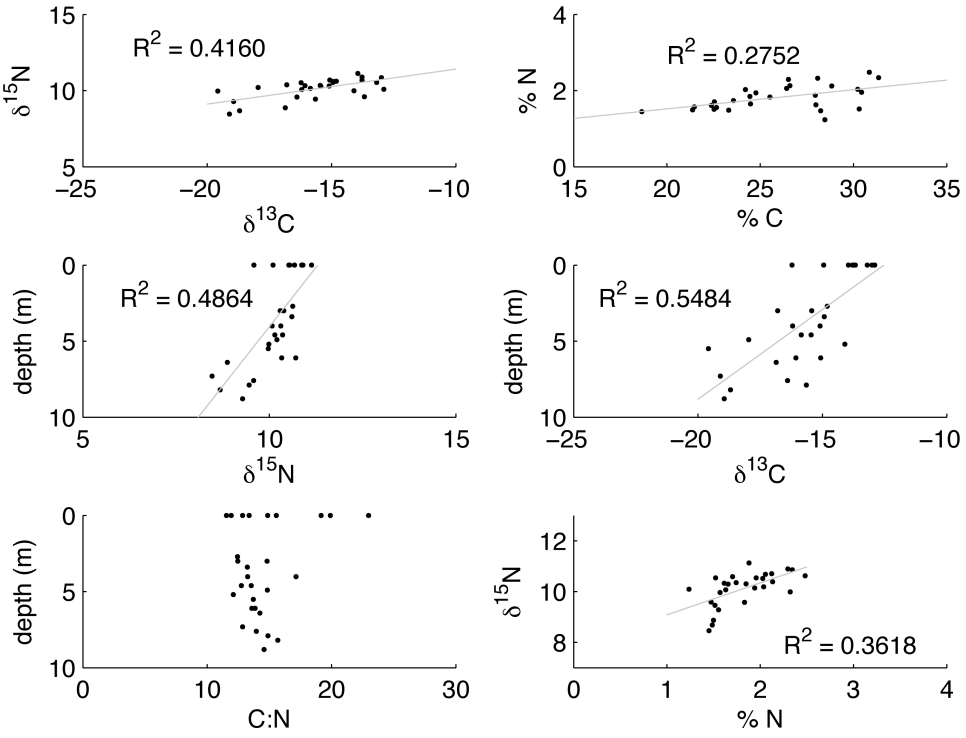

Figure A1.4: Monterey *Macrocystis pyrifera* stable isotope and percent carbon and nitrogen data for 11 individuals collected during the summer. R^2 values shown if p-value < 0.01

Table A1.1: Summary of stable isotope data collected

Sites (sampling depths)	Sampling dates (# individuals)	$\delta^{13}C$		$\delta^{15}N$		% C		%N	
		range	mean	range	mean	range	mean	range	mean
La Jolla (0-21 m)	7 Jan 2009 (1)	-18.2 to -11.6	-14.5	9.2 to 10.7	10	33 to 39.5	37	2.6 to 5.0	3.7
	24 Jul 2009 (1)	-17.3 to -15.0	-15.6	7.9 to 11.5	9.1	34.6 to 39.4	36	1.6 to 4.0	3
	31 Jul 2009 (1)	-15.4 to -14.6	-14.9	7.2 to 9.7	8.9	32.0 to 36.7	33.9	2.3 to 3.1	2.7
	6 Aug 2009 (1)	-17.6 to -15.7	-16.6	7.3 to 10.4	9	32.2 to 36.0	34.6	2.4 to 3.2	2.8
	13 Aug 2009 (2)	-18.0 to -14.0	-16.5	5.3 to 12.1	8.2	32.5 to 40.2	35.6	.7 to 3.4	2.1
Del Mar (0-12 m)	16 Jan 2009 (3)	-20.6 to -13.6	-17.7	7.8 to 12.2	10.1	29.8 to 40.8	37.2	1.7 to 4.2	2.8
	18 Jun 2009 (1)	-18.2 to -15.3	-16.9	6.7 to 9.6	7.9	34.4 to 37.8	36.3	1.9 to 3.0	2.5
Monterey (0-9 m)	28 Aug 2009 (6)	-19.1 to -13.2	-15.7	8.5 to 11.1	9.9	18.6 to 30.4	24.9	1.5 to 2.3	1.7
	31 Aug 2009 (5)	-19.6 to -12.9	-15.5	10.0 to 10.9	10.4	21.5 to 31.3	27.4	1.3 to 2.5	1.9

Table A1.2: Range of reported *Macrocystis* stable isotope values

$\delta^{13}C$	$\delta^{15}N$	*Location*	*Citation*
-25 to -13 ‰	2 – 10 ‰	Big Sur, CA	(Foley & Koch, 2010)
-13.8 to -12.2 ‰ (mean values)	8.5 – 9.7 ‰ (mean values)	Santa Barbara, CA	(Page et al., 2008)
-20.7 to -11.1 ‰	N/A	Multiple	(Appendix, Raven et al., 2002)
-20.6 to -11.6 ‰	5 – 12 ‰	San Diego & Monterey, CA	This study

References

Casciotti, K.L., Sigman, D.M., Hastings, M.G., Böhlke, J.K., and Hilkert, A. (2002). Measurement of the oxygen isotopic composition of nitrate in seawater and freshwater using the denitrifier method. Analytical Chemistry *74*, 4905–4912.

Cornelisen, C., Wing, S., Clark, K., Bowman, M., Frew, R., and Hurd, C. (2007). Patterns in $\delta^{13}C$ and $\delta^{15}N$ signature of *Ulva pertusa*: Interaction between physical gradients and nutrient source pools. Limnology and Oceanography *52*, 820–832.

Evans, R. (2001). Physiological mechanisms influencing plant nitrogen isotope composition. Trends in Plant Science *6*, 121–126.

Foley, M., and Koch, P. (2010). Correlation between allochthonous subsidy input and isotopic variability in the giant kelp *Macrocystis pyrifera* in central California, USA. Marine Ecology Progress Series *409*, 41–50.

Ostrom, N., Macko, S., Deibel, D., and Thompson, R. (1997). Seasonal variation in the stable carbon and nitrogen isotope biogeochemistry of a coastal cold ocean environment. Geochimica Et Cosmochimica Acta *61*, 2929–2942.

Page, H., Reed, D., Brzezinski, M., Melack, J., and Dugan, J. (2008). Assessing the importance of land and marine sources of organic matter to kelp forest food webs. Marine Ecology Progress Series *360*, 47–62.

Raven, J., Johnston, A., Kübler, J., Korb, R., McInroy, S., Handley, L., Scrimgeour, C., Walker, D., Beardall, J., Vanderklift, M., et al. (2002). Mechanistic interpretation of carbon isotope discrimination by marine macroalgae and seagrasses. Functional Plant Biology *29*, 355–378.

Simenstad, C.A., Duggins, D.O., and Quay, P.D. (1993). High turnover of inorganic carbon in kelp habitats as a cause of delta^{13}C variability in marine food webs. Marine Biology *116*, 147–160.

Wada, E., Kadonaga, T., and Matsuo, S. (1975). ^{15}N abundance in nitrogen of naturally occurring substances and global assessment of denitrification from isotopic viewpoint. Geochemical Journal *9*, 139–148.

Wankel, S., Kendall, C., Pennington, J., Chavez, F., and Paytan, A. (2007). Nitrification in the euphotic zone as evidenced by nitrate dual isotopic composition: Observations from Monterey Bay, California. Global Biogeochemical Cycles *21*.

APPENDIX 2

Preliminary Investigations into the Bacteria Associated with the Blades of *Macrocystis pyrifera*

Microorganisms are abundant in the marine environment, occupying both the water column and surfaces of macroorganisms. There is rising interest in algal-microbe interactions in recent years (Goecke et al., 2010). These symbiotic relationships span the spectrum of mutualistic, commensalistic, and parasitic relationships. In a mutualistic relationship, the surface of macroalgae provides an organic rich material and oxygen environment favorable for bacterial colonization; in return, bacteria remineralize organic materials and provide the algae with products such as carbon dioxide, ammonia, or vitamins (Croft et al., 2006). Other potential benefits provided by bacteria to macroalgae include chemical defense via secondary metabolites against biofouling or defense against pathogens. A commensal relationship scenario would be consumption by microbes of kelp-derived carbon with no return benefit to the macroalgae. Negative bacterial interactions with macroalgae include competition for nutrients, or inhibition of gas exchange and light absorption. Parasitic bacteria can cause disease (Vairappan et al., 2001; Wang et al., 2008).

Early studies characterizing bacteria associated with macroalgal surfaces were culture and microscopy based and emphasized count and morphological (e.g. cocci vs. rod) differences associated with different incubation conditions (Laycock, 1974). Seasonal and habitat specific differences were observed using these approaches (Laycock, 1974; Mazure, 1978; Mazure and Field, 1980). Recently, molecular

biology approaches have been employed to characterize bacteria associated with macroalgae in a culture-independent way. A recent review thoroughly examines the research from the last 40 years on macroalgal-bacterial interactions (Goecke et al., 2010). For brown algae (Phaeophyceae), culture-dependent techniques remain the dominant approach though molecular techniques have begun to be applied in the last decade (Figure A2.1).

The epibacterial community can be highly specific to a given algal species; community composition was more similar between individuals of the same species occupying different habitats than those from different species inhabiting the same habitat (Lachnit et al., 2009). Study of these species-specific associations has led to the discovery of new bacterial species (Goecke et al., 2010). The composition and roles of the *Macrocystis*-associated microbial community remains largely unstudied. *M. pyrifera* is the largest alga on earth, with individuals reaching tens of meters in height, and provides both a food source and habitat for many species. Young kelp blades exposed to antibiotic solutions (i.e. polymyxin, dihydrostreptomycin, chloromycetin, and magnamycin) showed marked reductions in photosynthesis and respiration (North, 1971) suggesting that some of these bacteria provide a benefit to *Macrocystis* (though an alternate explanation might be that the antibiotics were negatively affecting the kelp blades). Bacteria play an important role in the degradation of marine macrophyte material and contribute to the energy balance in kelp communities and surrounding waters (Laycock, 1974; Koop et al., 1982; Newell et al., 1982). With emerging molecular biology techniques, we hope soon to be able to answer ecological questions relating to *M. pyrifera*-associated unculturable bacteria.

For example, during summer months, when stratification is pronounced, *M. pyrifera* blades at the ocean surface are bathed in nitrate deplete water. Could a symbiotic relationship with bacteria capable of catalyzing transformations such as nitrification, nitrogen fixation or ammonia oxidation provide a nitrogen source? A recent study found bacterial ammonia oxidizing communities on macroalgal surfaces, including one Phaeophyte (however, this study failed to rinse the surfaces with filtered sea water thus rendering the conclusions tenuous) which has important implications for nitrogen cycling in these species (Trias et al., 2011).

In the mucus associated with *M. pyrifera* blades, I have observed filamentous bacteria by using the fluorescent DNA-stain, DAPI, and epifluorescence microscopy. Scanning electron micrographs also confirmed the presence of filamentous, rod-shaped and cocci bacteria associated with the blades of *Macrocystis* (Figure A2.2). I attempted to characterize the microbial community using both culture-based and molecular biology techniques with mixed success.

Scanning Electron Microscopy

Kelp blades were rinsed with sterile seawater to remove loosely associated bacteria and were fixed in 2.5% v/v EM grade gluteraldehyde (Electron Microscopy Sciences). Fixed samples were processed through an ethanol dehydration series (10%, 25%, 50%, 75% 100%), each 1h in duration. Dehydrated samples were critically point dried in a Tousimis Autosamdri (R) - 815 Critical Point Drier, to preserve the cellular structure. Samples were mounted on Aluminum stubs with carbon adhesive pads, coated with Pt/Pd to prevent charging, and imaged at 2 kV on a Zeiss 1540 Field

Emission Scanning Electron Microscope at the Center for Nanoscale Science & Engineering at the University of California Riverside. Electron microscopy was done with the help of G. Wanger (J. Craig Venter Institute).

Several different morphotypes were observed: filamentous (Figure A2.4), rod shaped (Figure A2.2), and cocci (Figure A2.3). The bacteria appear to preferentially be located in the depressions on the surface of the kelp—each of the pillow-like bumps is a cell of kelp (Figure A2.2). Some of the bacteria appear to be connected via wire-like structures (Figures A2.2, A2.4, A2.5). The nature of these connections remains unknown and may represent dehydrated extracellular polymeric substances (EPS) secreted by the bacteria, polysaccharides in the kelp mucus, or possibly, bacterial nanowires. Bacteriral nanowires have been described in several species of bacteria ranging from dissimalatory metal reducing bacteria (i.e. *Shewanella oneidensis* and *Geobacter sulfurreducens*) (Reguera et al., 2005; Gorby et al., 2006; El-Naggar et al., 2010; Summers et al., 2010), phototropic bacteria (i.e. *Synechosystis* sp. (Gorby et al., 2006) and a marine pseudomonad (i.e. *Pseudomonas stutzeri*, Wanger unpublished results). Bacterial nanowires are proposed to function as electrical connections between microbes and extracellular terminal electron acceptors or transfer electrons between individual cells (Reguera et al., 2005). Unfortunately, it is not possible to discern from electron micrographs if the filamentous structures observed connecting the bacteria on kelp blades to each other are a collapse of extracellular polymers dehydration (Dohnalkova et al., 2011) or nanowires (El-Naggar et al., 2010). El-Naggar et al. have developed advanced tools used to evaluate bacterial nanowires that have been adopted from the field of micro electromechanical

systems (MEMS), and which use nanolithographic techniques to connect the putative nanowires into an electrical circuit. Once fabricated, these bio-electrical devices can be used to measure the electrical properties of the bacterial nanowires (El-Naggar et al., 2010). The implications of electrical connections between kelp-associated bacteria, while intriguing thus far, remain elusive.

Culture-dependent Sequencing

Mannitol is the main carbon storage product found in *M. pyrifera*. Plumes of mannitol-fermenting bacteria associated with kelp forests can extend for several kilometers offshore (Koop et al., 1982). The approach described below was used to isolate bacteria that utilize mannitol as a carbon source.

Recipe for D-mannitol carbon source plates[1] (per 1 L):

500 ml 0.2 μm filtered seawater

495 ml milli-Q water

1 ml PO_4 (37.5 mM stock) KH_2PO_4

1 ml NH_4 (200 mM stock) NH_4Cl

2 ml Tris buffer for seawater plates (5% Tris-H_2SO_4 pH 7.8)

10 g bacterial agar

10 g D-mannitol (carbon source)

20 ml 0.01% phenol red stock

Autoclave, then add 1 ml of trace metal mix and 1 ml of f/2 vitamin mix.

[1] I also attempted to make plates with 1% alginic acid from brown algae as the alternate carbon source, but the agar would not dissolve and I was unable to make the plates at these concentrations.

I employed two methods for transferring the bacteria: pressing the *M. pyrifera* blades directly onto the plate and taking a swab to transfer to the plates. The two methods of inoculation resulted in growth of bacteria under both the light and dark growing conditions at 37°C. Control plates (no carbon source) did not show any growth. The phenol red pH indicator in the plate media turns yellow in the presence of acid by-products of mannitol fermentation. The plates where the kelp blades were directly pressed onto the agar showed that ~80% of the surface of the plate turned yellow as compared to ~10% of the swab method.

Eight cultures made from individual colonies grown on the D-mannitol plates grown in the light were incubated in a 3 ml Luria broth + 1.5 µl of Kanamycin (50 ng/ml) medium overnight on a 37ºC shake table. Plasmids were isolated using QIAprep Miniprep kit (Qiagen, Valencia, CA, USA). Four samples had the expected 16S rRNA band size and were sent for sequencing (Genewiz, La Jolla, CA, USA). Taxonomic assignment of returned sequences was done using Ribosomal Database Project (Cole et al., 2009) and returned the following sequences: two *Psychromonas* sp.*,* one *Psuedoalteromonas* sp. and one *Cobetia* sp. (Table A2.1).

The selective bias introduced by culture-based methods vastly under samples the bacteria consortia; it is generally accepted that <1% of bacteria are culture-able (Amann et al., 1995). However, this approach does provide a starting point to characterizing the kelp-associated microbial community.

Bacterial DNA Extraction

I tried several methods for isolating bacterial DNA from the mucus of kelp blades in order to create 16S rRNA libraries in an attempt to assess the full complement of bacteria in a culture-independent way. Table A2.2 lists the protocols and variations attempted. Common problems included high peaks in the 220-230 nm region resulting in low 260/230 and 260/280 ratios, which is indicative of contamination. Potential contaminants include carbohydrate carryover (common with plants and perhaps algae as evidenced in my samples by increased viscosity compared to water), residual phenol or salts from the extraction process or proteins. A lysis buffer that includes polyvinylpyrolidone and BSA in a high salt concentration was used to bind polyphenols and lower the amount of coextracted polysaccharides (Snirc et al., 2010). Despite the addition of various clean-up steps, qPCR attempts with universal bacterial primers did not work for the macroalgal-associated bacteria, though the *E. coli* controls showed PCR products indicating appropriate cycling conditions and reagents. Much progress is being made in this fruitful area of research and I expect these challenges for isolating bacteria from *M. pyrifera* will be overcome in the near future.

Conclusions

The existence of bacteria living on *M. pyrifera* blades was confirmed through scanning electron microscopy and the ability to culture bacteria on a mannitol carbon source was demonstrated. Emerging interest in this area (Bengtsson et al., 2011; Lachnit et al., 2011; Trias et al., 2011), has provided new protocols and information

that will aid in overcoming the methodological challenges of extracting *M. pyrifera*-associated bacterial DNA. Many questions remain unexplored for almost all algal species including the distributional patterns of bacteria through space and time, and the ecological function of associated bacteria even with the recent expansion in methodological capabilities (Goecke et al., 2010). Hopefully, future studies using these culture-independent techniques will be able to examine the biodiversity and begin to explore the complex ecology of these symbiotic interactions in the ecologically important giant kelp, *M. pyrifera*. This appears to be a rich area for future research especially associated with rapid advances in molecular tools.

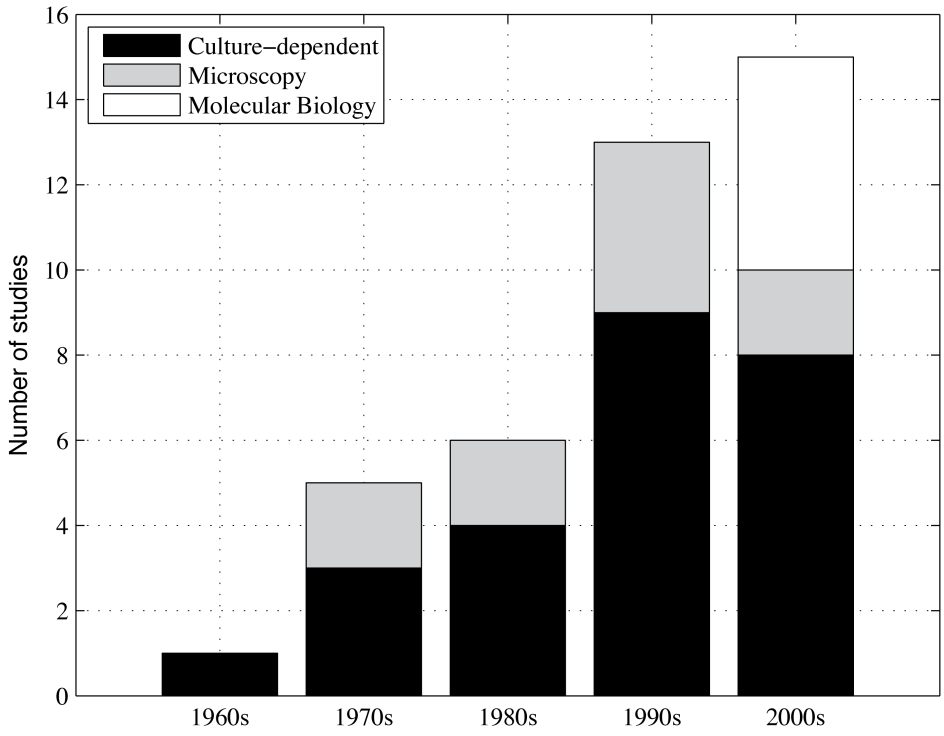

Figure A2.1: Total number of published studies of bacterial communities associated with Phaeophyceae (brown algae) in the last 50 years, separated by the methodology used for the analysis. Adapted from data found in Appendix 1 of Goecke et al. (2010). Microscopy techniques include epiflourescence microscopy and scanning electron microscopy. Molecular biological approached include cytogenic fluorescence *in situ* hybridization, cloning, denaturing gradient gel electrophoresis, and immunofluorescent detection.

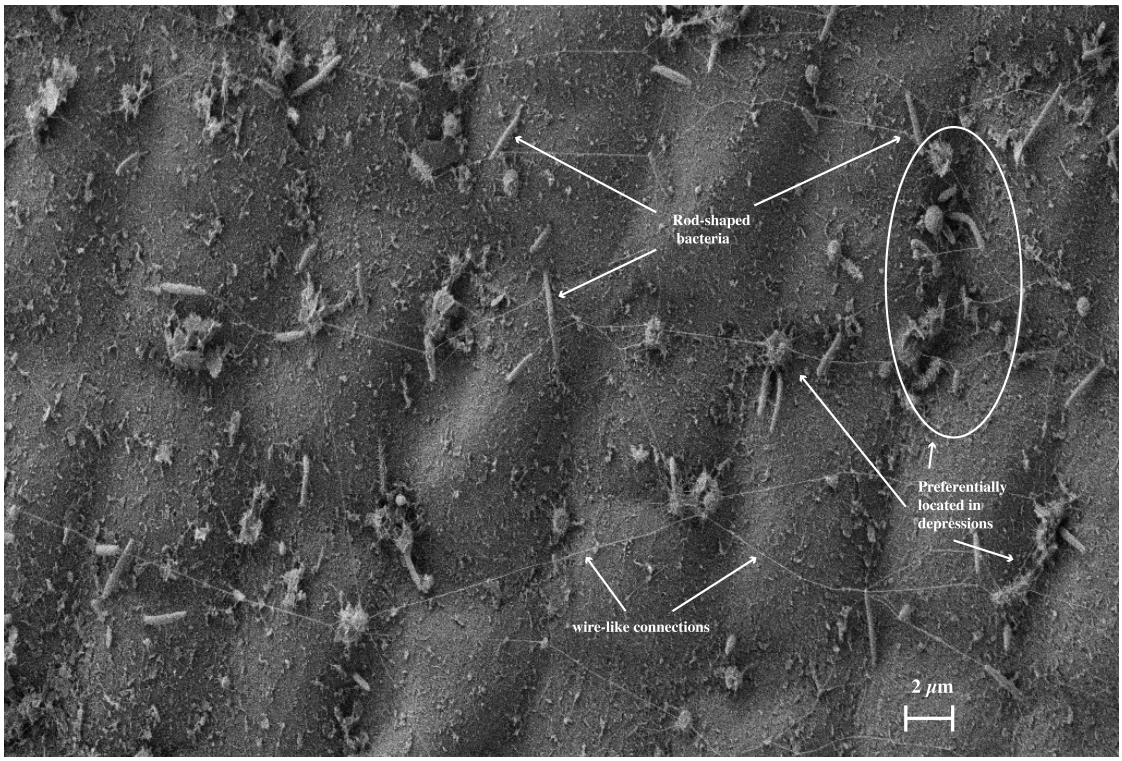

Figure A2.2: Scanning electron micrographs of bacteria on the surface of a *M. pyrifera* blade, scale bar = 2 μm. The bacteria seem to be preferentially located in the depression on the surface of the *M. pyrifera* blade. Examples of rod-shaped bacteria and wire-like structures are indicated with arrows.

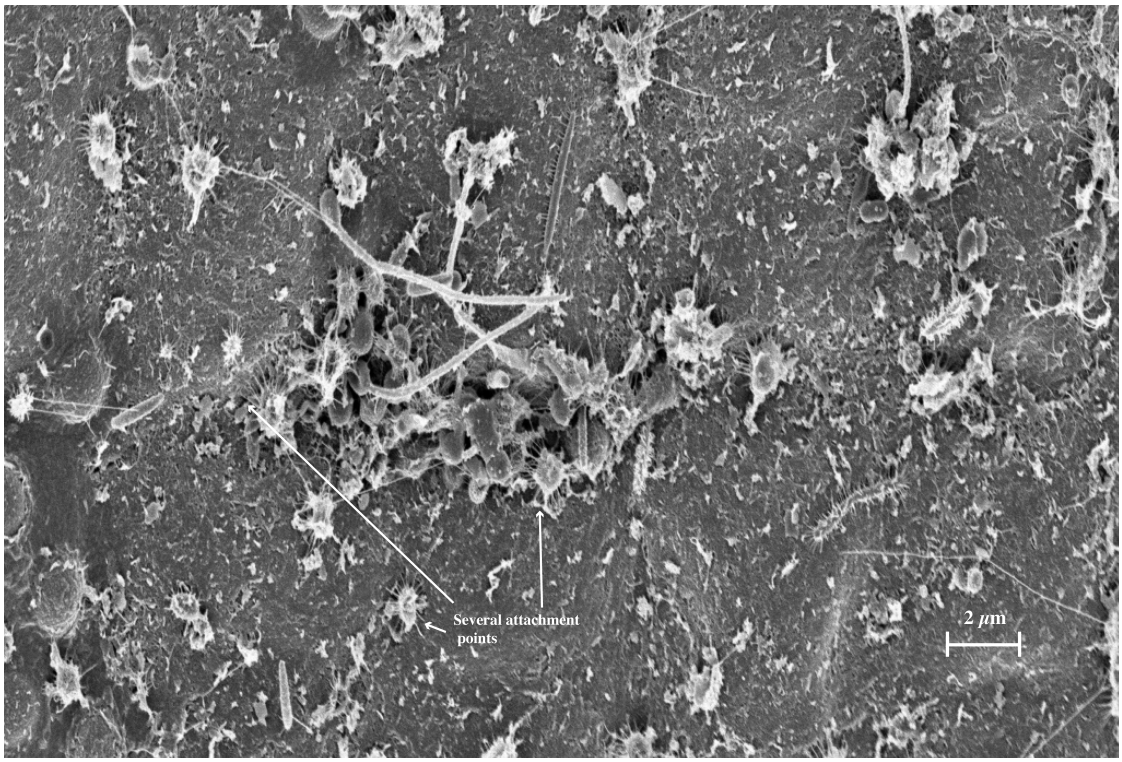

Figure A2.3: Scanning electron micrographs of bacteria on the surface of a *M. pyrifera* blade, scale bar = 2 μm. Some of the bacteria have multiple attachment points suggesting strong surface attachment. Additionally, the large aggregation of bacteria in the center of the figure could possibly be a small microcolony or represent bacteria entering the kelp tissue via degradation of the kelp tissue.

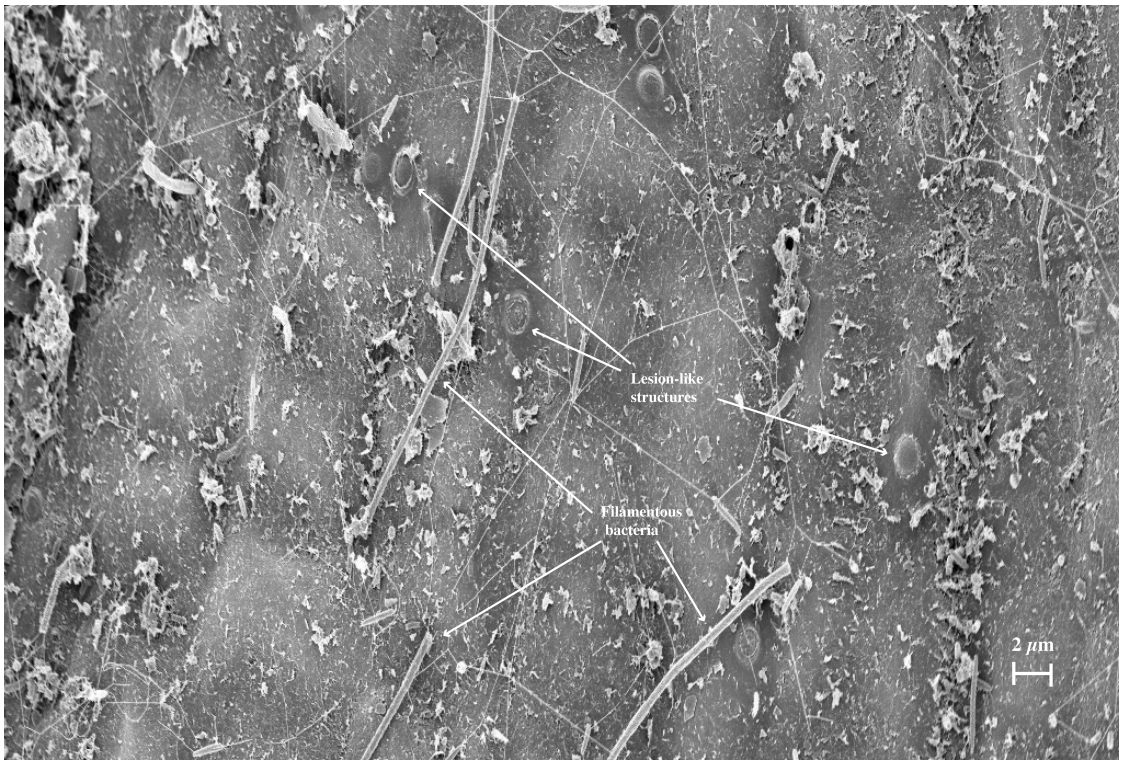

Figure A2.4: Scanning electron micrographs of bacteria on the surface of a *M. pyrifera* blade, scale bar = 2 μm. Examples of filamentous bacteria are indicated with arrows. There are also structures that appear to be lesions, perhaps resulting from pathogenic bacteria. Their size is perhaps too large to be viral. Wire-like structures are also visible connecting bacteria possibly dehydrated EPS or bacterial nanowires.

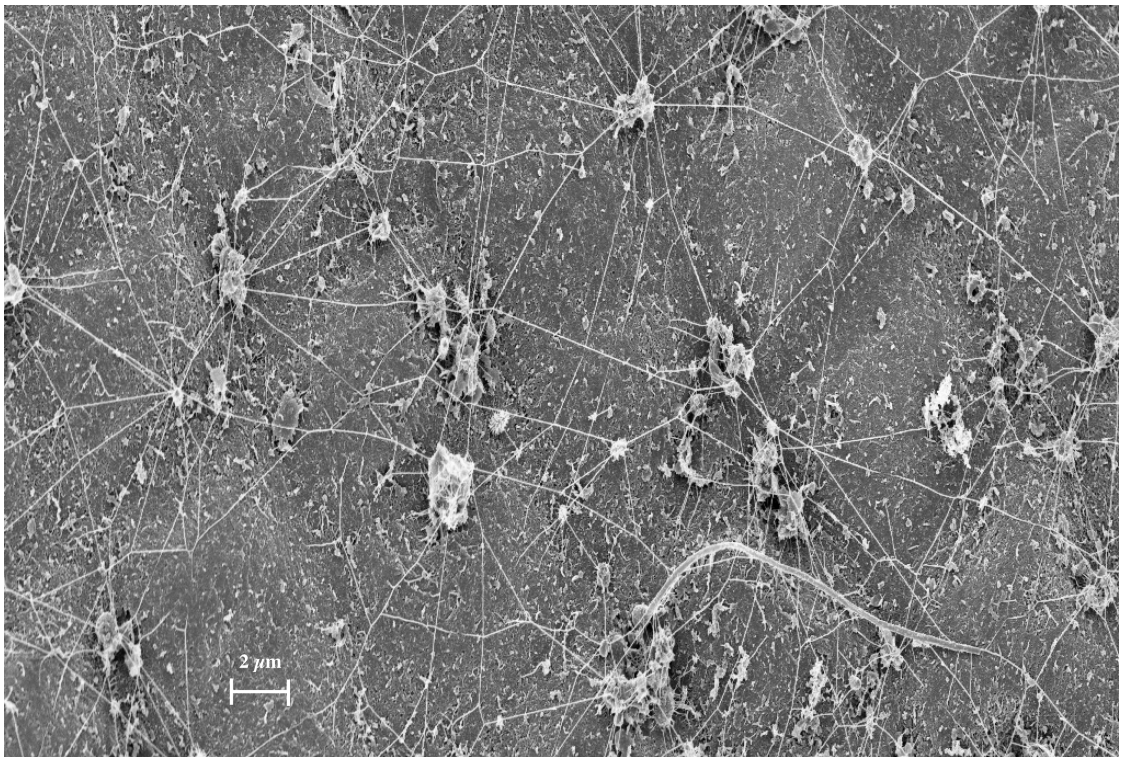

Figure A2.5: Scanning electron micrographs of bacteria on the surface of a *M. pyrifera* blade, scale bar = 2 μm, displaying an extensive network of wire-like structures.

Table A2.1: A list of the taxonomic assignment of 16S rRNA sequences isolated from bacteria grown on a mannitol carbon source.

Bacterial genus	**Info/characteristics**
Psychromonas	Found in marine environments at temps less than 22°C (Garrity, 2001)
Psychromonas	Found in marine environments at temps less than 22°C (Garrity, 2001)
Pseudoalteromonas	Aerobic, requires Na+ for growth, isolated from marine algae, some produce autotoxic antibiotic compounds (Garrity, 2001)
Cobetia	a slightly halophilic bacterium isolated from fermented seafood in Korea (Kim et al., 2010)

Table A2.2: Methods used to extract bacterial DNA from *M. pyrifera* blades. PCR amplification using universal bacterial primers of the DNA products generated using the protocols below was unsuccessful.

Original Protocol	Modifications
Burke et al. 2008	protocol followed by additional extraction[1]
	protocol followed by protein clean-up[2] and additional clean-up[1]
	follow protocol until first supernatant removal, then equal volume supernatant:CTAB buffer[3]
	follow protocol until first supernatant removal, then spin down[4]
.2 μm filtered 10mM EDTA and/or 30mM EGTA as extraction buffer	Place kelp material into extraction buffer (EDTA only, EGTA only, or 50:50 mix) and shake at 250 rpm at 30ºC for 1 hour. EGTA solutions completely broke apart kelp cells turning them into sludge[5]
	EDTA extraction buffer dilutions: 10 mM, 5 mM, 1 mM, 0.5 mM[5]
	As above but concentrate DNA using speedvac
	1 mM & 0.5 mM EDTA extraction buffer, shake at 250 rpm at 30ºC for 1 hour[6], then clean-up[1]
	As above, followed by a PowerClean DNA clean-up kit (MO BIO)
Snirc et al. 2010	using material from 1mM EDTA extraction buffer[5], then Snirc modification to Plant DNeasy kit
Apt et al. 1995	Extract *M. pyrifera* DNA using this protocol, then use bacterial universal primers on that material

[1]Clean-up protocol:
Add equal volume phenol:chloroform:isoamyl alcohol to sample, mix well
Centrifuge 14,000g for 30 min at 4ºC
Keep supernatant
Add 1/10 volume sodium acetate, 2x volume EtOH
Place in -20ºC overnight
Centrifuge 14,000g for 30 min at 4ºC
Air dry, then add DEPC water to resuspend

[2]1:75 volume proteinase K:sample; incubate at 37ºC for 10 min

[3]Extraction buffer:
2% CTAB
2% PVP
1.4 M NaCl
20mM EDTA
100mM Tris-HCl
Incubate at 65ºC for 30 min
Add 750 µl chloroform-isoamyl alcohol, mix by inversion
Centrifuge 13,400 rpm for 25 min at room temperature
Keep supernatant
Add 1000 µl 100% EtOH
Add 175 µl 3M sodium acetate pH 7.0-8.0
Place at -20ºC overnight
Centrifuge 13,200 rpm for 25 min at 4ºC
Remove liquid, 70% EtOH wash x2
Resuspend in DEPC water

[4]Centrifuge at 15,000g for 15 min at 4ºC
Keep supernatant
Phenol:chloroform extraction on 10x and 20x dilutions
Take 750 µl of each sample and add to phase lock gel 2mL tubes
Add 750 µl phenol:chloroform:isoamyl alcohol, pipette mix
Centrifuge 14,000g for 30 min at 4ºC
Keep supernatant
Add 75ul sodium acetate
Add 1000 µl 100% EtOH
Place in -20ºC for 1 hour
Centrifuge 14,000g for 30 min at 4ºC

[5]Discard kelp material
Centrifuge at 4000 rpm for 10 min at room temperature
Remove supernatant, leaving a few ml liquid above the pellet
Mix the remaining solution onto 0.1 µm VVLP Millipore filter
Follow Plant DNeasy kit protocol (Qiagen)

[6]Discard kelp material
Filter onto 0.1 µm VVLP Millipore filter, then freeze at -80ºC
Grind filter on liquid nitrogen
Follow Plant DNeasy kit protocol (Qiagen)

References

Amann, R., Ludwig, W., and Schleifer, K. (1995). Phylogenetic identification and in situ detection of individual microbial cells without cultivation. Microbiology and Molecular Biology Reviews *59*, 143–169.

Bengtsson, M., Sjøtun, K., Storesund, J., and Øvreås, J. (2011). Utilization of kelp-derived carbon sources by kelp surface-associated bacteria. Aquatic Microbial Ecology *62*, 191–199.

Cole, J.R., Wang, Q., Cardenas, E., Fish, J., Chai, B., Farris, R.J., Kulam-Syed-Mohideen, A.S., McGarrell, D.M., Marsh, T., Garrity, G.M., et al. (2009). The Ribosomal Database Project: improved alignments and new tools for rRNA analysis. Nucleic Acids Research *37*, D141–D145.

Croft, M., Warren, M., and Smith, A. (2006). Algae Need Their Vitamins. Eukaryotic Cell *5*, 1175–1183.

Dohnalkova, A., Marshall, M., Arey, B., Williams, K., Buck, E., and Fredrickson, J. (2011). Imaging hydrated microbial extracellular polymers: comparative analysis by electron microscopy. Applied and Environmental Microbiology *77*, 1254–1262.

El-Naggar, M., Wanger, G., Leung, K., Yuzvinsky, T., Southam, G., Yang, J., Lau, W., Nealson, K., and Gorby, Y. (2010). Electrical transport along bacterial nanowires from *Shewanella oneidensis* MR-1. In Proceedings of the National Academy of Sciences, pp. 18127–18131.

Goecke, F., Labes, A., Wiese, J., and Imhoff, J. (2010). Chemical interactions between marine macroalgae and bacteria. Marine Ecology Progress Series *409*, 267–300.

Gorby, Y., Yanina, S., McLean, J., Rosso, K., Moyles, D., Dohnalkova, A., Beveridge, T., Chang, I., Kim, B., Kim, K., et al. (2006). Electrically conductive bacterial nanowires produced by *Shewanella oneidensis* strain MR-1 and other microorganisms. In Proceedings of the National Academy of Sciences, pp. 11358–11363.

Koop, K., Carter, R., and Newell, R. (1982). Mannitol-fermenting bacteria as evidence for export from kelp beds. Limnology and Oceanography *27*, 950–954.

Lachnit, T., Blümel, M., Imhoff, J., and Wahl, M. (2009). Specific epibacterial communities on macroalgae: phylogeny matters more than habitat. Aquatic Biology *5*, 181–186.

Lachnit, T., Meske, D., Wahl, M., Harder, T., and Schmitz, R. (2011). Epibacterial community patterns on marine macroalgae are host-specific but temporally variable. Environmental Microbiology *13*, 655–665.

Laycock, R.A. (1974). The detrital food chain based on seaweeds. I. Bacteria associated with the surface of *Laminaria* fronds. Marine Biology *25*, 223–231.

Mazure, H., and Field, J. (1980). Density and ecological importance of bacteria on kelp fronds in an upwelling region. Journal of Experimental Marine Biology and Ecology *43*, 173–182.

Mazure, H.G.F. (1978). The seasonal cycle of marine bacteria in a west-coast kelp bed. Transactions of the Royal Society of South Africa *43*, 119–124.

Newell, R., Field, J., and Griffiths, C. (1982). Energy balance and significance of micro-organisms in a kelp bed community. Marine Ecology Progress Series *8*, 103–113.

North, W. (1971). The biology of giant kelp beds (Macrocystis) in California (Beihefte Zur Nova Hedwigia, Heft).

Reguera, G., McCarthy, K., Mehta, T., Nicoll, J., Tuominen, M., and Lovley, D. (2005). Extracellular electron transfer via microbial nanowires. Nature *435*, 1098–1101.

Snirc, A., Silberfeld, T., Bonnet, J., Tillier, A., Tuffet, S., and Sun, J.-S. (2010). Optimization of DNA extraction from brown algae (Phaeophyceae) based on a commerical kit. Journal of Phycology *46*, 1–6.

Summers, Z., Fogarty, H., Leang, C., Franks, A., Malvankar, N., and Lovley, D. (2010). Direct exchange of electrons within aggregates of an evolved syntrophic coculture of anaerobic bacteria. Science *330*, 1413–1415.

Trias, R., García-Lledó, A., Sánchez, N., Lopez-Jurado, J., Hallin, S., and Baneras, L. (2011). Abundance and composition of epiphytic bacterial and archaeal ammonia oxidizers of marine red and brown macroalgae. Applied and Environmental Microbiology *78*, 318–325.

Vairappan, C., Suzuki, M., Motomura, T., and Ichimura, T. (2001). Pathogenic bacteria associated with lesions and thallus bleaching symptoms in the Japanese kelp *Laminaria religiosa* Miyabe (Laminariales, Phaeophyceae). Hydrobiologia *445*, 183–191.

Wang, G., Shuai, L., Li, Y., Lin, W., and Zhao, X. (2008). Phylogenetic analysis of epiphytic marine bacteria on Hole-Rotten diseased sporophytes of *Laminaria japonica*. Journal of Applied Phycology *20*, 403–209.